UNIVERSITÀ DI PISA

Department of Energy, Systems, Territory, and Construction Engineering

Master Degree Course in Energy Engineering

IN COOPERATION WITH

Lawrence Livermore National Laboratory

Master Dissertation

Modeling of a compressor-less thermal compression H_2 refueling station: design and optimization

Author:

Michael Melchionda

Supervisors:
Prof. Dr. Umberto Desideri,
Dr. Guillaume Petitpas,
Dr. Salvador Aceves

Academic year 2015-2016

ABSTRACT

The compressor-less thermal compression hydrogen refueling station concept is being analyzed as a cost-effective alternative to “traditional” fueling stations. A transient thermodynamic model was developed and used in this study to evaluate the pathways that minimize both operating (venting losses) and capital (size of cascade of cryogenic vessels) costs. Various conditions were simulated, including operating conditions and vessel design. Results were given as a ratio of venting losses per kg H_2 dispensed, and as a material balance (liner and overwrap) for the cascade necessary to meet a certain given size. Typical HDSAM assumptions were used for station sizing, including the utilization profile, also known as “Chevron” profile.

A refueling station for cryogenic hydrogen, that uses the technique of thermal compression, requires accurate model to simulate all the transient thermodynamic conditions we are facing during the several steps and to design the vessels that are going to be used in the cascade. The cost of the refueling stations covers a big role on the final cost of the dispensed hydrogen. Hence, it is important understand how the several variables we can control are playing in the global system.

Such a station saves the high cost and outages due to the maintenance of high pressure compressor here not necessary, this at the expenses of an amount of hydrogen that has to be vented during the cascade recharging process.

To understand how the system reacts at the input parameters of design, have been written two codes with Fortran 90. One to study and the boil-off and the second to study the refueling process.

With these it was possible to understand which are the controllable parameters to optimize and the goals to follow to have an optimal design.

ACKWONLEDGEMENTS

This dissertation is the result of the support and work of many people. I am grateful for the opportunity I had to work in such an interesting topic in a really professional and high level environment surrounded by awesome people.

First, I want to say that I have been very fortunate to work with my Univeristy of Pisa's supervisor Prof. Umberto Desideri, without him I would have never had this experience. He has always been supportive with my choices and guided me through my path.

I would also like to thank my supervisor Dr. Salvador Aceves for giving me the chance to work with his team. I would like to thank him for welcoming me as a family member, helping me with any situation or trouble I had living out of my country.

I am really thankful to my supervisor Dr. Guillaume Petitpas, for his endless patience and availability, his door (not that there actually was one) was always open to solve my problems and answer my questions. I would like to thank him for the strong support that helped me overcome many crisis situations in both my scientific research and daily life. Without him none of this would have been possible.

Furthermore, I would like to express my gratitude to my other LLNL colleagues, Francisco Espinoza-Loza that helped me uncountable times with my daily problems, gave me precious advice for my research, and has always been available for any need I had. Russel Whitesides that had great patience teaching me to write a code, helping me with all the troubles I had. To Nicholas Killingsworth and Matthew Mcnenly always being supportive, for the fruitful discussions, and great friendship.

Most importantly, none of this would have been possible without the love and patience of my family. Finally, I would like to take the opportunity to thank LLNL and all people who have ever helped me before, all my friends and relatives.

TABLE OF CONTENTS

ABSTRACT ..... **I**

ACKWONLEDGEMENTS ..... **II**

LIST OF TABLES ..... **V**

LIST OF FIGURES ..... **VI**

1.INTRODUCTION **1**

2.HYDROGEN PRODUCTION **6**

2.1 THERMAL PROCESSES 10
Production from natural gas by steam reforming *11*
Production from hydrocarbon partial oxidation *16*
Hydrocarbon decomposition *20*
Production from coal gasification *22*
Capture and storage of CO_2 ..... *25*
Production from biomass gasification *26*
High-temperature decomposition *28*
Thermochemical methods *29*
2.2 ELECTROLYTIC PROCESSES 31
2.3 PHOTOLYTIC PROCESSES 37
Photo-electrolysis (photolysis) *37*
Photo-biological production (biophotolysis) *39*

3. HYDROGEN STORAGE **41**

3.1 PHYSICAL- BASED STORAGE 43
Off-board hydrogen storage *44*
Compressed and cryo-compressed gas storage *44*
Liquid storage *49*
3.2 MATERIAL- BASED STORAGE 53
Hydride hydrogen storage *54*
Activated carbon based hydrogen storage and other high surface area materials *57*
Other hydrogen storage system (Glass Microspheres, Organic fluid sorption) *58*

4.HYDROGEN DELIVERY AND REFUELING STATION **61**

4.1 HYDROGEN DISTRIBUTION 61
Centralized hydrogen manufacture *63*
Distributed hydrogen manufacture *64*
4.2 DELIVERY SYSTEMS 65
Road liquid tanker transport *65*
Ship liquid hydrogen transportation *66*
Compressed hydrogen tube trailer transport *69*
Gaseous hydrogen pipeline transport *70*

4.3 HYDROGEN FUELING STATION 71
Compressed gas hydrogen refueling station *74*
Liquid hydrogen refueling station *75*
Mobile refueling station *76*
Station fuel demand *77*

5. COMPRESSOR-LESS THERMAL COMPRESSION LH_2 REFUELING STATION: PHYSICAL MODEL AND TANK DESIGN 80

5.1 DESCRIPTION OF THE COMPRESSOR-LESS THERMAL COMPRESSION CONCEPT 84
Step 1: Recharging of the cascade from the Dewar *86*
Step 2: Warm up of the full cryogenic vessels *87*
Step 3: Refueling vehicles *88*
Step 4: Recycle hydrogen left in the cascade into the Dewar *90*
Step 5: Venting unusable hydrogen leftover in the cascade *91*
5.2 DESCRIPTION OF THE TANK DESIGN MODEL 91
Mechanical analysis for the design *92*
Thermal mass estimation *95*

6.MODEL CODING AND IMPLEMENTATION 98

6.1 VENTING LOSSES MINIMIZATION SIMULATIONS 100
Input parameters selection *101*
Logic and code routine *103*
6.2 OPTIMIZATION OF THE CASCADE DESIGN 108
Input parameter selection *109*
Logic and code routine *109*

7. RESULTS AND CONCLUSIONS 114

FUTURE WORKS 125

APPENDIX A: REFPROP 9.1 126

APPENDIX B: HDSAM 128

APPENDIX C: SOBOL SEQUENCE 129

APPENDIX D: HDMR 131

BIBLIOGRAPHY 134

LIST OF TABLES

Table 1 World Hydrogen Production Capacity From Different Sources..... 8
Table 2 Comparison of technologies for H_2 production from natural gas..... 20
Table 3 Overview of solid storage options..... 53
Table 4 Comparison between the two path to deliver hydrogen: LH_2 delivery trucks and CH_2 tube trailer delivery trucks 80
Table 5 Capital Cost Contribution to the Liquid Refueling Station of the Delivered Real Levelized Hydrogen Cost ($/kg of Hydrogen)..... 82
Table 6 Coefficients for the specific thermal masses of the two methods 96
Table 7 Parameters range for the optimization process..... 101
Table 8 Parameters range for the optimization process 109
Table 9 Symbol meaning in the HDMR analysis results 115
Table 10 Parameters managing to optimize cascade cost and boil-off. Arrow pointing up: increase value. Arrow pointing down: decrease value..... 124

LIST OF FIGURES

Figure 1 Hydrogen powered vehicle on the left. Gasoline powered vehicle on the right. Time-sequence fuel leakage. 3
Figure 2 Feedstocks and technologies for hydrogen production [7] 6
Figure 3 Flowsheet of the main hydrogen production technologies 9
Figure 4 Simplified scheme including all main process steps involved in hydrogen production 12
Figure 5 Simplified scheme of an integrated gasification plant 24
Figure 6 Generic flow sheet for methanol, hydrogen or FT diesel production 27
Figure 7 Principle drawing of iodine/sulfur thermo-chemical process[7] 31
Figure 8 Simplified principle scheme for alkaline (a), PEM (b) and solid oxide (c) cells for water 33
Figure 9 Scheme of a HTE plant based on nuclear power[8] 36
Figure 10 Principle of photo-electrolytic cell[7] 38
Figure 11 Principle of photo-biological hydrogen production[7] 40
Figure 12 Potential hydrogen storage technologies 42
Figure 13 Tank for liquid H_2 against a high pressure hydrogen cylinder, made from carbon fiber composite/metal with a working pressure of 350 bar, produced by Dynetek Industries LTD 43
Figure 14 Commercial hydrogen delivery technologies 44
Figure 15 Schematic of a typical high-pressure, C-fiber-wrapped H2 storage composite tank 45
Figure 16 High pressure storage system by Quantum Technologies 46
Figure 17 Thecnologies for hig pressure copressed gas tank 47
Figure 18 Cryogenic pressure vessel design 48
Figure 19 Cryogenic pressure vessel installed onboard a hydrogen-fueled Toyota Prius experimental vehicle 49
Figure 20 LH_2 storage system 50
Figure 21 H2 liquefier block diagram (Linde cycle) 51
Figure 22 Energy density (LHV per liter of storage) in LH_2 and CGH_2 at a different pressures 52
Figure 23 Scheme of a vehicular hydrogen fuel cell system using some form of hydrite storage 54
Figure 24 Left illustration is a shell, tube and fin hydride bed configuration. The right illustration is a cross-section of the storage system. 54
Figure 25 Mass and volume characteristics of various hydride materials 55
Figure 26 Schematic of a rechargeable metal hydrite battery 56
Figure 27 Schematic of (a) Fullerene carbon buckyballs, (b) multi-wall nanotubes, (c) single-wall nanotubes 57
Figure 28 Schematic glass membrane hydrogen storage and working concept 59

Figure 29 Snapshot of glass microspheres for hydrogen storage 59
Figure 30 (*a*) The volume of 4 kg of hydrogen compacted in different ways, together with the weight of hydrogen storage material (note: weight and volume of a container are excluded). (*b*) At normal conditions, 4 kg of hydrogen occupies a volume of 48 m^3, the volume of a medium size balloon 60
Figure 31 H2 supply options in centralized and distributed approaches 62
Figure 32 Principle sketch for large scale centralised hydrogen production 63
Figure 33 Hydrogenics Hy-STAT A alkaline electrolysis unit. This packaged unit has an integrated compressor to deliver hydrogen at storage pressures. 64
Figure 34 Three pathways to deliver hydrogen when the production is off-site..... 65
Figure 35 Cryogenic Liquid Hydrogen Tanker Truck 66
Figure 36 Liquefied Natural Gas ship transportation 67
Figure 37 Conceptual Design of 160000 m^3 LH2 carrier ship 68
Figure 38 Conceptual Design of 2500 m^3 LH2 carrier ship 68
Figure 39 Truck with tube trailer for compressed hydrogen delivery 69
Figure 40 New generation of tube trailer 70
Figure 41 Pipeline..... 71
Figure 42 Shell Hydrogen station in Washington D.C. 72
Figure 43 Scheme of a typical hydrogen refueling station with pipeline GH_2 delivery 74
Figure 44 Scheme of a typical hydrogen refueling station with CcH2 delivery and storage 74
Figure 45 Scheme of a typical hydrogen refueling station with LH2 delivery and storage 75
Figure 46 Mobile hydrogen refueling station 76
Figure 47 Seasonal variation in production plants and storage operation..... 77
Figure 48Weekly distribution of fuel transaction or “fills”..... 78
Figure 49 Hydrogen daily average demand 78
Figure 50 Percentage in the final cost influence of production, delivery and dispensing CH_2 vs. LH_2 refueling station. The costs considered are for a steam methane reforming production plant..... 81
Figure 51 Cost break down LH_2-CcH_2 Refueling Station 82
Figure 52 Schematic thermal-compression compressor less refueling station..... 83
Figure 53 Operational configuration Thermal-compression compressor less LH_2 refueling station 85
Figure 54 Cycle of charging-discharging for a cryogenic vessel of the cascade. Refers to a station that dispenses vehicles with 700 bar tank and come with 90 bar initial pressure, so the minimum pressure of discharge will be 91.4 bar considering 1.4 bar of pressure drop along the hose and dispenser 85
Figure 55 Trend Pressure and Venting during the Step 1 (Recharge Cryogenic Vessel). The Red line show the pressure trend inside of the cryogenic vessel, while the green one indicate the pressure in the Dewar, the dotted blue line indicates the

overall quality of the hydrogen inside the cryogenic vessel, as shown at the beginning is super-heated then be-phase with decreasing quality. The purple line shows the mass of hydrogen that needs to be vented in correspondence of that time to guarantee the flow continuously without interruptions 87
Figure 56 Vessel pressures (red line) vs. vehicles pressures (blue lines). Cryogenic cascade vessels with rating pressure of 860 bar, inner volume of 1 m^3 and the dispensing minimum pressure of 150 bar. Vehicles with 140 liter of tank volume rated for 700 bar pressure and 5.6 kg of capacity. 89
Figure 57 Tries of strategies to a better use of the cascade to minimize the vessels number 89
Figure 58 Dewar pressure cycles 90
Figure 59 Pressure in the Dewar, and pressure and temperature of the cryogenic vessel, as function of the hydrogen mass in the cryogenic vessel during step 4 and 5 91
Figure 60 Filament winding process 92
Figure 61 Thermal mass for aluminum and carbon fiber[38] 97
Figure 62 Excel spreadsheet to simulate step-3 with 20 cryogenic vessels in the cascade 98
Figure 63 Screenshot of the input file for the transient cascading sub-routine..... 99
Figure 64 Pseudorandom sampling vs. Sobol' sequence sampling..... 100
Figure 65 Density vs. pressure for saturated Para-Hydrogen (at equilibrium) 102
Figure 66 Main logic of the program to simulate the entire process of the fueling station. The green blocks are referring at the tank design, the blue ones is the actual fueling station 103
Figure 67 Main logic of the transient cascading simulation code 108
Figure 68 Logic of the Step3 transient model code, the red block is the actual refueling process, the blue are the vehicles and bank of cryogenic vessels implementation, the green are for the timestep change 110
Figure 69 Maximum station demand profile, for a Friday of summer[30]..... 111
Figure 70 First order Sobol indices for the input parameters 115
Figure 71 Second order Sobol indices for coupled parameters 116
Figure 72 Comparison of first order and total Sobol indices 117
Figure 73 Output data map. Total percentage venting function of two input parameters. Red dots boil-off < 10%, blue dots all the values..... 118
Figure 74 Time window influence and number of needed vessel in the cascade .. 120
Figure 75 Comparison during the peak of the demand (16.00) of two minimum dispensing pressure scenario. Cryogenic vessels pressures vs. vehicles pressures. Scenario (A) 250 bar, scenario (B) 92 bar 121
Figure 76 (A) Estimation of the cost of the entire bank of cryogenic vessel in the cascade correlated with their volume. (B) Average number of cycles per day for one cryogenic vessel. (C) Correlation number of cryogenic vessels in the cascade Vs. internal volume of the vessel 122

Figure 77 Venting-Cascade Design comparison at a fixed target price for the dispensed hydrogen. Blue line considering the energy input for the pressurization process, the red line this cost is considered negligible.....123

1.INTRODUCTION

Nowadays, there is an increasing energy demand in all sectors, the world's population growth and the low-cost fossil fuel energy sources such as oil, natural gas, and coal are rapidly being depleted. In the 21st century, these are some of the most important issues that the world is facing. Fossil-fuel, cannot be considered as a sustainable and permanent solution to the global energy requirements and any shortage of it, could lead to fluctuations in the oil price, threatening the global energy security and world's economy. Moreover, the concerns about green-house gas (GHG) emissions are rising, as fossil-fuel usage is increasing worldwide, local air quality falls. Indeed, some studies have estimated the cost of transportation-related emissions on public health to be between $40 billion and $60 billion every year. This is making develop new sets of technological requirements[1].

These are the reasons underlining the considerable interest to reach an ideal future world, driven by renewable, pollution-free sources for every need from the electrical grid to the vehicles.

Hydrogen has seen by a growing number of studies, having a crucial role to play in this future, as one of the most promising energy carriers with a possible development of a global "hydrogen economy" (The hydrogen economy is a proposed system of delivering energy using hydrogen as major carrier[2]. The term *hydrogen economy* was coined by John Bockris during a talk he gave in 1970 at General Motors (GM) Technical Center). It is considered an energy-efficient and low-polluting fuel as an alternative to gasoline and diesel in the transportation field and as an energy store to ensure reliable and continuous supply from intermittent and variable renewable energy sources. When hydrogen is used in a fuel cell to generate electricity or is combusted with air, water and a small amount of NO_x are the only products.

Hydrogen is renewable and is the most common element in the universe, its molecule (H_2) has the highest energy content per unit of weight of any known fuel,

but it never occurs by itself on earth, it can be found in many compounds such as water (combined with oxygen O_2), fossil fuels (combined with carbon C), and biomass. Hydrogen produced through non-fossil fuel sources by using the different forms of sustainable energy sources, such as solar, hydropower, wind, nuclear, etc., (so-called: renewable energy based hydrogen production) can be considered to be a prime fuel in meeting some quantity of energy supply and security, transition to hydrogen economy leads to, environmental, social, societal, sectoral, technological, industrial, economical and governmental sustainabilities in a country. Thus, renewable energy based hydrogen system can be one of the best solution for accelerating and ensuring the global energy stability and sustainability.

For example, there is a study[3] investigating the transition to hydrogen energy in the United States of America (USA) for light and heavy-duty vehicles, marine vessels and trains as a central plank of a sustainable energy strategy. The study found that hydrogen fuel cell electric vehicles (FCEVs), in conjunction with electric and other low-emission vehicles, could lead to a reduction of GHG pollution by 80% in 2100 compared with that of 1990. Further, it would enable the USA to remove almost all controllable air pollution in urban areas and become essentially independent of gasoline fuel by the 2100s.

The most concern in using hydrogen is about safety issues. It is important to underline, however, that in the early years of using gasoline and diesel existed exactly the same situation. Hydrogen gas is nontoxic, environmentally safe, and has low radiation level, which reduce the risk of a secondary fire. But special care must be taken since hydrogen burns with a colourless flame that may not be visible (it can be visible in presence of some impurities or particulate in the environment where the combustion takes place because such impurities can burn emitting radiation in the visible length-scale). Hydrogen has a faster laminar burning velocity (2.37 m/s), and a lower ignition energy (0.02 mJ) than gasoline (0.24 mJ) or methane (0.29 mJ). The explosion limits by volume for hydrogen in air of 18.3–59% are much higher than those for gasoline (1.1–3.3%) and natural gas (5.7–14%). The self-ignition temperature of hydrogen (585 °C) is significantly higher than for gasoline (228–501 °C) and natural gas (540 °C). It is almost impossible to make hydrogen explode in an open area due to its high volatility. Since hydrogen is 14 times lighter

than air, it rises at 20m/s if gas is released. Hydrogen is thus usually safer than other fuels in the event of leaks; in this matter there is an interesting study conducted by Ford, that compares the damages caused to a vehicle due to fuel leakage[4], in Figure 1 below is shown the time sequence of the experiment. Cold burns and increased duration of leakage area concern about liquid hydrogen, although hydrogen disperses in air much faster than gasoline.

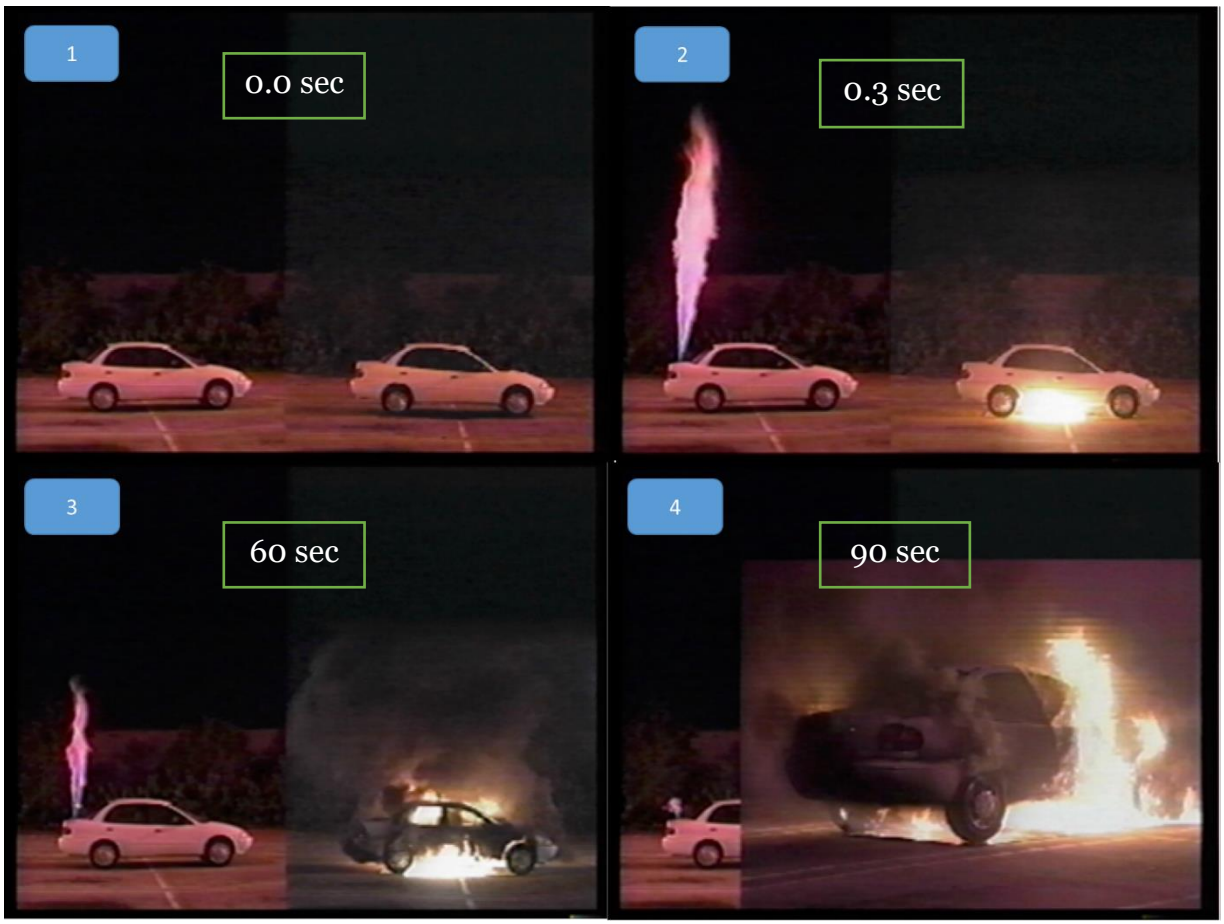

FIGURE 1 HYDROGEN POWERED VEHICLE ON THE LEFT. GASOLINE POWERED VEHICLE ON THE RIGHT. TIME-SEQUENCE FUEL LEAKAGE.

Hydrogen is as safe as other fuels if appropriate standards and safe working practices are followed. When stored at high pressures, the usual regulations and standards for pressurised gas vessels and usage must be implemented, and detection systems need to be employed to avoid any accident or components failure due to hydrogen attack or hydrogen embrittlement. All components used in hydrogen fueling stations must be certified by the appropriate safety authority. The California

Energy Commission has identified 153 failure modes at hydrogen delivery stations (using liquid hydrogen and/or compressed hydrogen stations), and at on-site hydrogen production stations (using steam reforming-SMR and electrolysis hydrogen production)[5]. Stations with liquid hydrogen delivery have the most serious potential failures due to factors such as collisions, overfilling tanks, and relief valve venting. For stations with electrolysers, there are two low-potential failure modes and one medium failure mode. The low failure modes are related to the electrolyser leak (oxygen, hydrogen, or KOH) and high voltages electrocution hazard. The medium failure is related to the dryer failure, which causes moisture to go into downstream components. Station with SMR has one medium-frequency rating failure, which is condensate separator failure that can cause fire or explosion. Other SMR station failures are rated low frequency. Tube trailers have medium failure modes, such as dispenser cascade control failure, as well as hydrogen leaks due to trailer impact in accidents. Other failure modes with lower probability and less consequences have not been mentioned here.

Automotive companies have done a great deal of research on and have produced many types of successful fuel cell vehicle. Some of these companies, like Daimler, Ford and Nissan, have entered into agreements to develop and commercialise zero-emission vehicles based on hydrogen fuel cell vehicles[6].

Hydrogen fueling stations are one of the most important parts of the distribution infrastructure required to support the operation of hydrogen-powered vehicles, both FCEVs and hydrogen internal combustion engine (HICE) vehicles. Without hydrogen refueling network, hydrogen vehicles cannot operate, and their commercial deployment will be very limited. Without a significant fleet of operational hydrogen fuel cell vehicles, it is not viable to invest in setting up a network of hydrogen fueling stations. Hence, if there is to be substantial market penetration of hydrogen vehicles in the transport sector, to meet greenhouse gas reduction targets and enhance energy security, the introduction of commercial hydrogen vehicles and the network of fueling stations to supply them with hydrogen must take place simultaneously.

Hydrogen still has many challenges we need to work on. To begin, even though it can be manufactured from a wide set of sources, hydrogen molecules are very light, which makes it very difficult to retain in the atmosphere from our planet's gravitational force, thus it does not occur naturally in high concentration, only the 0.00005% of the air. Normally hydrogen is found bounded with other elements, such as water, hydrocarbons, hydrides of diverse kinds, and in a wide variety of organic materials. Unlike natural gas, molecular hydrogen it is not found in large accumulations in geologic strata, either. This means that hydrogen more than an actual primary energy source is a mean to transport energy like electricity. In the same way as electrical power, hydrogen must be produced and transported, though hydrogen can be stored for later use, this peculiarity makes it more attractive for some kind of applications, and it is a useful feature to power vehicles and other portable devices.

Moreover, the application of hydrogen in the transportation sector introduces additional problems correlated to the creation of a large infrastructure network for fuel utilization, strictly related to the selected production technologies. The development of specific on-board storage technologies is necessary to match the high energy densities typical of the traditional liquid fuels (gasoline, diesel, LPG) used to feed internal combustion engines in passenger cars.

Current production of hydrogen is about 50 Mt/yr, 90% of which is coming from fossil fuel sources, mostly it is for industrial use in chemical and petro-chemical applications.

2.HYDROGEN PRODUCTION

One of the advantages of using hydrogen as energy carrier is that can be produced following several pathways and using a wide range of feedstocks; all primary resources such as fossil fuels, renewable energy sources (solar, wind, hydro, geothermic, biomass) and nuclear power. In particular, it can be extracted from any substance containing hydrogen atoms, such as hydrocarbons, water, and even some organic matter. Thus, the different technologies utilize mainly these compounds as starting materials for the final H_2 molecule formation, and renewable energy can be used as input of the process. In addition, it can be readily produced from synthesized hydrogen carriers such as methanol, ammonia, and synthetic fuels.
An overview of the different feedstocks and process technologies is shown in the following Figure 2.

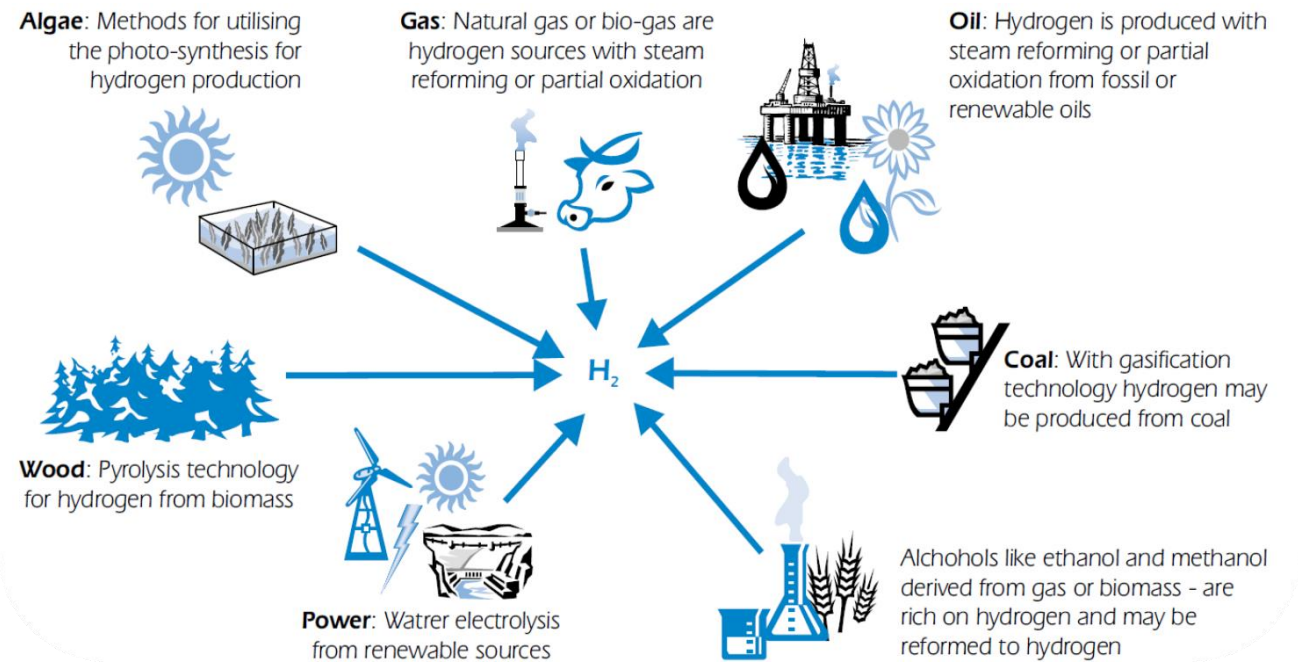

FIGURE 2 FEEDSTOCKS AND TECHNOLOGIES FOR HYDROGEN PRODUCTION [7]

Several of the technologies for industrial production of hydrogen are already available in the marketplace. The first one commercialized dates the late 1920s, it

was the electrolysis of water to produce pure hydrogen. In the 1960s, the industrial production of hydrogen shifted slowly towards a fossil-based feedstock, which is the main source for hydrogen production today.

Hydrogen can be produced directly from fossil fuels by the following processes by steam methane reforming (SMR), thermos cracking (TC), partial oxidation (POX), and coal gasification (CG). The main processes for producing hydrogen from biomass are biochemical and thermochemical (via gasification). Hydrogen can also be produced by dissociating water by electrolysis (HE), photo electrolysis (PHE) or photolysis (also called photo electrochemical or photocatalytic water splitting), water thermolysis (WT) (also called thermochemical water splitting), and photo biological processes.

All these processes require inputs of energy. In the case of conventional electrolysis, for example, the electrical energy input can be electricity generated by fossil fuel, nuclear or renewable energy power stations. Greenhouse gas emission and other environmental impacts of hydrogen production processes depend crucially on the primary energy source used to supply the process energy, as well as the raw material input, irrespective of whether water, biomass or fossil fuel. Crucially important to note here, is that hydrogen is a zero greenhouse gas emission fuel only if it is produced entirely using renewable.

As shown in Table.1 almost half of the hydrogen used worldwide (48%) comes from steam reforming of natural gas (SMR), as it is the most economical route from hydrocarbon feedstock.
The other contributions to hydrogen production are based mainly on partial oxidation of refinery oil (about 30%) and coal gasification (18%), whereas only 4% of the produced hydrogen derives by water electrolysis. The hydrogen is mainly used to make ammonia for fertilizers, in refineries to make reformulated gasoline, and also in the chemical, food, and metallurgical industries.
The pathways involving fossil fuels (natural gas, refinery oil, and coal) that provide for almost 96% of the total production of hydrogen, release carbon dioxide in the atmosphere.
Innovative strategies able to capture and sequestrate carbon dioxide emissions, so-called Carbon Capture and Sequestration (CCS) technologies, are the object of several analysis and heated debate. CCS technologies should be applied for an

environmental-friendly diffusion of fossil fuel-based H_2 production methods, but they are presently in the embryonic stage of development and certainly would involve a great growth of costs[8].

TABLE 1 WORLD HYDROGEN PRODUCTION CAPACITY FROM DIFFERENT SOURCES		
Raw Material	**Technology**	**%**
Natural Gas	Catalytic Steam Reforming	**48**
Refinery Oil	Partial Oxidation	**30**
Coal	Gasification	**18**
Water	Electrolysis	**4**

On the other hand, water electrolysis, which is an intrinsic carbon-free method as it involves splitting water into its component parts, hydrogen (H_2) and oxygen (O_2), is strongly limited because of the present high costs of electricity generation. Thus, the costs will certainly represent one of the most important barriers to be overcome for a sustainable massive production of hydrogen.

The different methods could be classified as: *thermal*, *electrolytic* or *photolytic* processes.

An overview of the main forms of energy input (thermal, electricity, or solar radiation) required by each of the principal processes for producing hydrogen are shown in Figure 3, along with the primary energy options for supplying this input (fossil fuels, nuclear or renewable energy of various kinds).

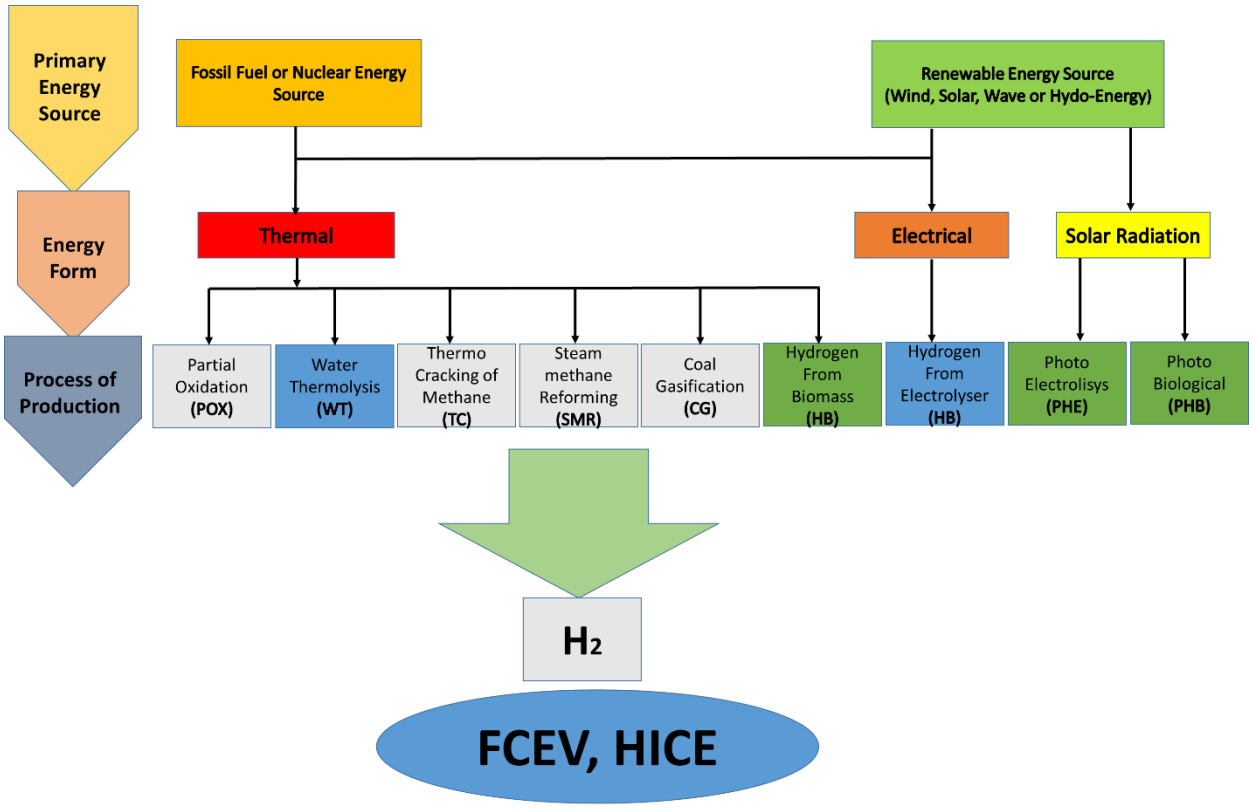

FIGURE 3 FLOWSHEET OF THE MAIN HYDROGEN PRODUCTION TECHNOLOGIES

The heart of the *thermal* processes consists of using the energy associated with chemical reactions to obtain directly hydrogen. Hydrocarbon reforming reactions as well as coal gasification are part of this type of processes. In SMR the fuel reacts with steam at relatively high temperature, producing hydrogen and carbon dioxide. In partial oxidation and gasification processes, the fuels react with a controlled oxidant mixture (air or/and oxygen, and steam) producing similar product mixtures. A further method that should be considered as "thermal" is the technology based on thermochemical cycles involving different chemical reagents. In these processes, hydrogen is extracted from water thanks to heat combined with closed-chemical cycles, necessary to reduce the very high water decomposition temperatures (> 2500 °C), difficult to be reached for heavy limitations due to materials and heat source.

Electrolysis uses electricity to split water into hydrogen and oxygen by means of an electrochemical approach. Hydrogen produced via electrolytic processes can result in zero greenhouse gas emissions, depending on the selected primary source of the

electricity. In addition to renewable and nuclear power, fossil fuels or biomass could be also used in stationary power plants to produce electricity for water electrolysis.

The analysis of *photolytic* methods completes the discussion about hydrogen production. They use sunlight energy to split water into hydrogen and oxygen by photo-electrochemical and photo-biological approaches. These direct sunlight-based processes are currently in the very early stages of research, but could offer long-term potential for sustainable hydrogen production with low environmental impact.

2.1 Thermal processes

The thermal processes require the use of thermal energy to favor the advance of chemical reactions providing hydrogen as direct product. Thermal approaches involve, as reactants, various resources which contain hydrogen atoms as part of their molecular structure, such as hydrocarbons or water, and the conversion advance aimed at directly obtaining high hydrogen yield can be further improved by catalyst addition (hydrocarbon reforming) or should require chemical compound usage (water splitting by thermochemical cycles).
Steam methane reforming, hydrocarbon partial oxidation or coal gasification are all examples of "thermal" methods. The theoretical possibility to overcome the problem of carbon dioxide emissions without using the CCS technology is based on other possible "thermal" methods, such as the hydrocarbon cracking, or gasification of biomass-derived fuels. Also, the thermal production of hydrogen based on thermochemical cycles appears quite promising, being its overall reaction based on the decomposition of water aided by intervention of chemicals, anyway completely recycled.
The feasibility of the processes will vary with respect to a centralized or distributed production plant.

Currently the main production of hydrogen from hydrocarbons such as natural gas is by means of three different chemical processes:

- Steam reforming (steam methane reforming- SMR);
- Partial oxidation (POX);
- Auto-thermal reforming (ATR).

Although several new production concepts have been developed, none of them is close to commercialization.

Production from natural gas by steam reforming

The reforming is a chemical process, in principle, an energy transformation process. The HHV (Higher Heating Value) energy contained in the original substance can be transferred to the HHV energy of hydrogen.
The steam reforming process was introduced in Germany at the beginning of the twentieth century to produce hydrogen for ammonia synthesis, and it was further developed in the 1930s when natural gas and other hydrocarbon feedstocks such as naphtha became available on large scale. H_2 is currently produced from natural gas in large quantities in mixtures with nitrogen or carbon oxides for manufacture of ammonia, alcohols (mainly methanol) and for Gas to Liquid (GTL) processes. In particular, steam reforming produces a mixture of H_2 and CO (synthesis gas or syngas) that could be used directly for the synthesis of methanol or higher alcohols, and for Fischer–Tropsch synthesis.
Natural Gas feedstock is mainly constituted by methane molecule (CH_4), which represents the hydrocarbon with the highest H/C ratio. The composition of the natural gas could slightly change in dependence of the geographic region where it is extracted, but generally, the mixture contains mainly small amounts of light hydrocarbons (C_2–C_4). The compound present in the highest concentration is the ethane (C_2H_6) that can reach in some mixtures a volumetric concentration of 5%. Not negligible traces of sulfur are often detectable in the hydrocarbon mixture.
A simplified scheme of SMR is shown in Figure 4, which includes all main process steps involved in hydrogen production plants based on the steam reforming reaction[8].

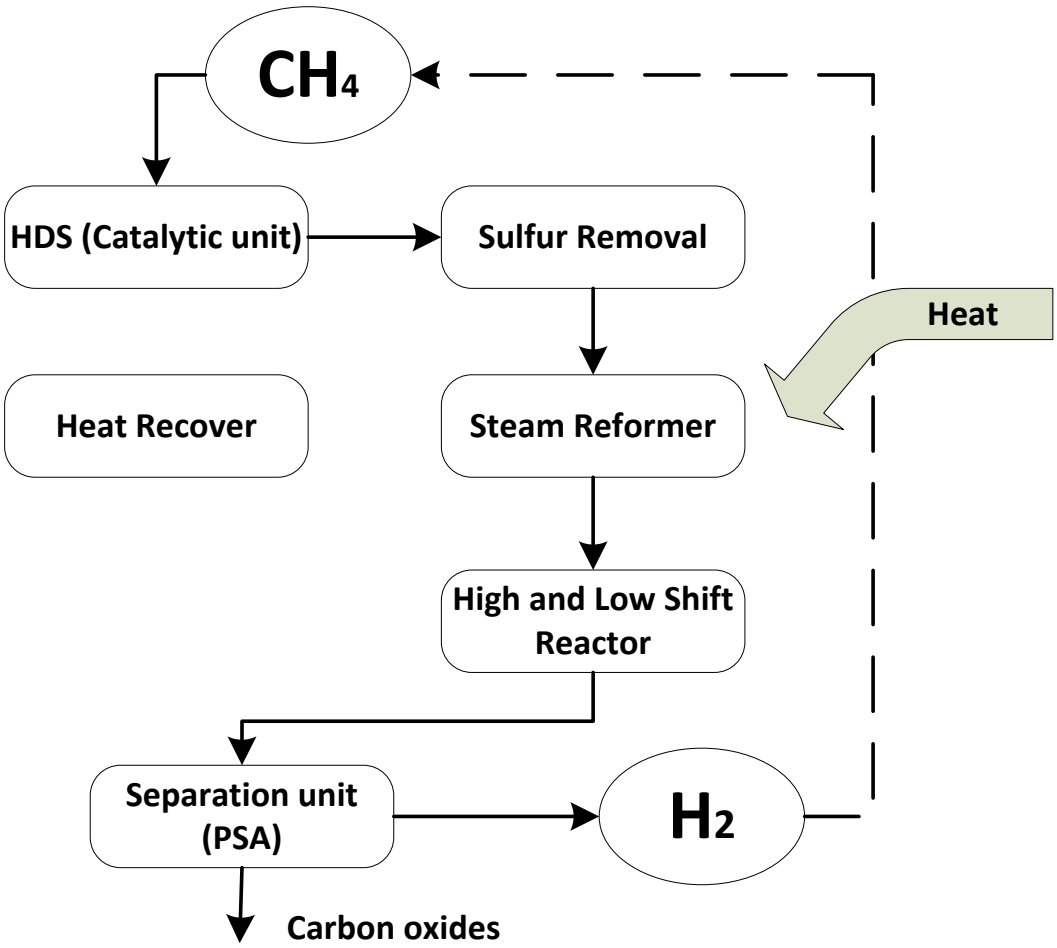

FIGURE 4 SIMPLIFIED SCHEME INCLUDING ALL MAIN PROCESS STEPS INVOLVED IN HYDROGEN PRODUCTION

Two units remove the sulfur concentrations (ppm), added to natural gas as an odorant for safety detection, or present in higher hydrocarbon feedstocks, to protect downstream catalysts (sulfur is a poison for steam reforming catalysts) and process equipment. In particular, the organosulfur species are converted to H_2S at pressures exceeding about 35 bar and temperatures higher than 350°C by catalytic hydro-desulfurization (HDS unit), and Co and Mo alumina-based particulates are used as catalysts. This step is not required for methanol but would be necessary for any sulfur-containing petroleum-based fuels. A second unit permits the H_2S produced in the first step to be removed by a particulate bed of Z_nO. When necessary a further step for chloride removal should be included (not reported in Figure 4).

The third step is the heart of the process (steam reformer). Ni-based ($Ni\text{-}Al_2O_3$) catalysts, loaded in tubular reactors, favor the advancement of the following reactions:

$$CH_4 + H_2O \rightleftarrows CO + 3H_2 \quad \Delta H = +206\,\frac{kJ}{mol} \quad (2.1)$$

Or for higher hydrocarbons:

$$C_nH_m + nH_2O + heat \rightleftarrows nCO + \frac{m+2n}{2}H_2 \quad (2.2)$$

Simultaneously in high- and low-temperature shift reactors, the so-called water gas shift reaction produces further H2 converting the CO contained in the product gas (approximately 12%) according to the exothermic equation:

$$CO + H_2O \rightleftarrows CO_2 + H_2 \quad \Delta H = -41\frac{kJ}{mol} \quad (2.3)$$

The SMR process involves the endothermic conversion showed in the equations 2.1 and 2.2 that are highly energy intensive requiring high energy inputs, in dependence of the fuel.

The heat needed to produce the steam is often supplied from the combustion of some of the methane feed-gas and some waste gas. The process typically occurs at temperatures of 700 to 900 °C and pressures of 3 to 25 bar.

Expensive alloy reaction tubes have to be used to withstand the severe operating conditions.

The array of tubes filled with the catalyst is suspended in a furnace that supplies heat for the highly endothermic reforming reactions.

In some cases, carbon dioxide may replace steam to give a more favorable H_2/CO ratio for subsequent reactions of the products:

$$CH_4 + CO_2 \rightleftarrows 2CO + 2H_2 \quad \Delta H = +247\frac{kJ}{mol} \quad (2.4)$$

The product selectivity for all these reactions is controlled predominantly by thermodynamics, i.e. the final product composition can be foreseen by multicomponent chemical equilibria calculations.
When other hydrocarbons (for example propane) are used as feedstocks, CH_4 is the favored product at lower temperatures, while hydrogen is preferred at temperatures superior to 700–800 °C, then the product gas leaves the tubular reactor at temperatures between 700 and 950°C, in dependence of the particular application. The necessity to operate at these temperatures introduces several potential problems. In particular, the thermal stability of catalysts needs to be carefully verified, because steam tends to favor catalyst and support sintering. However, the major problem lies in the formation of coke, according to the following thermodynamically possible reactions[8]:

$$CH_4 \rightleftarrows C + 2H_2 \ (methane\ decomposition)\ \Delta H = +74.7\frac{kJ}{mol} \quad (2.5)$$

Or for higher hydrocarbons:

$$C_nH_{2n+2} + heat \ \rightleftarrows nC + (n+1)H_2 \quad (2.6)$$

$$2CO \rightleftarrows C + CO_2 (Boudouard\ equilibrium)\ \Delta H = -173\frac{kJ}{mol} \quad (2.7)$$

$$CO + \ H_2 \rightleftarrows C + H_2O \quad \Delta H = -131\frac{kJ}{mol} \quad (2.8)$$

The coke can affect the performance of active sites of steam reforming catalysts, determining their partial deactivation, with progressive loss of selectivity towards synthesis gas production, blockage of reformer tubes and increasing pressure drop. The above reactions are in equilibrium and the formation of coke via reactions 2.7 and 2.8 becomes less favored as the temperature increases. However, coke formation via reactions 2.5 or 2.6 becomes increasingly important at higher temperatures and, depending on the nature of the feed, can rapidly deactivate the steam reforming catalyst and block the reactor.

Therefore, the minimization of coking is one of the major factors controlling the industrial application of steam reforming. The thermodynamic of the process dictates reaction conditions that favor coke formation cannot be avoided, but operating conditions can be chosen to minimize coke. Temperature, pressure, and feed composition must be carefully controlled to avoid catalysts deactivation due to coking. Perhaps, the most obvious way is to increase the steam to hydrocarbon ratio to favor the reverse of reaction 2.8.

The outlet from the secondary reformer contains about 10–14% CO (dry gas) which is fed to a high-temperature water gas shift (WGS) reactor in Figure 4, typically loaded with Fe or Cr particulate catalyst at about 350°C. This further increase the H_2 content lowering CO content to about 2% as governed by the thermodynamic and kinetics of the equation 2.3, that is an exothermic reaction. Water gas shift reaction equilibrium is sensitive to temperature with the tendency to shift towards products when temperature decreases.

Then the product gas is fed to a low-temperature reactor where a $Cu/Zn–Al_2O_3$ particulate WGS catalyst works at about 200°C. Outlet CO concentration is decreased to <0.5%, while the remaining CO, which can poison downstream ammonia or methanol synthesis catalysts, is removed by pressure swing adsorption (PSA) unit. This method exploits the adsorption capacity of different molecular sieves or active carbon, which selectively permit the crossover of hydrogen but not of the other compounds present in the effluents. This technology has been introduced relatively few years ago and results highly reliable and flexible.

Starting exclusively from equations 2.1 and 2.3, considering a stoichiometric mixture of CH_4 and H_2O completely converted to H_2 and CO_2, and taking into account the heat of reaction supplied by combustion of CH_4, it is possible to calculate the theoretical energy associated with lower heating value (LHV) of methane to produce H_2. The minimum energy consumption which can be reached by this process corresponds to 2.59 Gcal/1000 Nm^3 H_2 when starting from water vapor, and 2.81 Gcal/1000 Nm^3 H_2 when starting from liquid water, as the real process.

Hydrogen plants designed with conventional technology utilize reforming temperatures below 900°C and high steam to carbon ratios (>2.5), to limit coke formation problems. These plants are characterized by quite poor energy efficiency, as significant amounts of process steam have to be condensed by large air and water

coolers. Moreover, investment costs are high, as large volumetric process flows have to be handled.

Modern hydrogen plants utilize the new developments in steam reforming and shift technology, allowing apparatus to be designed with reforming temperatures above 900°C and steam to carbon ratios even lower than 2.0. These advanced steam reforming plants have improved energy efficiency and reduced hydrogen production costs.

Currently, the processes require about 2.98 Gcal/1000 Nm^3 H_2 implying that an advanced reforming technology consumes about 6% more energy than the theoretical minimum.

In recent years, new concepts to produce hydrogen by SMR have been proposed to improve the performance in terms of capital costs reducing with respect to the conventional process.

As interest in using hydrogen as an energy carrier has increased, attention has been focused on the generation of hydrogen via reformation at a smaller-scale. Systems are being developed with output as low as 20 kg/day, sufficient for refueling 5 passenger cars per day, and there is interest in developing even smaller systems for home-based reformers or even reforming on-board the vehicle.

In particular, different forms of in situ hydrogen separation, coupled to reaction system, have been studied to improve reactant conversion and/or product selectivity by shifting of thermodynamic positions of reversible reactions towards a more favorable equilibrium of the overall reaction under conventional conditions, even at lower temperatures. Several membrane reactors have been investigated for SMR in particular based on thin palladium membranes[8]. More recently, the sorption-enhanced steam methane reforming (Se-SMR) has been proposed as innovative method able to separate CO_2 in situ by addition of selective sorbents and simultaneously enhance the reforming reaction.

On-site scale reformers are a developmental technology, but there are a number operating at H_2 refueling stations around the world.

Production from hydrocarbon partial oxidation

Partial oxidation (POX) is an alternative route to produce synthesis gas starting from hydrocarbon feedstocks. This reaction utilizes the oxygen in the air as oxidant

and results moderately exothermic. The oxygen to carbon ratio is lower than that required by stoichiometric complete combustion.
The stoichiometric equation for methane conversion is:

$$CH_4 + \frac{1}{2}O_2 \rightarrow CO + 2H_2 \quad \Delta H = +35.6\frac{kJ}{mol} \quad (2.9)$$

Or for higher hydrocarbons:

$$C_nH_m + \frac{n}{2}O_2 \rightleftarrows nC + \frac{m}{2}H_2 \quad (2.10)$$

The theoretical H_2 to CO ratio results lower than that of steam reforming (about 2/3), as the main oxidant is O_2 instead H_2O. However, a small amount of water is often added to the reactor feed, to better control reaction temperature and coke formation[8]. The reactions 2.9 or 2.10 are not the exclusive routes of the process as other stoichiometric equations are thermodynamically compatible with the mixture composition fed to the reactor. Equations 2.1–2.8 involved in hydrocarbon steam reforming might occur also in partial oxidation, i.e. they are possible reaction pathways in addition to 2.9 or 2.10. On the other hand, it is necessary to consider that further equations related to several oxidation reactions could occur during fuel conversion:

$$CH_4 + 2O_2 \rightarrow CO_2 + H_2O \quad \Delta H = -801.6\frac{kJ}{mol} \quad (2.11)$$

$$CO + \frac{1}{2}O_2 \rightarrow CO_2 \quad \Delta H = -282.7\frac{kJ}{mol} \quad (2.12)$$

$$H_2 + \frac{1}{2}O_2 \rightarrow H_2O \quad \Delta H = -241.6\frac{kJ}{mol} \quad (2.13)$$

POX involves the combustion of hydrocarbon feedstock in a flame with less than stoichiometric oxygen required by complete combustion with production of carbon dioxide (CO_2) and water (H_2O), according to the equations 2.11-2.13, which in turn

react with the unreacted hydrocarbon (equations 2.1 and 2.4), to produce carbon monoxide and hydrogen. Usually, a slight excess (20–30%) of oxygen with respect to the stoichiometric value required by equations 2.9 or 2.10 is fed to the system. The most recognized reaction mechanism hypothesis is that the highly exothermic total oxidation reaction consumes essentially all the available oxygen, and the large amount of thermal power produced by the combustion is exploited by endothermic reforming reactions. However, the POX process remains globally exothermic.

A non-catalytic partial oxidation process based on the above reactions has been largely used for the past five decades for a wide variety of feedstocks, in particular heavy fractions of refinery, such as naphtha, vacuum fuel oil, asphalt residual fuel oil, or even whole crude oil. The absence of catalysts implies that the operation of the production unit is simpler (decreased desulfurization requirement) but the working temperatures results higher than 1200°C. The high values of this parameter permit satisfactory yield to H_2 and CO to be obtained without using a selective catalyst.

A catalytic partial oxidation (CPO) reaction permits operation temperature to be lowered and meets the requirements of recently proposed decentralized applications based on small-scale reformer plants[8], better than the steam reforming or the non-catalytic partial oxidation process. This evaluation is based on the dependence of costs associated with both SMR and CPO manufacture and management plants by power size. The potentialities of small-scale plants suggest a deeper discussion about hydrogen distribution network scenarios that is carried out in.

The scientific community interest has been focused in recent years especially on H_2 catalytic production by partial oxidation of methane, due to the large diffusion of natural gas as primary feedstock. Coke formation and its deposition on catalyst active sites represent, as well as for SMR process, the main barrier to be abated for a practical utilization of CPO in hydrogen production plants.

Methane CPO has been intensively studied to select new advanced catalysts able to maximize hydrocarbon conversion, hydrogen yield and specially to control catalytic deactivation phenomena, strictly connected to coke deposition problem, similar to SMR process. The role of transition metal-based catalysts in methane CPO reaction mechanism has been detailed, evidencing that fuel dissociation step is crucial for a

viable overall process rate at reasonable temperatures, as expected taking into account the stability of methane molecule.
LPG could be another favorable feedstock for distributed hydrogen production since it is easy to store and transport. Furthermore, LPG and natural gas appear attractive because hydrocarbon mixtures with short aliphatic chains (C1–C4) and no-sulfur or other electronegative atoms (Cl, P) could limit carbon deposition and catalyst poisoning. Commercial Ni catalysts used for SMR plants have resulted very active also for CPO of methane and propane, but deactivation resistance due to coke is not yet acceptable. Ni-based catalyst modification with rare-earth metal oxide La_2O_3 can reduce the Lewis acidity of the catalyst surface and enhance its ability to suppress carbon deposition, while among the various noble metal catalysts Rh has been reported as active and stable. Bi-metallic Ni–Pt catalysts supported on Al_2O_3 result very promising if compared with monometallic catalytic solids. Mixed oxides containing Ce seem useful to formulate a catalyst suitable for a durable hydrogen production, in particular CeO_2 is known to be an oxy-transporter, i.e. it is capable to oxidize deposited carbon particles and to actively participate in mechanism of redox catalytic reactions. On the other hand, the incorporation of ZrO_2 into CeO_2 lattice promotes the CeO_2 redox properties, increasing the oxygen mobility within the solid solution formed[8].

If the water quantity added as feed increases up to a value corresponding to neutral energetic balance between exothermic and endothermic reaction steps, the overall process is denominated auto-thermal reforming (ATR) this approach is a combination of both steam reforming and partial oxidation catalytic processes, it has been recently proposed to optimize the performance in terms of compactness and efficiency of small-medium production plants. Theoretically, no external energy is needed to convert a hydrogen-rich energy carrier like methane (CH_4) or methanol (CH_3OH) into hydrogen by an auto-thermal reforming process. However, in reality, thermal losses cannot be avoided and the HHV energy contained in the generated hydrogen is always less than that in the original hydrocarbon fuel.
The total reaction is exothermic, and so it releases heat. The outlet temperature from the reactor is in the range of 950 to 1100 °C, and the gas pressure can be as high as 100 bar. Again, the CO produced is converted to H_2 through the water-gas shift reaction. The need to purify the output gases adds significantly to plant costs and

reduces the total efficiency. This technology could permit a compromise between the good efficiency of SR and the fast start up of POX. However, it needs a careful control of in going mass stream.

TABLE 2 COMPARISON OF TECHNOLOGIES FOR H_2 PRODUCTION FROM NATURAL GAS

Technology	SMR	ATR or POX
Benefits	**High efficiency** **Emissions**	**Smaller size** **Costs for small units** **Lower efficiency**
Challenges	**Costs for large units** **Complex system** **Sensitive to natural gas qualities**	**Lower efficiency** **H_2 purification** **Emissions/flaring**

Hydrocarbon decomposition

The direct thermal decomposition of methane or higher hydrocarbons represents the unique approach for a theoretical direct decarburization strategy.
Equation 2.5, moderately endothermic, already involved in steam reforming or partial oxidation processes as secondary undesired reaction, written for a general hydrocarbon

$$C_nH_m + heat \rightarrow nC + \frac{1}{2}mH_2 \quad (2.14)$$

evidences that theoretically hydrogen produced by this route results carbon dioxide emission-free, with the additional potentiality of producing a valuable carbon material.

The non-catalytic route, as for the other fuel processing processes, requires a too high temperature (1300–1600°C) to obtain high reactant conversions, while a catalytic approach would permit the working temperature to be lowered to more practical values. Various Ni supported catalysts, and more recently innovative systems doped with other transition metals such as Fe and Co, greatly reduce the working temperature, but fast deactivation occurs, due to carbon deposition. The activity loss strongly limits both efficiency and environmental benefits, as catalyst regeneration is necessary, consuming additional energy and producing carbon dioxide emissions.

Carbon-based catalysts and in particular their kinetics have been intensively studied, because they should reduce the disadvantages related to metal-based catalysts. Carbon materials are more available, have the potential of cost reduction, do not require periodic regeneration because it is not necessary to separate the carbon-product from the catalyst. The fluidized bed reactor technology represents the optimal choice for this kind of hydrocarbon cracking process as it can withdraw the carbon particles evermore, permitting a reliable storage of produced carbon for further use.

The presence of small amount of O_2 in an auto-thermal approach seems to be the best solution to minimize CO_2 emissions in the overall process.

Plasma technology has been proposed as alternative solution to be used in different fuel processing pathways[9]. Similar to catalysis, the plasma approach could drastically increase the rate of the key reaction steps, mainly related to fuel molecule dissociation, abating the activation barrier for the advance of the overall decomposition reaction. The most common method utilizes a high electric discharge produced by two electrodes ('arc'), which determines intense heat, and breaks down organic molecules into their elemental atoms. However, this kind of processes suffers by many limitations, in particular the electricity cost impact on overall efficiency needs to be accurately verified for a transition to large-scale hydrogen production.

Recently, a laboratory atmospheric pressure microwave plasma reactor has demonstrated to be useful for a single-stage, non-catalytic dry methane thermolysis, resulting active and selective towards hydrogen production[9]. Similarly, another novel process proposed for thermo-catalytic decomposition, based on plasma

generation of catalytically active carbon aerosol particles, has provided very high efficiency (higher than 80%) at working temperatures below 1000°C [10].

Production from coal gasification

Another important thermal method is based on the gasification process, currently used on industrial scale essentially to generate electricity.
This technology is also the oldest method for hydrogen production and could convert any type of organic material, such as coal and other petroleum or biomass-derived mixtures. The interest towards this approach comes from the practical possibility of using coal as fuel that is the most world-wide available and relative cheap fossil fuel[11].
The gasification of coal or other carbonaceous substances was largely used in the past century especially for iron making. The process consists of a series of chemical reactions finally producing, similar to reforming reactions, carbon monoxide and hydrogen mixtures, also called 'town gas', which represented in the past century an important chemical feedstock in North American, Europe and China for domestic heating and lighting, public street lighting and domestic fertilizer industry. However, the popularity of town gas decreased significantly by the 1950s as natural gas became widely available. Gasification takes place at high pressure (up to 60 bar) and temperature superior to 700°C, with a controlled amount of oxygen and/or steam. Similar to hydrocarbon reforming-derived synthesis gas, the effluent mixture may be used to produce hydrogen or methanol, burned directly in internal combustion engines, or converted via the Fischer–Tropsch process into synthetic fuel.
Coal substances have complex chemical structures and their compositions are highly variable. For example, a carbon/hydrogen composition in bituminous coal may be represented as about one atom of hydrogen per atom of carbon. For a generic gasification process based on the above coal feedstock, selected as reference carbonaceous fuel, the following (not balanced) overall chemical equation can be written as:

$$CH + O_2 + H_2O \rightleftarrows CO + CO_2 + H_2 + other\ species \quad (2.15)$$

The carbonaceous particles are heated and volatilized at temperatures ranging from 1000 to 1500°C producing carbon oxides and hydrogen gaseous mixtures and simultaneously char (pyrolysis).
A limited amount of oxidant (oxygen or air) is introduced into the reactor and is mixed with crushed/pulverized coal feed (either dry or as slurry) to allow volatile products and some of the char reacts with oxygen to form carbon dioxide and carbon monoxide. The basic reactions for the CO and CO2 formation are the partial and total combustion of C, respectively

$$C + \frac{1}{2}O_2 \rightarrow CO \quad \Delta H = -110.4\frac{kJ}{mol} \quad (2.16)$$

$$C + O_2 \rightarrow CO_2 \quad \Delta H = -393.1\frac{kJ}{mol} \quad (2.17)$$

The exothermicity of the above reactions provides heat for the subsequent gasification reactions. The char (or other resulting hydrocarbons) reacts with steam (but also with carbon dioxide) to produce carbon monoxide and hydrogen, according to the following equation that is the reverse of equation 2.8

$$C + H_2O \rightleftarrows CO + H_2 \quad \Delta H = +131\ kJ/mol \quad (2.18)$$

In addition, the reversible gas phase water gas shift reaction (2.3) reaches very fast equilibrium at temperatures typical of a gasifier. The above chemical equations balance all the product (CO, CO_2, H_2O, H_2) concentrations of the process.
Gasification process could be inserted in an Integrated Gasification Combined Cycle plant (IGCC) to improve the overall process efficiency. The syngas produced in the gasifier is used as fuel in the gas turbine generator of the integrated combined-cycle technology, which consists also of a heat recovery steam generator and a steam turbine/generator. A simplified scheme of a proposed gasification overall plant for generation of both electricity and hydrogen is reported in Figure 5.

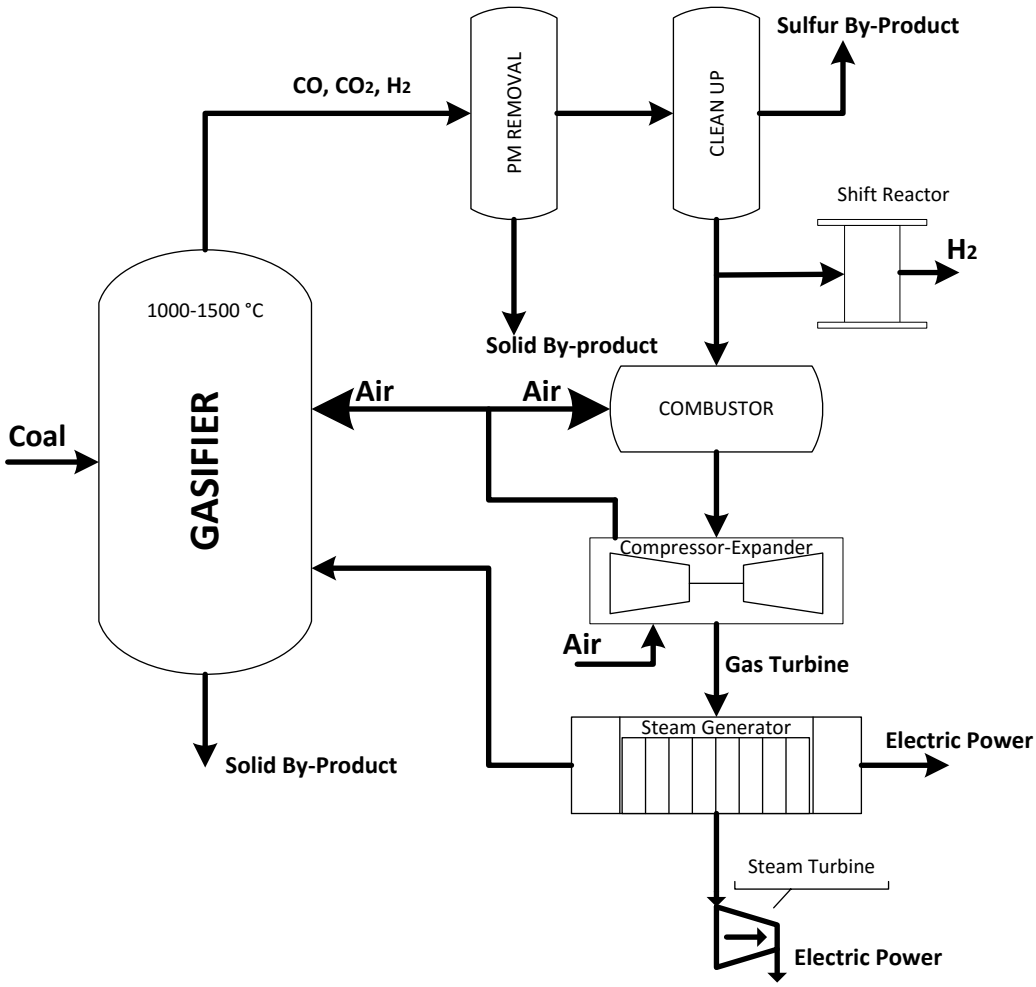

FIGURE 5 SIMPLIFIED SCHEME OF AN INTEGRATED GASIFICATION PLANT

The scheme evidences different steps to produce electricity and hydrogen. The heart of the overall process remains the gasifier. The coal fed to the reactor is exposed to steam and carefully controlled amounts of air or oxygen under high temperatures and pressures. Sulphur is converted to hydrogen sulfide (clean-up reactor in Figure 5) and can be captured by processes presently used in the chemical industry.

The exhaust heat from the combustion turbine is recovered in the heat recovery steam generator to produce steam. The waste heat is passed to a steam turbine system, while heat is recovered from both the gasification process and the gas turbine exhaust in advanced boilers producing steam. The steam is then used in steam turbines to produce additional electrical power, while the syngas mixture could also feed a fuel cell plant (IGFC).

A potential advantage of this technology is that carbon dioxide can be easily separated from the syngas and then captured, instead of being released into the atmosphere. If oxygen is used in a coal gasifier instead of air, carbon dioxide is

emitted as a concentrated gas stream in syngas at high pressure. In this form, it can be captured and sequestered more easily and at lower costs. Finally, plasma technology added to gasification plant has been recently proposed to improve energy performance and quality of product mixtures.
Hydrogen could be produced from coal gasification with near-zero greenhouse gas emissions only if CCS technology, in particular the crucial sequestration stage, will be successfully developed in the next decades. In this view, the coal gasification technology appears most appropriate for large-scale, centralized hydrogen production plants, where handling of large amounts of coal and CCS technologies could be more functionally managed. Significant technological efforts towards the development of an advanced apparatus capable to enhance efficiency, environmental performance and reliability appear necessary.

Capture and storage of CO_2

Carbon dioxide is a major exhaust in all production of hydrogen from fossil fuels. The amount of CO_2 will vary with respect to the hydrogen content of the feedstock. To obtain a sustainable (zero-emission) production of hydrogen, the CO_2 should be captured and stored. This process is known as de-carbonization. There are three different options to capture CO_2 in a combustion process:

- **Post-combustion.** The CO_2 can be removed from the exhaust gas of the combustion process in a conventional steam turbine or CCGT (combined cycle gas turbine) power plant. This can be done via the "amine" process, for example. The exhaust gas will contain large amounts of nitrogen and some amounts of nitrogen oxides in addition to water vapour, CO_2 and CO.
- **Pre-combustion.** CO_2 is captured when producing hydrogen through any of the processes discussed above.
- **Oxyfuel-combustion.** The fossil fuel is converted to heat in a combustion process in a conventional steam turbine or CCGT power plant. This is done with pure oxygen as an oxidizer. Mostly CO_2 and water vapor are produced in the exhaust or flue gases, and CO_2 can be easily separated by condensing the water vapor.

In post-combustion and oxyfuel-combustion systems, electricity is produced in near-conventional steam and CCGT power plants. The electricity produced could then be used for water electrolysis.
If the capture and storage of CO_2 is applied to an energy conversion process of relatively low efficiency, and the electricity is used to electrolyse water, then the overall efficiency of fuel to hydrogen would not exceed 30%.
The captured CO_2 can be stored in geological formations like oil and gas fields, as well as in aquifers, but the feasibility and proof of permanent CO_2 storage are critical to the success of de-carbonization.
The choice of the transportation system for the CO_2 (pipeline, ship or combined) will largely depend on the site chosen for the production plant and the site chosen for storage.

Production from biomass gasification

The choice of a carbon neutral source class as feedstock for hydrogen production, such as biomass substances, could permit the problem of carbon dioxide emissions to be overcome.
In recent years, several methods for hydrogen production starting from biomass materials have been investigated, and great efforts have been addressed in particular in selecting advanced solutions for optimization of the previously analyzed thermal processes, such as steam reforming or gasification, by substituting the fossil fuel feedstocks (coal or petroleum-derived fuels) with different types of biomass-derived fuels.
In particular, biomass-derived materials could be converted in gasifiers, to obtain a gaseous mixture of hydrogen, carbon monoxide, carbon dioxide and other compounds, by applying heat under pressure in the presence of steam and a controlled amount of oxygen, very similar to coal gasification process. On the other hand, the produced syngas could be reformed to maximize hydrogen production but it may also feed an electrical power plant coupled to an electrolysis unit. A typical flow sheet for the production of hydrogen from biomass is presented in Figure 6.

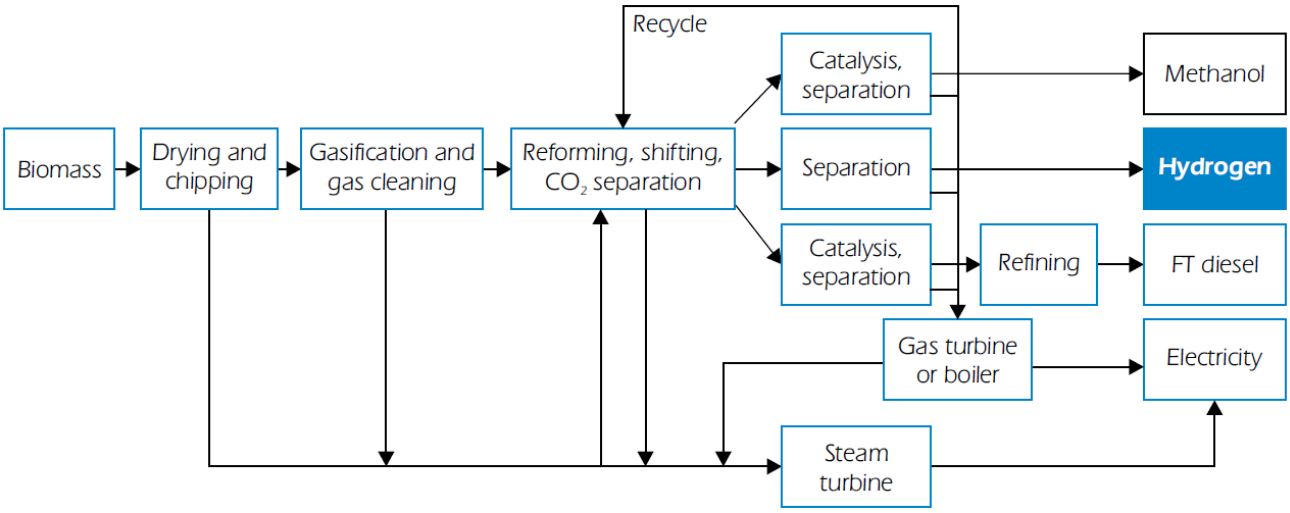

FIGURE 6 GENERIC FLOW SHEET FOR METHANOL, HYDROGEN OR FT DIESEL PRODUCTION

Typically, a biomass-derived material contains substances constituted by carbon, hydrogen and oxygen atoms. As an example, the simplified not balanced chemical equation representative of the overall gasification process for a reference substance such as glucose is:

$$C_6H_{12}O_6 + O_2 + H_2O \rightleftarrows CO + CO_2 + H_2 + other\ species \quad (2.19)$$

The exhaust gases contain CH_4, N_2, H_2O, tar, acidic and basic compounds (NH_3, HCN, H_2S) considered as impurities. Tar conversion has to be controlled to maximize the reliability of mechanical equipments and to assure the operation of the successive clean-up catalytic steps for final hydrogen separation and purification. This step involves the utilization of additional steam and selective catalysts, affecting the overall efficiency of the process. The operation with oxygen instead of air may improve the efficiency of the process but it suffers the costs associated with air liquefaction process, necessary for O_2/N_2 separation.

The current industrial concept for biomass gasification is conditioned by several problems, i.e. heterogeneity of material availability, relatively high costs of collection and transporting the feedstock, and a relatively low thermal efficiency due to the vaporization cost of the moisture contained in the biomass. In order to lower capital costs many efforts are addressed towards the development of advanced membrane technologies able to separate oxygen from air (when the gasifier utilizes

oxygen), replacing the cryogenic process of air liquefaction, and separate and purify hydrogen from the produced gas stream.
Similar to coal, biomass gasification technology seems to be more appropriate for large-scale, centralized hydrogen production, due to the nature of handling large amounts of biomass and the required economy of scale for this type of process, and it may be relevant in specific geographic zones where this feedstock is readily available. However, it will be also useful to explore the future possibilities to use biomass for improving economics of distributed and/or semi-central reforming processes. In this respect, heterogeneous waste and in particular municipal rubbish could represent an important feedstock, if thermally pretreated, in medium-sized power plants.

High-temperature decomposition

High-temperature splitting of water occurs at about 3000 °C. At this temperature, 10% of the water is decomposed and the remaining 90% can be recycled. To reduce the temperature, other processes for high temperature splitting of water have been suggested:

- Thermo-chemical cycles;
- Hybrid systems coupling thermal decomposition and electrolytic decomposition.
- Direct catalytic decomposition of water with separation via a ceramic membrane ("thermo-physic cycle").
- Plasma-chemical decomposition of water in a double-stage CO_2 cycle.

For these processes, efficiencies above 50% can be expected and could possibly lead to a major decrease of hydrogen production costs. The main technical issues for these high-temperature processes relate to materials development for corrosion resistance at high temperatures, high-temperature membrane and separation processes, heat exchangers, and heat storage media. Design aspects and safety are also important for high-temperature processes.

Thermochemical methods

The possibility to transform directly a high-temperature thermal source to chemical energy makes quite attractive the water thermolysis process. This approach represents a direct route for conversion of heat associated with a primary source into hydrogen without intermediate steps; the constraint is that theoretically attractive efficiency can be obtained only if primary sources producing high temperature energy are used. Thermochemical water-splitting cycles have been known for the past 35 years. They were extensively studied in the late 1970s and 1980s, but have been of little interest in the past 10 years.

While there is no question about the technical feasibility and the potential for high efficiency, cycles with proven low cost and high efficiency have yet to be developed commercially. Severe engineering barriers are correlated to the very high temperatures necessary to split water exclusively by heat, together with the problems connected to heat extraction and thermal management. These problems require the practical development of a more complex concept of water decomposition, based on multistep thermochemical processes. This approach is founded on the characteristics of several chemical reagents, capable to lower the temperatures of water decomposition down to a commercially viable value, inferior to 1200°C.

A schematic overall process involves at least two steps:

$$H_2O + 2X \rightleftarrows 2HX + \frac{1}{2}O_2 \quad (2.20)$$

$$2HX \rightleftarrows 2X + H_2 \quad (2.21)$$

where X represents the generic chemical agent. Obviously, the net balance reaction is the reverse of equation 2.13:

$$H_2O \rightleftarrows H_2 + \frac{1}{2}O_2 \quad \Delta H = +288\ kJ/mol \quad (2.22)$$

where ΔH is calculated considering the water in liquid form. The nature and the role of intermediate compounds (XH) are the key point for a successful process, strictly related to the reaching of the following targets:

- Gibbs free energy variation of all individual reaction steps must approach zero;
- The different steps should be minimal;
- Direct and reverse reaction rates of the different steps need to be very fast.

A lot of thermochemical cycles have been proposed in literature, potentially able to exploit the high-temperature energy coming from nuclear or concentrating solar plants (CSP).
In Figure 7 is shown the iodine–sulfur cycle [12] that results quite attractive. It consists of three steps at different operation temperatures, outlined in the equations 2.23-2.24-2.25, which involve the H_2SO_4 and HI dissociation and the re-production of both acids starting from I, SO_2 and H_2O. For this process, the research and development needs are to capture the thermally split H_2, to avoid side reactions and to eliminate the use of noxious substances. The corrosion problems associated with the handling of such materials are likely to be extremely serious.

The HI is then separated by distillation or liquid/liquid gravimetric separation.

$$(120°C)\ \ I_2 + SO_2 + 2H_2O \rightarrow H_2SO_4 + 2HI \qquad (2.23)$$

The water, SO_2 and residual H_2SO_4 must be separated from the oxygen byproduct by condensation.

$$(850°C)\ \ H_2SO_4 \rightarrow H_2 + \frac{1}{2}O_2 \qquad (2.24)$$

Iodine and any accompanying water or SO_2 are separated by condensation, and the hydrogen product remains as a gas.

$$(450°C)\ \ 2HI \rightarrow I_2 + H_2 \qquad (2.25)$$

Net reaction:

$$2H_2O \rightarrow H_2 + \frac{1}{2}O_2 \qquad (2.26)$$

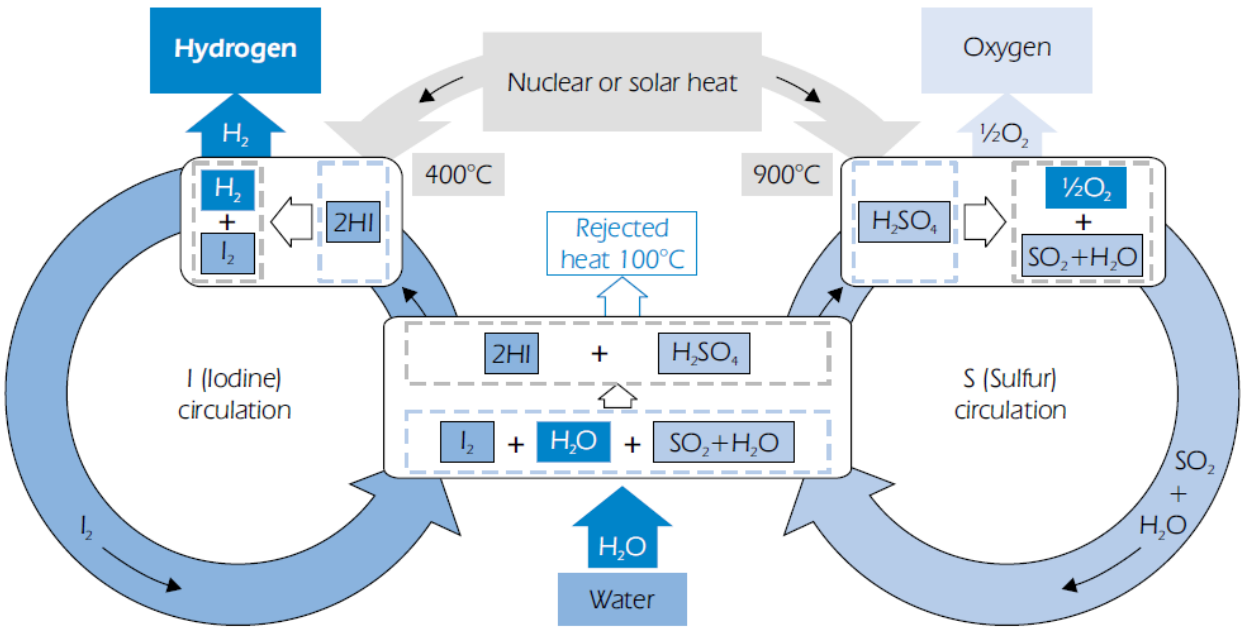

FIGURE 7 PRINCIPLE DRAWING OF IODINE/SULFUR THERMO-CHEMICAL PROCESS[7]

Particular interest is also focused on CeO_2/Ce_2O_3 cycle, cerium–chlorine cycle (Ce–Cl), Zinc–zinc-oxide cycle (Zn/ZnO), but also on a Cu–Cl cycle, which is a cycle with an electrochemical step.

This technology appears really promising for a massive efficient hydrogen production but it is still far to be practically realized in few years, basically because of engineering and material constraints associated with high operation temperature (not inferior to 900–1000°C).

2.2 Electrolytic processes

The possibility to store the surplus of electric energy produced by the power plants into a hydrogen carrier represents an attractive potential solution to optimize the

overall efficiency of energy production and utilization. This idea requires a technology able to transform the excess of produced electric energy into the chemical energy of hydrogen molecule.

A well-known electro-chemical method to obtain hydrogen using electricity is the water electrolysis, which permits the splitting of water molecule into H_2 and O_2 according to the equation 2.22 earlier reported.

The galvanic cells produce electric energy via electro-chemical reactions, while electrolytic cells, such as those used in water electrolysis, are electrochemical cells in which a chemical reaction is forced by added electric energy.

The galvanic cells are based on a spontaneous overall reaction characterized by a negative value of the Gibbs free energy, which corresponds to the theoretical electric work. The electrolytic cells represent exactly the reverse of the galvanic process, then the overall reaction, characterized by a positive value of the Gibbs free energy, is not spontaneous, and needs an external energy resource to force the advance towards the products.

Different electrolysis technologies could be applied, from the commercially available method based on alkaline cells to the new advanced cells based on proton exchange membrane (PEM) and solid oxide mixtures as electrolytes. The basic schemes of these electrolyzer are shown in Figure 8.

The alkaline device utilizes a solution of potassium hydroxide (KOH) as electrolyte (Fig. 8a). The two semi-reactions of reduction (cathode side) and oxidation (anode side) that occur in alkaline solution are, respectively

$$2H_2O + 2e^- \rightarrow H_2 + 2OH^- \qquad (2.27a)$$

$$2OH^- \rightarrow \frac{1}{2}O_2 + H_2O + 2e^- \qquad (2.27b)$$

The sum of the two semi-reactions (2.27a) and (2.27b) gives the overall equation 2.22. Hydroxyl-ions represent the chemical species that close the electric circuit through the electrolyte.

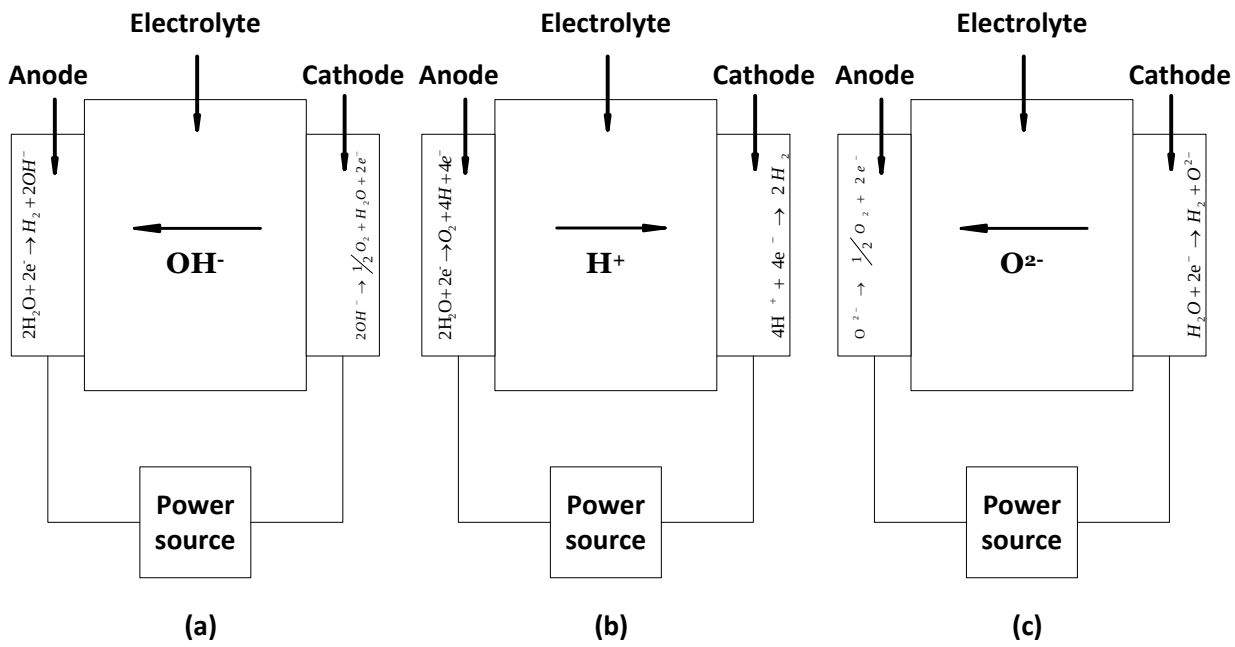

FIGURE 8 SIMPLIFIED PRINCIPLE SCHEME FOR ALKALINE (A), PEM (B) AND SOLID OXIDE (C) CELLS FOR WATER

The alkaline solution contains about 30 wt% of potassium hydroxide and operates at about 80°C. Today, this technology gives a very low contribution to the worldwide hydrogen production (see Table 1), because of the high costs of electricity and the high but not complete conversion efficiency. Furthermore, the KOH solution could limit the resistance of used materials because of corrosion phenomena. In the past years, many studies have been addressed towards a further improvement of catalyzed electrodes to optimize the efficiency and reliability of the electrolytic process involving alkaline cells, but the results have not yet satisfactory.

New advances of the other two electrolytic cells reported in Figure 8 have been recently encouraged to exploit the higher potentialities of PEM and solid oxide technologies, as electrolyzer components to be integrated in plants based on wind and solar renewable sources or nuclear power, respectively.

As regarding electrolysis with PEM cells (scheme b of Figure 8), which is just the reverse of fuel cell operation mode, the interest derives by greater energy efficiency, ecological cleanness, easy maintenance, smaller mass–volume characteristics and high degree of gases purity. Furthermore, it is expected that future costs could be progressively reduced due to foreseeable technological advances of PEM devices working as electric power generation.

The two semi-reactions involved in the process are:

$$2H_2O \rightarrow O_2 + 4H^+ + 4e^- \qquad (2.28a)$$
$$4H^+ + 4e^- \rightarrow 2H_2 \qquad (2.28b)$$

Equations 2.28a and 2.28b are the oxidation and reduction steps, occurring at anode and cathode side, respectively, while the protons represent the ion species passing through the solid polymer electrolyte. However, the overall electrochemical reaction is the same of alkaline electrolyzers.

Recent studies have been devoted to the optimization of the already existent PEM electrolyzers, first exploring the possibilities to increase the working pressure. The high pressure electrolysis (HPE) should reduce significantly the energy costs for the successive fuel compression step. Currently, the onboard storage of hydrogen in fuel cell cars requires a compression stage before fueling the vehicle, while the need for an external hydrogen compressor could be avoided by pressurizing the hydrogen in the electrolyzer. The energy required to produce high pressure hydrogen by high pressure water electrolysis is estimated to be about 5% less than that required for devices working in atmospheric conditions. However, high pressure operation could affect the performance of existent Nafion electrolytic membranes and yield additional problems regarding efficiency loss due to cross-permeation phenomena that implies also relevant safety issues. On the other hand, the application of this technology for electrolytic hydrogen production is mainly related to costs of noble metals used in membrane electrode assembly materials, requiring the development of new high performance and low cost materials.

PEM electrolysis process has been proposed especially for wind turbines or solar photovoltaic (PV) panel utilizations. In this case, the electrolysis represents only a step in the overall hydrogen production process. Efficiency, reliability and costs of overall integrated plants have to be carefully analyzed, in particular taking into account the typical intermittent operation mode of each renewable source.

Several configurations of PV arrays or wind turbines connected to an electrolyzer, based on PEM technology, have been considered evidencing the potentialities of each solution[13]. A possible optimal option is to select the PV panels so that their voltage–current output matches the polarization curves of the electrolyzer. Solar PV

energy has shown good potentialities as an electricity source for water electrolysis but recent analysis related to environmental and economical issues evidence that wind energy seems to be, at least for the existent technological level, a more promising option to produce electrolytic hydrogen.
The operative temperature could play a crucial role for the development of a very efficient electrolyser plant. Solid oxide cells (scheme c in Figure 8) have been proposed for high temperature electrolysis (HTE), because of the strong resistance at high temperatures of the related electrolytes[14]. With respect to traditional room-temperature electrolysis HTE modules presents two main advantages:

- Electrical energy requirement is reduced because of better recover of residual heat, which is cheaper than electricity;
- The power generating cycle, including also electrolysis reaction, is more efficient at higher temperatures.

Currently, yttria-stabilized zirconia and doped $LaGaO_3$ systems seem the most promising materials for developing high temperature (about or higher than 800°C) and intermediate temperature (between 400 and 800°C) electrolysis technologies, respectively[15]. This method could be used for nuclear, concentrating solar or geothermal power plants without carbon dioxide emissions.
The process is based on the following two electrochemical semi-reactions:

$$H_2O + 2e^- \rightarrow H_2 + O^{2-} \qquad (2.29a)$$

$$O^{2-} \rightarrow \frac{1}{2}O_2 + 2e^- \qquad (2.29b)$$

where the ionic species are oxygen anions. As for alkaline and PEM electrolyzer technologies the overall reaction is the equation 2.2.
In Figure 9, a simplified scheme of a high-temperature electrolysis plant based on nuclear power is reported.
Water is warmed up by outer heat in the boiler of the nuclear reactor, before entering as steam into cathode side, where it decomposes according to the equation 2.29a, hydrogen molecule is removed as product, and oxygen anion moves to anode

through a solid oxide electrolyte with high oxygen ion conductivity. Oxygen ion, losing electrons at the anode side, is the reactant of the oxidation semi-reaction, and is recovered as oxygen molecule, according to the equation 2.29b.

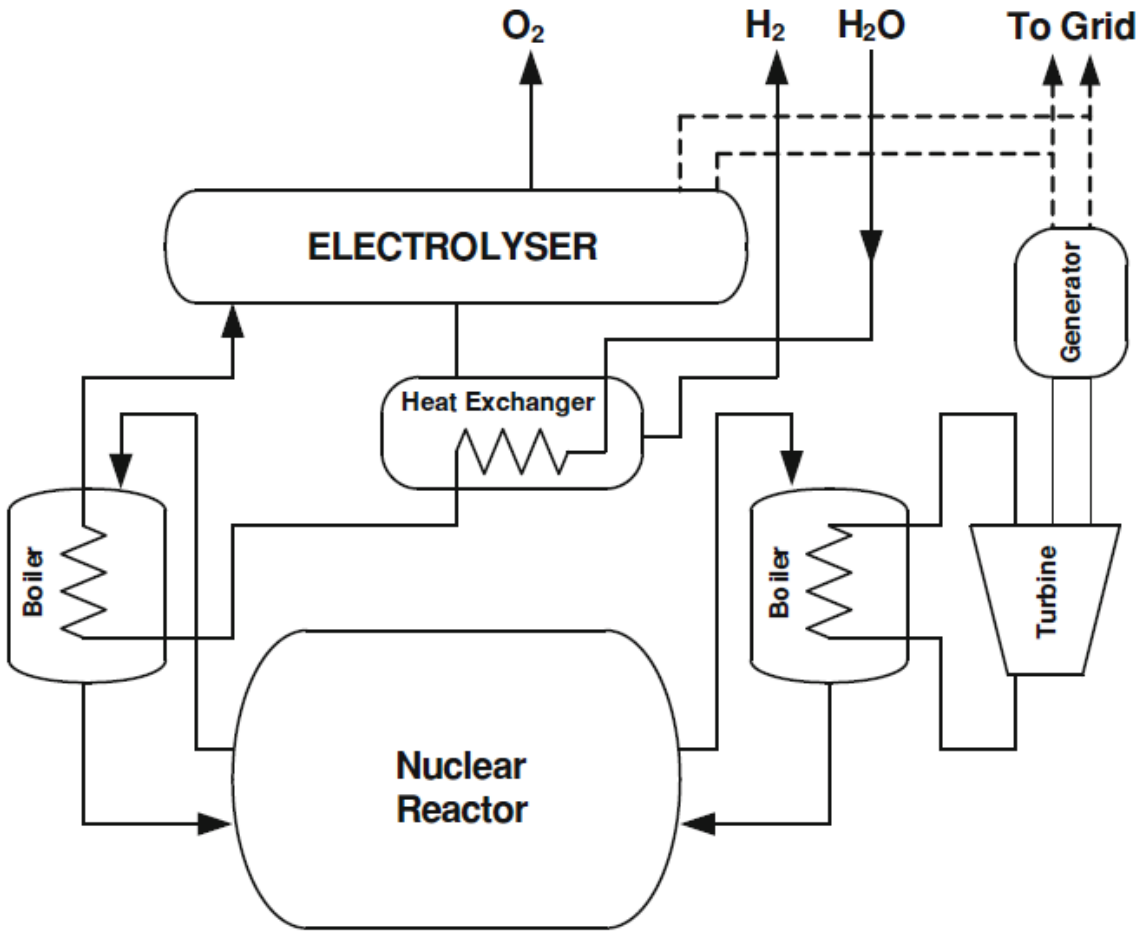

FIGURE 9 SCHEME OF A HTE PLANT BASED ON NUCLEAR POWER[8]

The steam–hydrogen mixture exits from the electrolyzer and the water/hydrogen gas mixture passes through a separator to obtain pure hydrogen, while a portion of the electricity produced by the reactor is used to feed the electrolyzer.

Electrochemical oxidation of coal has been investigated at the beginning of 1980s to evaluate the possibility to limit the high electric power required by H_2O electrolysis, simultaneously overcoming the limitations of the conventional hydrogen production starting from coal, related to the high costs due to working temperature and separation units. The electrolysis of coal takes place according to the following reactions:

$$C + 2H_2O \rightarrow CO_2 + 4H^+ + 4e^- \qquad (2.30a)$$

$$4H^+ + 4e^- \rightarrow 2H_2 \qquad (2.30b)$$

Coal is oxidized at the anode, while protons are reduced to form hydrogen molecule at the cathode. The low current densities achieved in the reaction (about 2.5 mA/cm^2 at 1 V) have discouraged further studies in the successive two decades, but recent works on the development of noble metal carbon fiber electrodes have demonstrated the possibility to improve their activity justifying further experimental tests aimed at fabricating a coal electrolytic cell (CEC) operating at intermediate temperatures (40–108°C). Finally, another potential advantage of the coal electrochemical oxidation is that downstream separation of gases is not necessary as pure H_2 and CO_2 are generated in different compartments of the cell.

2.3 Photolytic processes

The photolytic effect represents another technology able to directly exploit the sunlight, in addition to photovoltaic effect and concentrating solar technology.
This process could be theoretically used to directly dissociate water molecules into hydrogen and oxygen. The recent advances realized in this field encourage a wide research effort aimed at individuating technological pathways alternative to thermal, thermochemical and electrolytic approaches, for an useful contribution to medium–long term hydrogen production.
In particular, two kinds of processes are under investigation:

- The photoelectrochemical (PEC) process that uses photoactive cells in which doped semiconductor electrodes are immersed in aqueous solutions or water;
- The photobiological (PB) water splitting, related to the specific activity of specialized microorganisms.

Photo-electrolysis (photolysis)

Photovoltaic (PV) systems coupled to electrolysers are commercially available. The systems offer some flexibility, as the output can be electricity from photovoltaic cells or hydrogen from the electrolyzer. Direct photo-electrolysis represents an advanced

alternative to a PV-electrolysis system by combining both processes in a single apparatus. This principle is illustrated in Figure 10.

Photoelectrolysis of water is the process whereby light is used to split water directly into hydrogen and oxygen. Such systems offer great potential for cost reduction of electrolytic hydrogen, compared with conventional two-step technologies.

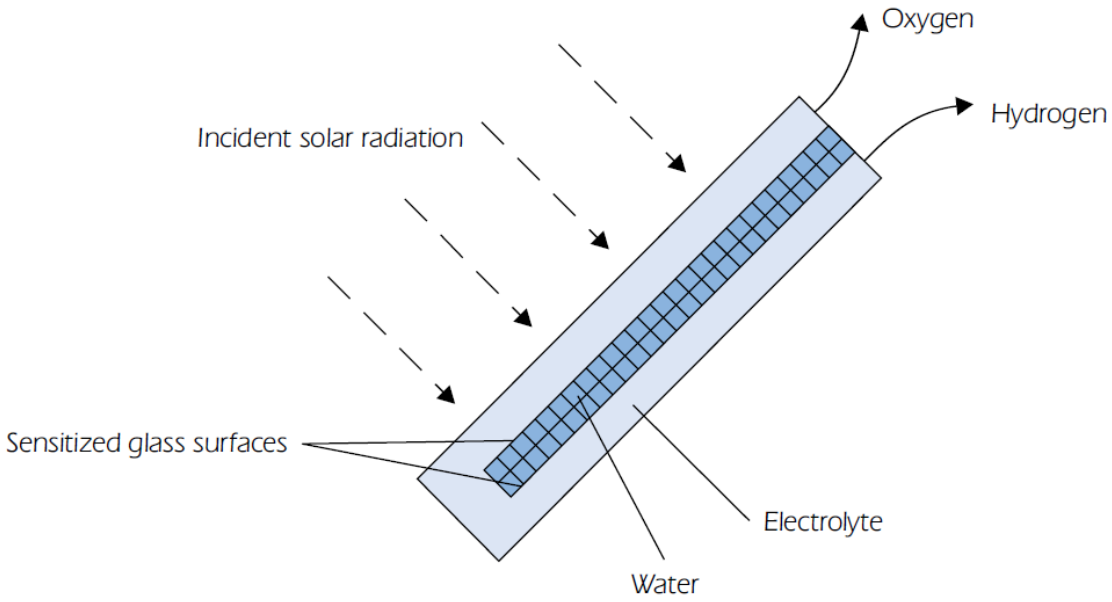

FIGURE 10 PRINCIPLE OF PHOTO-ELECTROLYTIC CELL[7]

PEC research is mainly focused into materials science and systems engineering for photo-electrochemical cells (PEC) are currently being undertaken worldwide, with at least 13 OECD (Economic Co-operation and Development) countries maintaining PEC-related R&D projects and/or entire programs.

Four major PEC concept areas are being studied, comprising two-photon tandem systems, monolithic multi-junction systems, dual-bed redox systems, and one-pot two-step systems. While the first two concepts employ thin-film-on-glass devices immersed in water, the latter two concepts are based on the application of photosensitive powder catalysts suspended in water. Various laboratory-scale PEC devices have been developed over the past couple of years, thus far demonstrating solar-tohydrogen conversion efficiencies of up to 16%.

The key challenges to advance PEC cell innovation toward the market concern progress in materials science and engineering. It is very important to develop photo-electrode materials and their processing technologies with high-efficiency

(performance) and corrosion-resistance (longevity) characteristics, paving the path toward smart system integration and engineering. Since no "ideal" photo-electrode material commercially exists for water splitting, tailored materials have to be engineered.

Combinatorial chemistry approaches offer fast-tracking experimental options for the necessary materials screening, while modelling capabilities of photo-oxidation based on quantum transition theory need to be developed. Most important, there is a need for fundamental research on semiconductor doping for band-gap shifting and surface chemistry modification, including studies of the associated effects on both surface and bulk semi-conducting properties. Corrosion and photocorrosion resistance present further significant R&D challenges to be addressed, with most of the promising materials options at hand. Current-matching between anode and cathode, in addition to ohmic resistance minimization, requires considerable systems design as well as sophisticated engineering solutions. Optimization of fluid dynamics (with its effects on mass and energy transfer) and gas collection and handling (with its effects on operational safety) will demand major conceptual and application-specific R&D attention.

Photo-biological production (biophotolysis)

Photo-biological production of hydrogen is based on two steps: photosynthesis (2.31a) and hydrogen production catalyzed by hydrogenases (2.31b), for example, green algae and cyanobacteria. Long-term basic and applied research is needed in this area, but if successful, a long-term solution for renewable hydrogen production will result. It is of vital importance to understand the natural processes and the genetic regulations of H_2 production. Metabolic and genetic engineering may be used to demonstrate the process in larger bioreactors. Another option is to reproduce the two steps using artificial photosynthesis.

$$2H_2O \rightarrow 4H^+ + 4e^- + O_2 \ (Photosynthesis) \qquad (2.31a)$$

$$4H^+ + 4e^- \rightarrow 2H_2 \ \ (Hydrogen\ production) \qquad (2.31b)$$

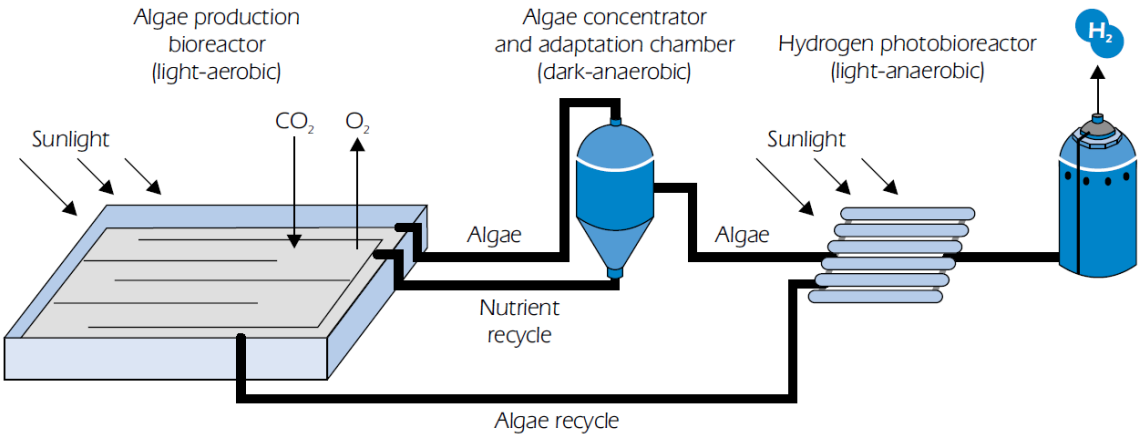

FIGURE 11 PRINCIPLE OF PHOTO-BIOLOGICAL HYDROGEN PRODUCTION[7]

3. HYDROGEN STORAGE

Hydrogen off-board storage is normally in a liquid form (into Dewar) or as compressed gas. For the off-board systems we have issues similar to the one we face in the on-board ones; in these systems though the weight of the canisters is less important than for the vehicular application, because systems are stationary or truck delivered.

The researches efforts, are mostly focused to vehicular on-board systems, because even though hydrogen is highly energy dense in terms of its energy content per kg of mass compared to other fuels, it is a gas at ambient temperature and pressure and for this reason the storage systems tend to be heavy, affecting the overall cost of the system (more material) and its efficiency.

Vehicles need compact, light, safe and affordable containment for on-board energy storage. There are essentially two ways to run a road vehicle on hydrogen. First, hydrogen in an internal combustion engine (ICE) is burnt rapidly with oxygen from air. Second, hydrogen is 'burnt' electrochemically with oxygen from air in a fuel cell (FCEV), which produces electricity (and heat) and drives an electric engine.

A modern, commercially available car is optimized for mobility and not for prestige. For a range of 400km, a normal vehicle burns about 24 kg of petrol in a combustion engine. To cover the same range only 8 kg hydrogen is needed for the ICE version or 4 kg hydrogen for an electric car with a fuel cell[16].

The technologies available and under R&D are many, we can split it in two main categories (Figure 12):

- Physical-based (liquid and gas hydrogen);
- Material-based (metal hydrite, absorption and adsorption).

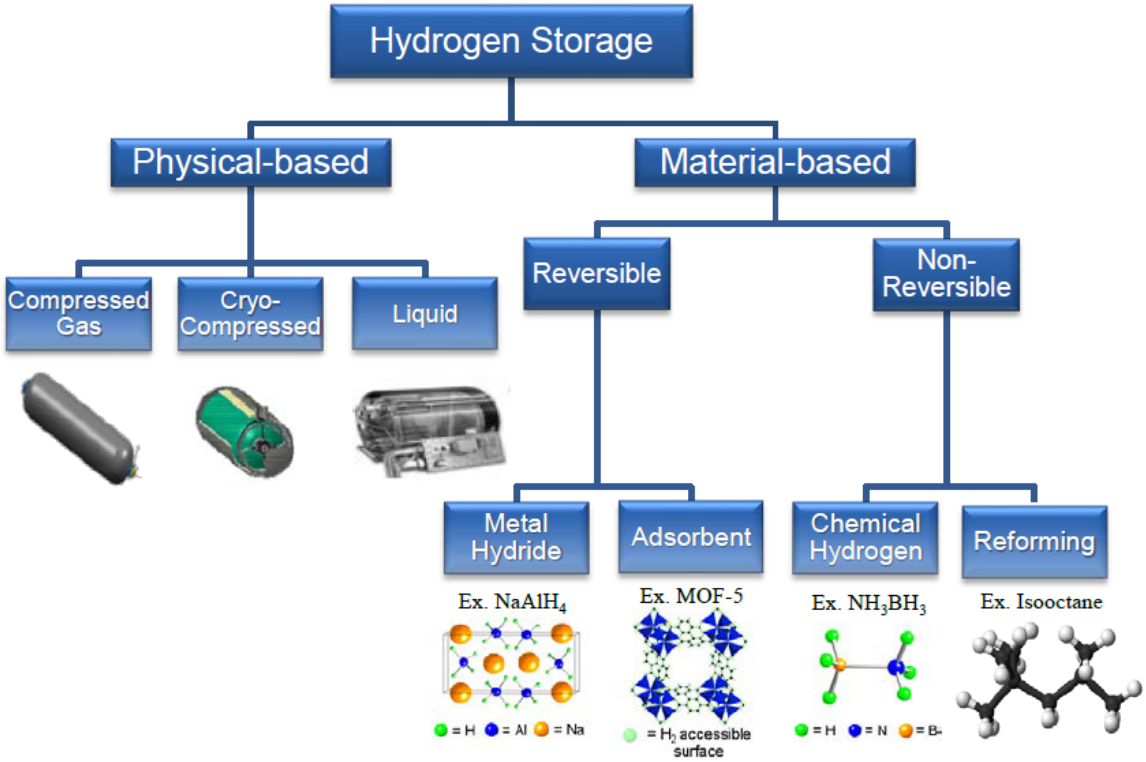

FIGURE 12 POTENTIAL HYDROGEN STORAGE TECHNOLOGIES

The immediate challenge is to find a storage material that satisfies three competing requirements including:

- High hydrogen density;
- Reversibility of the release/charge cycle at moderate temperatures in the range of 70–100 °C to be compatible with the present generation of fuel cell sand;
- Fast release/charge kinetics with minimum energy barriers to hydrogen release and charge.

The first one needs materials with strong chemical bonds and close atomic packing. The second necessitates materials structures with weak bonds that are breakable at moderate temperature. The third requires loose atomic packing to facilitate fast diffusion of hydrogen between the bulk and the surface, as well as adequate thermal conductivity to prevent decomposition by the heat released upon hydrating.

It is important to note that all H_2 storage systems, except gaseous systems, require a heat exchanger. In general, heat must be added during discharging and removed

during recharging. In practical systems, waste heat from the fuel cell or internal combustion engine (ICE) should be utilized.

Hence, the propulsion technology dictates the required discharge temperature of the hydrogen storage medium (*e.g.* approximately 80 ˚C for PEM fuel cells). A key challenge is the ability to recharge the system in 3 minutes. A typical 5 kg H_2-hydride bed, for instance, would require 500 kW of heat removal. That means that off-board recharging may be required.

3.1 Physical- based storage

As noted previously, there are a number of ways to physically store hydrogen. These technologies include liquid hydrogen, gaseous hydrogen.

Some of these options have moved beyond the laboratory stage into prototype vehicles. These are high-pressure storage at 350 bar and 700 bar in carbon fiber-composite tanks, liquid hydrogen in cryogenic tanks.

Each option has advantages and disadvantages.

FIGURE 13 TANK FOR LIQUID H_2 AGAINST A HIGH PRESSURE HYDROGEN CYLINDER, MADE FROM CARBON FIBER COMPOSITE/METAL WITH A WORKING PRESSURE OF 350 BAR, PRODUCED BY DYNETEK INDUSTRIES LTD

Off-board hydrogen storage

Today's hydrogen delivery technologies occupy the extremes of the phase diagram (Figure 14). Hydrogen is often delivered as a compressed gas (red dot) at ambient temperature (horizontal axis), high pressure (dotted lines), and relatively low density (vertical axis). Hydrogen is also delivered at much higher density as a cryogenic liquid (blue dot) with higher energetic cost (solid lines indicate the theoretical minimum work, also known as thermomechanical exergy necessary to densify hydrogen).

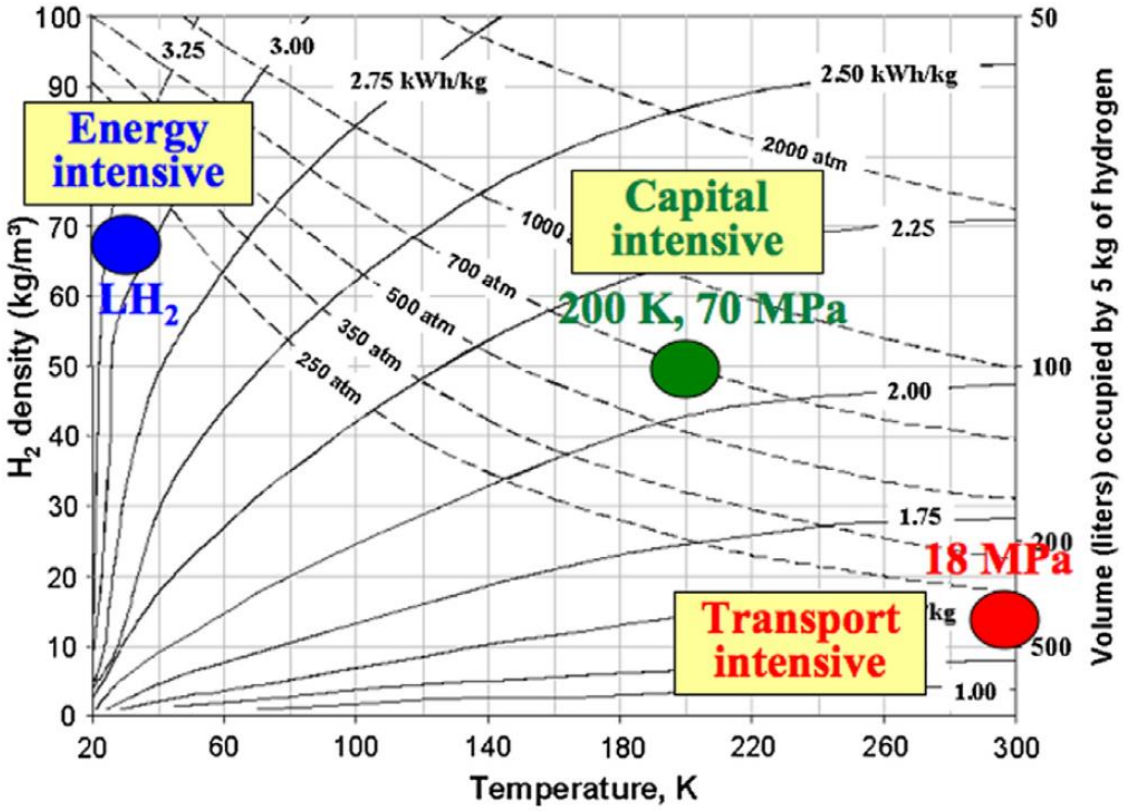

FIGURE 14 COMMERCIAL HYDROGEN DELIVERY TECHNOLOGIES

Compressed and cryo-compressed gas storage

Hydrogen storage in high-pressure cylinders is the most convenient and industrially-approved method. Usually, steel gas cylinders of the low (up to 12 liters) or medium (20 to 50 liters) capacity are in use for the storage and transportation of moderate quantities of compressed hydrogen at temperatures from -50 to +60°C.

Higher pressure compressed gas storage has clear benefits for vehicle onboard storage, giving increased range between refills.

Compressed hydrogen gas (CGH_2) at 345 bar has a density of 23.5 kg/L. A storage of 5.6 kg would require a volume of 255 L for the gas alone, not including the tank or supporting equipment. This additional volume over a 49 L tank for conventional ICE vehicle would be difficult to package in a vehicle without compromising the utility of the vehicle. Typical compressed hydrogen storage cylinders (i.e. steel cylinders containing hydrogen at 200 bar pressure) comprise < 1.5wt% H_2 (which expresses the percentage of the stored hydrogen mass and the mass of the tank i.e. >98.5% of the total weight is the cylinder). The weight of energy storage is very important for vehicle and portable applications, so there is a great deal of interest in increasing the wt% of hydrogen storage. One means of doing this is by storing in lighter-weight cylinders at higher pressures. Cylinders fabricated from wrapped carbon fiber composites (Figure 15) are becoming available that can store compressed hydrogen at pressures of 700 bar and above. This can increase the weight percent of hydrogen to ~ 6wt%.

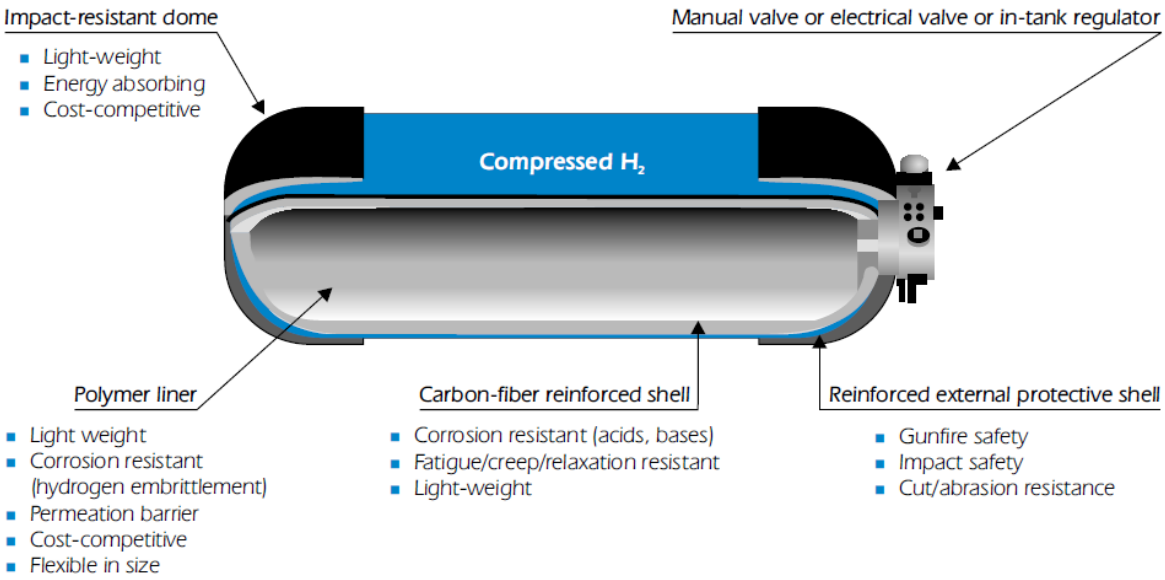

FIGURE 15 SCHEMATIC OF A TYPICAL HIGH-PRESSURE, C-FIBER-WRAPPED H2 STORAGE COMPOSITE TANK

Compressing the hydrogen to 350 bar requires about 8.5% of the energy content of the hydrogen being compressed. Typically fill times are not a problem; however, the fill rate must be monitored and regulated to reduce the temperature increase of the gas in the tank due to rapid filling[17]. At a pressure of 700 bar, the density of the

hydrogen is 38.7 g/L resulting in a tank volume of 155 L which is still much larger than for the gasoline tank. A typical example of high-pressure hydrogen cylinder is made by Quantum Technologies, shown in Figure 16, that they deployed in a fleet of hydrogen Prius in southern California. This high-pressure system is able to store hydrogen at 345 bar and room temperature, for those conditions the amount of hydrogen mass stored is 1.6 kg in an approximate internal volume of 68 liters. Assuming an efficiency of 25.5-42.5 km/L equivalent it is possible to drive from 155-256 km per tank fill-up. It's seen that compressed hydrogen technology is limited to small amounts of hydrogen storage onboard limiting the driving distance per fill-up.

FIGURE 16 HIGH PRESSURE STORAGE SYSTEM BY QUANTUM TECHNOLOGIES

The advantage of compressed gaseous hydrogen (CGH_2) storage is the technological maturity of both pressure vessels and refueling infrastructure. Automotive companies consider CGH_2 a viable near-term option while alternative technologies develop, and therefore CGH_2 is being used in all OEM prototype H_2 vehicles in use today. Negative aspects of CGH_2 are their low capacity that presents a challenge to achieve a practical range (500+ km), high cost due to the large amount of xpensive high strength material (carbon fiber), and the potential for destructive failure due to large expansion energy.

High-pressure tanks can be categorized into five types, four from the regulation (Figure 17), and the last one at its early stages.

- TYPE I: Metal tank (aluminum ~175 bars, steel ~200 bars);
- TYPE II: Metal tank (aluminum) with filament windings like glass fiber/aramid or carbon fiber around the metal cylinder (aluminum/glass ~260 bar, steel/carbon or aramid ~ 300 bar)
- TYPE III: Tanks made from composite material, fiberglass/aramid or carbon fiber with a metal liner (aluminum or steel). Approximate maximum pressure, aluminum/glass 305 bar, aluminum/aramid 440 bar, aluminum/ carbon 700 bars (70 MPa; 10,000 psi).
- TYPE IV: Composite tanks such as carbon fiber with a polymer liner (thermoplastic). Approximate maximum pressure, plastic/carbon 660 bar and up.
- TYPE V: All-composite, linerless Type V tank (under R&D).

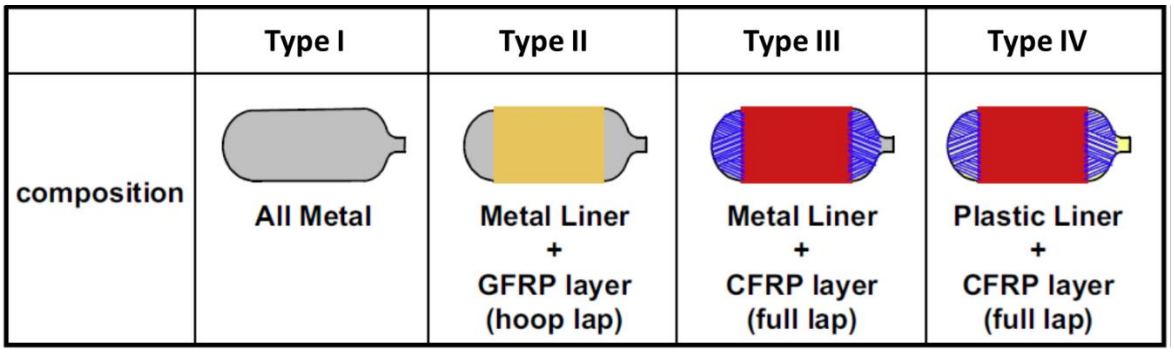

FIGURE 17 THECNOLOGIES FOR HIG PRESSURE COPRESSED GAS TANK

The mainstream of the hydrogen tank is carbon composite Type III and Type IV. This is different from the compressed natural gas vehicle, which mainly employs Type I and II. It is because the hydrogen vehicle uses higher pressure than the natural gas vehicle.
Optimization of material and winding strategy has resulted in 65% more hydrogen storable for the same vehicle[18].

Cryo-gas, gaseous hydrogen cooled to near cryogenic temperatures, is another alternative that can be used to increase the volumetric energy density of gaseous hydrogen.
In particular, LLNL (Lawrence Livermore National Laboratory) has developed a concept consisting of storing hydrogen in a pressure vessel that can operate at

cryogenic temperatures (as low as 20 K) and high pressures (e.g. 350 bar). Cryogenic pressure vessels comprise a high-pressure inner vessel made of carbon fiber coated metal, of the available pressure vessel technologies commonly used for vehicular storage of H_2, aluminum-lined, composite-wrapped (Type III) vessels have been used because they have the most desirable combination of properties for cryogenic application: no H_2 permeation, moderate weight, and affordable price. A vacuum space filled with numerous sheets of highly reflective metalized plastic (for high performance thermal insulation), and metallic outer jacket (Figure 18). This vessel can be fueled with LH_2, compressed gaseous H_2 (e.g. ~350 bar CGH_2) or with cryogenic hydrogen at elevated supercritical pressures, namely cryo-compressed hydrogen[19].

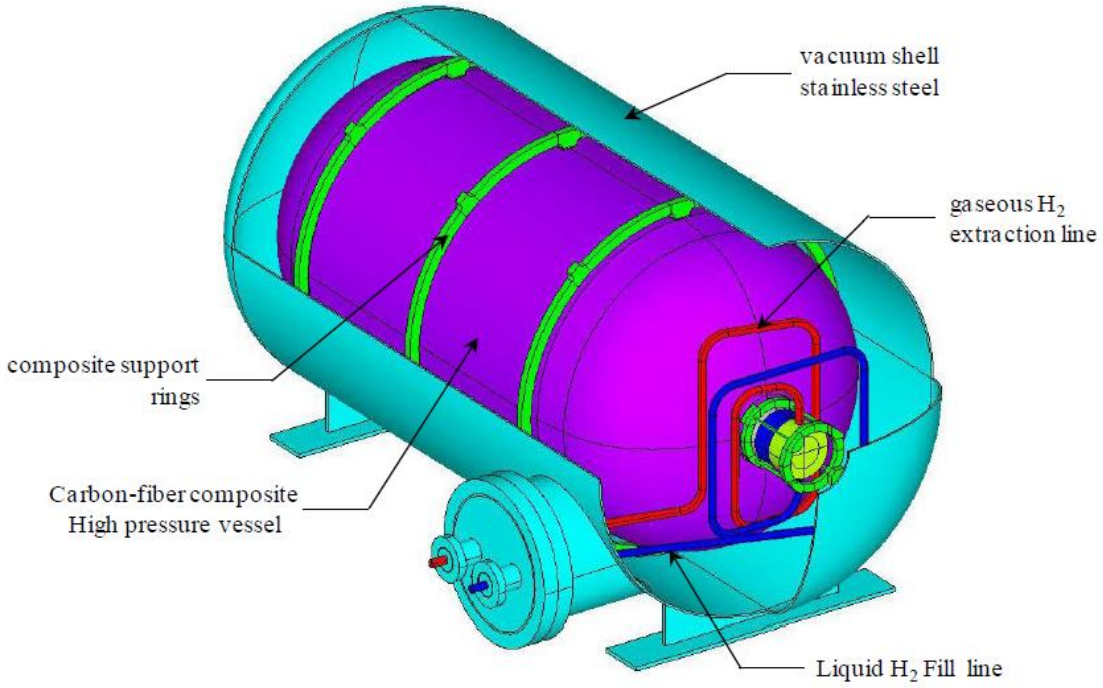

FIGURE 18 CRYOGENIC PRESSURE VESSEL DESIGN

After satisfactory pressure, cryogenic and vacuum testing the vessel was installed in an experimental hydrogen hybrid vehicle (Figure 19). The hydrogen vehicle was then test driven 1050 km on a single tank fill of LH_2 –the longest for a hydrogen vehicle [1.22]. The drive was conducted on-site at LLNL so traffic and speeds were atypical. Under typical driving, 800 km driving range is likely based on the vehicle's EPA fuel economy rating (80 km/kg H2) and the capacity of the storage tank.

FIGURE 19 CRYOGENIC PRESSURE VESSEL INSTALLED ONBOARD A HYDROGEN-FUELED TOYOTA PRIUS EXPERIMENTAL VEHICLE

Liquid storage

Liquid hydrogen (LH_2) has a density of 70.8 g/L, which requires much less volume for the same quantity of hydrogen than CGH_2.

Nowadays the technology of hydrogen liquefaction and liquid hydrogen storage is well developed. Cryogenic vessels having vacuum multilayer heat isolation allow to reach maximum weight capacity as compared to the other hydrogen storage methods (Figure 20).

Significant recent developments have resulted in a creation of highly efficient cryogenic tanks, fueling infrastructure, as well as the improvement in safety for all complex systems providing liquid hydrogen storage. The 5.6 kg requires only 85 L excluding the volume of the auxiliary systems to contain and fuel/refuel the cryogenic hydrogen.

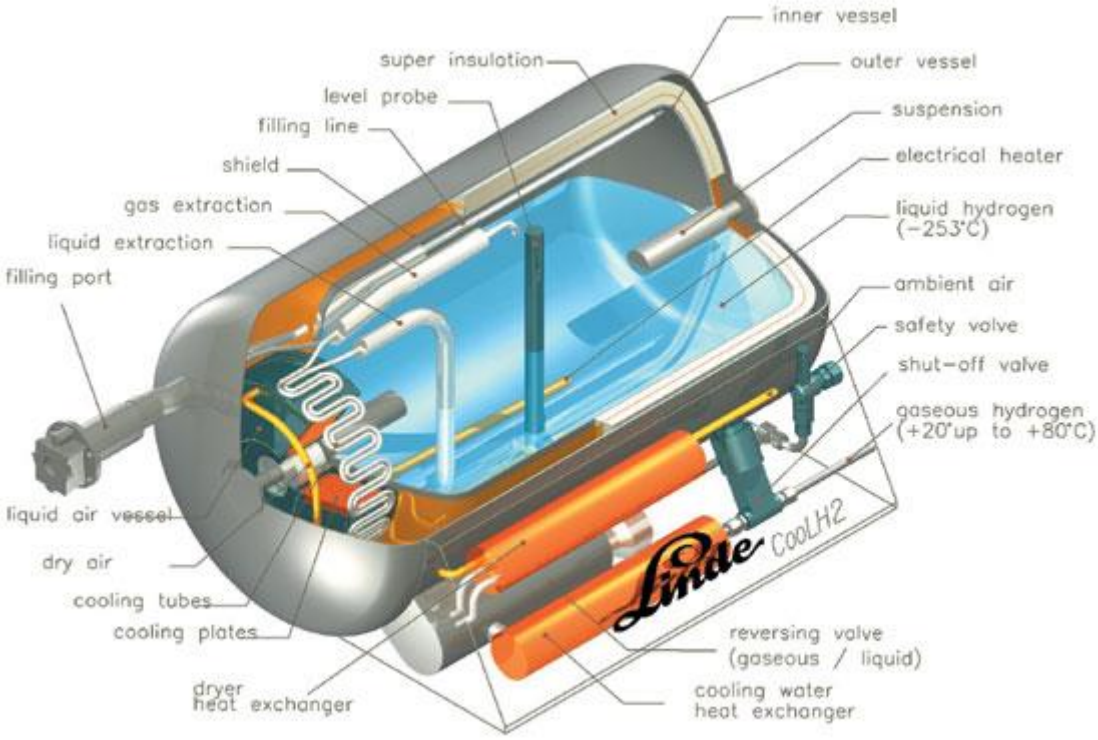

FIGURE 20 LH_2 STORAGE SYSTEM

The main problem with LH_2 compared to other technologies is its energy intensity (efficiency). Hydrogen once produced undergoes liquefaction at a temperature of 20K (-253°C) by a Linde cycle, that is a simple cryogenic process based on Joule–Thompson effect. It is composed of different steps: the gas is first compressed, then preliminarily cooled in a heat exchanger using liquid nitrogen, finally it passes through a lamination throttle valve to exploit the benefits of Joule–Thomson expansion. Some liquid is produced, and the vapor is separated from the liquid phase and returns back to the compressor through the heat exchanger. A simplified scheme of the overall process is reported in Figure 21.

Theoretically, only about 4 MJ/kg must be removed from the gas but the cooling process has a very low Carnot cycle efficiency so even large plants require 30 MJ/kg to liquefy hydrogen[20].

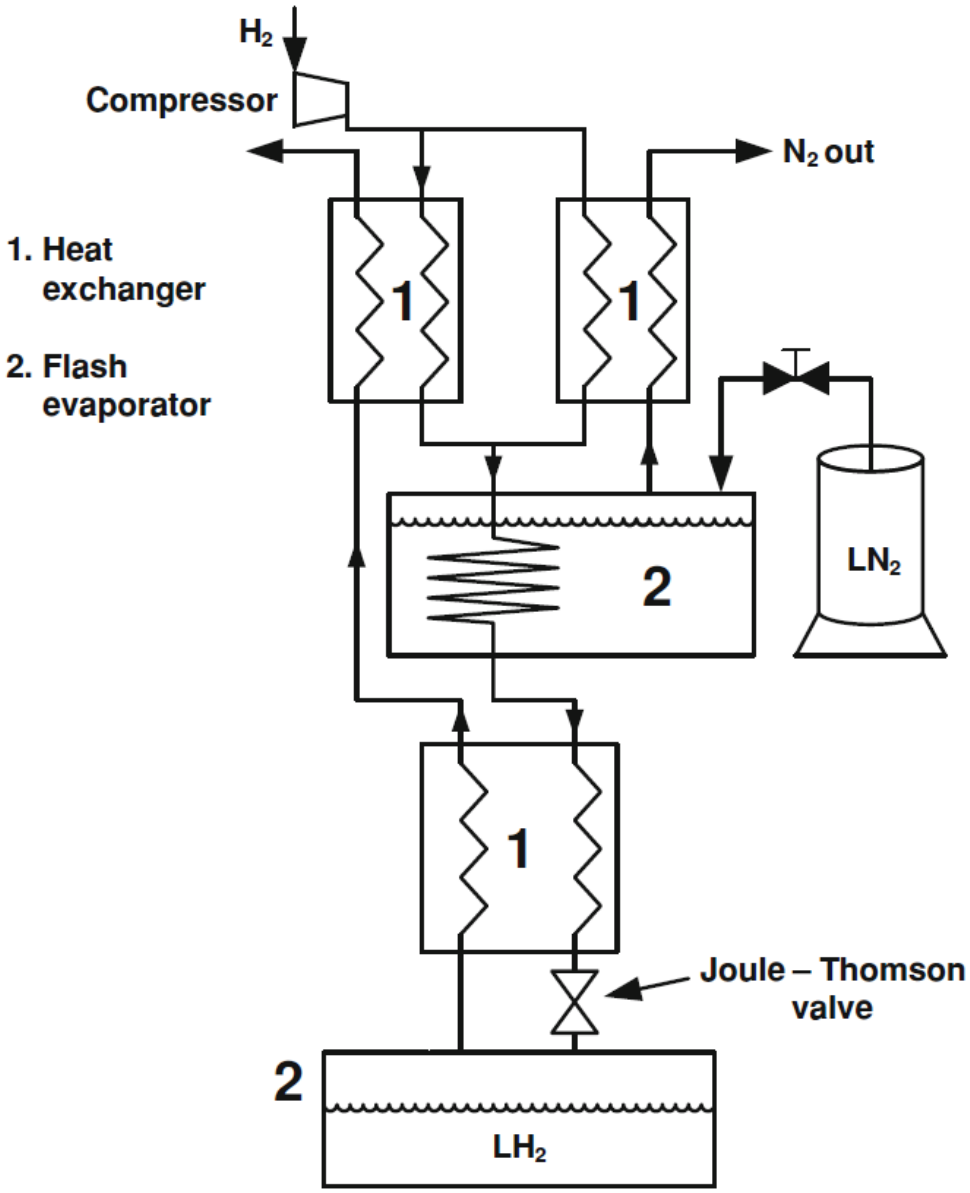

FIGURE 21 H2 LIQUEFIER BLOCK DIAGRAM (LINDE CYCLE)

For a LH_2 tank system, the typical nominal operational pressures are in the range from 1 to 3.5 bar, compared to compressed gaseous H_2 (CGH_2) at 240 bar, 350 bar, or 700 bar, as can be seen in Figure 22, the specific energy density (lower heating value, LHV per liter) of LH_2 is 1.5-2 times higher, even as compared with the existing prototypes of 700 bar composite pressure cylinders.

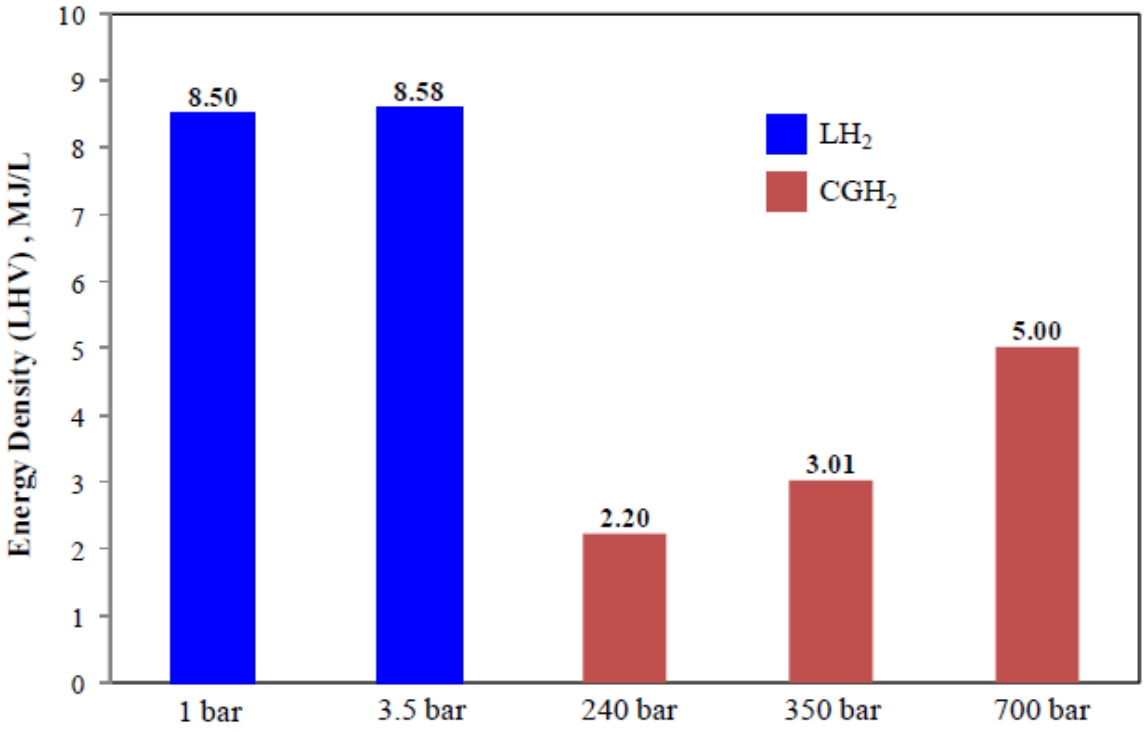

FIGURE 22 ENERGY DENSITY (LHV PER LITER OF STORAGE) IN LH_2 AND CGH_2 AT A DIFFERENT PRESSURES

Liquid hydrogen systems operate at low pressure and they are therefore light. The high density of LH_2 also results in high energy density (kWh/L). Liquid hydrogen vessels, however, proved to be too sensitive to environmental heat transfer, after a certain amount of time, some of the hydrogen will warm and change from its liquid state to a gaseous state. The time at which the vent pressure is reached and the gas cannot be contained within the LH_2 tank is called the dormancy or time to first venting (boil-off). General Motors estimates a boil-off rate of 4% per day for a 4.6 kg tank; in this case, the hydrogen would last for 25 days[21]. Heavy reliance on high performance insulation results in expensive and thick vacuum gaps that reduce system hydrogen storage density. While still potentially practical for large vehicles with low heat transfer rate per kg stored.

Filling LH_2 tanks from LH_2 storage is not a major challenge; however, the transfer lines must be cooled to liquid hydrogen temperature and lines must be provided to capture vented gas during filling to reduce boil-off losses. Refueling of LH_2 to CGH_2 storage onboard the vehicle requires both heat exchangers and a compressor and is thus more difficult and expensive than from high pressure gas storage at the station.

3.2 Material- based storage

Currently, material-based storage technologies include metal hydrides, sorbent-based materials, and chemical hydrogen storage materials. Complex and conventional metal hydrides store hydrogen in solid form where hydrogen atoms are chemically bonded to other metal or semimetal atoms through ionic, covalent, or metallic-type bonds. All sorbents, such as micro-porous activated carbons or metal-organic frameworks (MOF), generally share a common mechanism of utilizing the weak van der Waals bonding between molecular hydrogen and the sorbent (on the order of 1 to 10 kJ/mol H_2 for most sorbents), which results in the need for storage temperatures at or near that of liquid nitrogen (77 K). A third class of hydrogen storage materials are chemical hydrogen storage materials, which have the potential to contain large quantities of hydrogen by mass and volume on a material basis and can be prepared in either a solid or liquid form. These materials can be heated directly, passed through a catalyst-containing reactor, or combined with water (i.e., hydrolysis) or other reactants to produce hydrogen.

TABLE 3 OVERVIEW OF SOLID STORAGE OPTIONS

Carbon and other high surface area materials	Chemical hydrides (H_2O-reactive)
• Activated charcoals • Nanotubes • Graphite nanofibers • MOFs, Zeolites, etc. • Clathrate hydrates	• Encapsulated NaH • LiH & MgH_2 slurries • CaH_2, $LiAlH_4$, etc
Rechargable hydrides	**Chemical hydrites (thermal)**
• Alloy & intermetallics • Nanocrystalline • Complex	• Ammonia borozane • Aluminum hybride

Hydride hydrogen storage

Storage of hydrogen in solid materials has the potential to become a safe and efficient way to store energy, both for stationary and mobile applications.

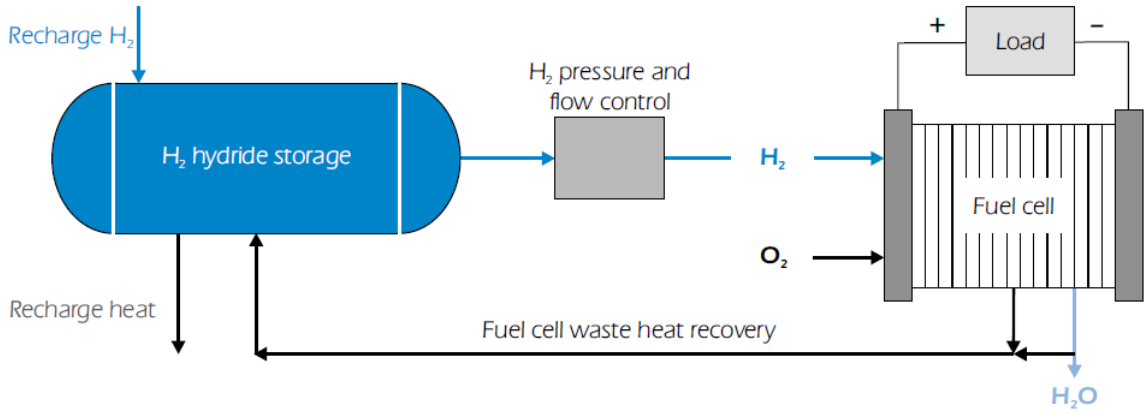

FIGURE 23 SCHEME OF A VEHICULAR HYDROGEN FUEL CELL SYSTEM USING SOME FORM OF HYDRITE STORAGE

There are a number of reversible hydrides that have been studied for hydrogen storage.

Figure 25 Mass and volume characteristics of various hydride materials are shown in Figure 25, and it clearly shows the theoretical potential of low volumetric densities for solid-state storage systems.

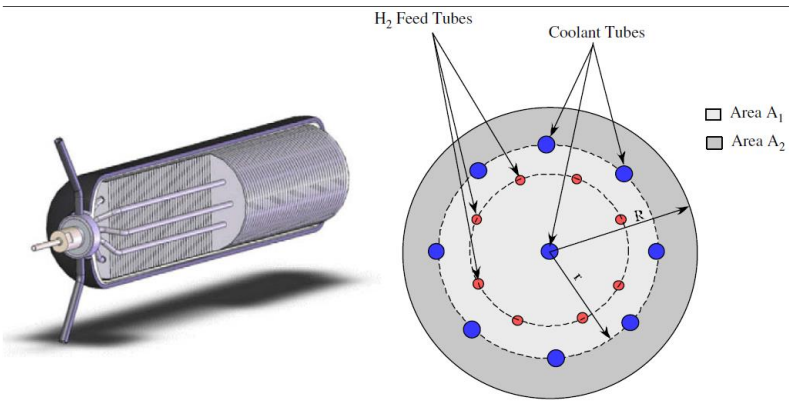

FIGURE 24 LEFT ILLUSTRATION IS A SHELL, TUBE AND FIN HYDRIDE BED CONFIGURATION. THE RIGHT ILLUSTRATION IS A CROSS-SECTION OF THE STORAGE SYSTEM.

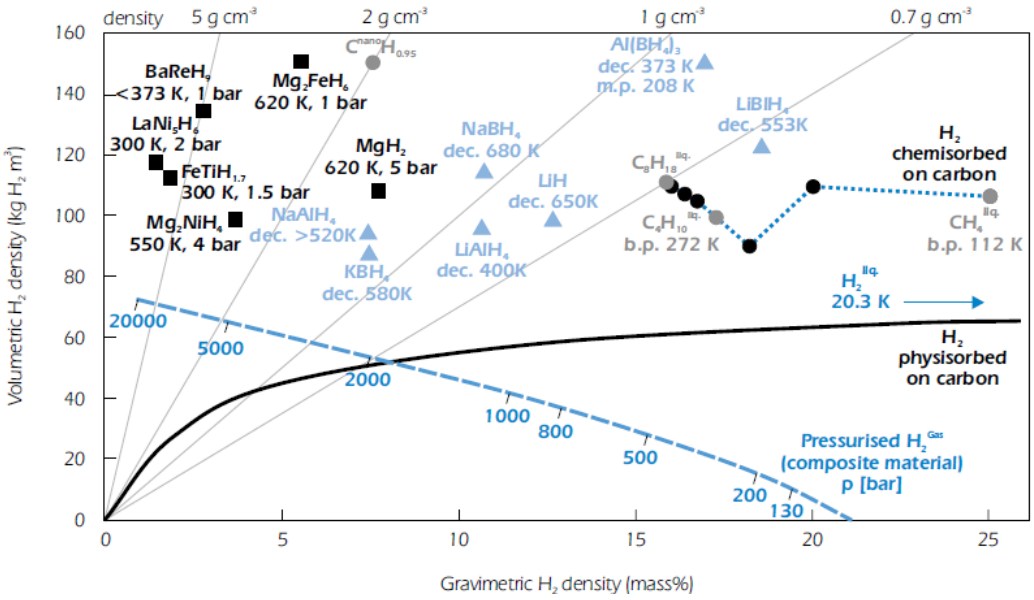

FIGURE 25 MASS AND VOLUME CHARACTERISTICS OF VARIOUS HYDRIDE MATERIALS

The simplest of the hydrides are the so-called metal or intermetallic hydrides such as LaNi and FeTi, which operate at relatively low temperatures near 100 °C and moderate pressures less than 100 bar. These hydrides have high volumetric hydrogen storage density (0.10-0.12 kgH_2/L), but store only a few percent (2-3wt%) hydrogen per unit weight of material. The result is relatively attractive system volumetric density and unattractive system gravimetric properties (kgH_2/kg system).

Higher gravimetric and volumetric storage densities can be attained using high temperature hydrides such as MgH_2 and $MgNiH_2$ which operate at 300-350 °C and at pressures as low as 5-10 bar. The metrics on a material basis for the high temperature hydrides are 3-8 wt.% and 0.13-0.15 kgH_2/L. These metrics, especially the wt %, are significantly better than the low temperature hydrides, but the high temperature requirement probably precludes their use in light-duty vehicles. In principle, higher wt % with hydrides can be attained using the alanates, which are combinations of alkali metals and aluminum. These are high temperature hydrides operating at 300-400 °C and relatively low pressures (less than 10 bar). At these conditions, the metrics for the alanates are 5-12 wt % and 8-12 kg H_2/L. The most studied of the alanates for hydrogen storage is $NaAlH_4$. It has been found that by doping it with a catalyst containing Ti and Zn compounds, the operating temperature of $NaAlH_4$ can be reduced to about 100 °C comparable to that of the

low temperature hydrides. The pressures are low being less than 10 atm. The metrics for the $NaAlH_4$ is 4-5wt% and .08 kgH_2/L. This material with the catalyst has been cycled (hydrogen adsorbed and desorbed) at relatively fast rates and cycle time is not thought to be a problem $NaAlH_4$ is considered to be one of the most promising hydrides because its wt% is 2 to 3 times higher than typical low temperature hydrides. The volumetric hydrogen storage (kgH_2/L) of $NaBH_4$ is lower than that of the low temperature hydrides, but in an acceptable range. It is also a relatively low cost material.

Another class of hydrides for storing hydrogen is the chemical hydrides, such as sodium borohydride ($NaBH_4$). These hydrides undergo a chemical reaction to release the hydrogen. In the case of $NaBH_4$, the hydride is mixed in solution with water and pumped through a chamber containing a catalyst to release the hydrogen. The reaction is exothermic generating about 35 kJ/ gm H_2. This corresponds to 35 MJ/kg H_2 which is 29% of the energy content of the hydrogen and indicates that cooling the reaction chamber will not be a simple matter. The $NaBH_4$ chemical contains 10 wt% hydrogen and in solution with water about 7 wt%.

The rate of hydrogen release is controlled by the flow rate of the $NaBH_4$ /water solution through the reaction chamber. Refueling involves removing the spent $NaBH_4$ as $NaBO_2$ and returning it to a processing plant to produce more $NaBH_4$. Providing a recycling infrastructure is one of the serious disadvantages of this approach to storing hydrogen. In addition, the reprocesses of the spent fuel is energy intensive as indicated by the high heat release when the $NaBH_4$ is reacted with the water to release the hydrogen. The round-trip efficiency of the formation/H_2 release processes will be less than 70%. The $NaBH_4$ system has been demonstrated by Millennium Cell [7] in two hydrogen fueled ICE vehicles and three fuel cell vehicles. This indicates that the system is technically feasible as far as operation in a vehicle is concerned.

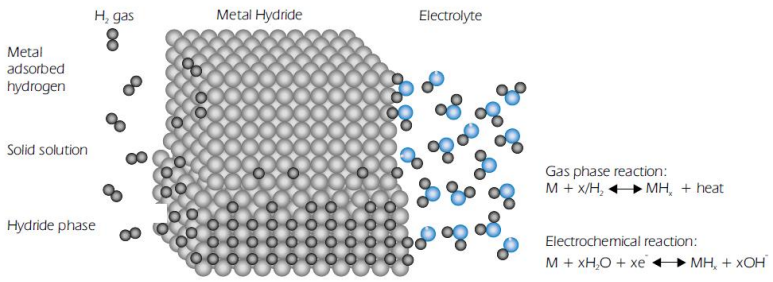

FIGURE 26 SCHEMATIC OF A RECHARGEABLE METAL HYDRITE BATTERY

Activated carbon based hydrogen storage and other high surface area materials

Carbon-based materials, such as nanotubes (Figure 27a-c) and graphite nanofibers (Figure 27d), have received a lot of attention in the research community and in the public press over the last decade.

The general consensus today is that the high H2-storage capacities (30-60 wt%) reported

a few years ago are impossible and were the result of measurement errors. Pure H_2 molecular physisorption has been clearly demonstrated, but is useful only at cryogenic temperatures (up to ca. 6 wt.% H_2), and extremely high surface area carbons are required. Pure atomic H-chemisorption has been demonstrated to ca. 8 wt.% H_2, but the covalent-bound H is liberated only at impractically high temperatures (above ca. 400 °C). Room temperature adsorption up to a few wt.% H_2 is occasionally reported, but has not been reproducible. This requires a new bonding mechanism with energies between physisorption and strong covalent chemisorption. The surface and bulk properties needed to achieve practical room temperature storage are not clearly understood, and it is far from certain that useful carbon can be economically and consistently synthesize. Hence, the potential for H2 storage in carbon-based materials is questionable, and some even suggest cessation of all research work in the area. A more moderate approach would be to continue carbon work for a limited additional time, say two years.

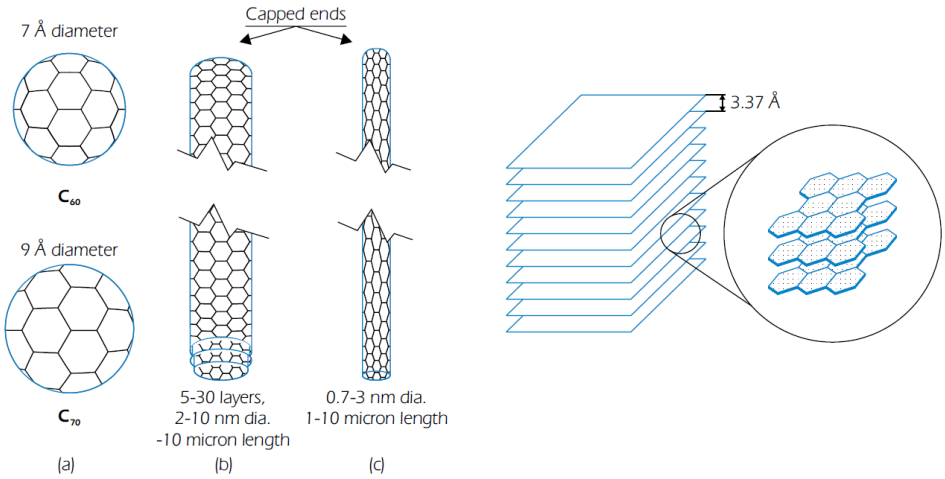

FIGURE 27 SCHEMATIC OF (A) FULLERENE CARBON BUCKYBALLS, (B) MULTI-WALL NANOTUBES, (C) SINGLE-WALL NANOTUBES

The most predominant examples of other high surface area materials are zeolites, metal oxide frameworks (MOFs) and clathrate hydrates. The definitions and main features for these materials are as follows:

- *Zeolites:* Complex aluminosilicates with engineered pore sizes and high surface areas. Well known as "molecular sieves". The science for capturing non-H_2 gases is well known.
- *Metal oxide frameworks (MOFs):* Typically, ZnO structures bridged with benzene rings. These materials have an extremely high surface area, are highly versatile and allow for many structural modifications.
- *Clathrate hydrates:* H_2O (ice) cage structures, often containing "guest" molecules such as CH_4 and CO_2. The cage size and structure can often be controlled by organic molecules (*e.g.* THF).

The materials are all characterized by extremely high surface areas that can physisorb molecular H_2. They have been shown to store a few wt.% H_2 at cryogenic temperatures. However, the main R&D question is whether they can be engineered to reversibly store high levels of H_2 near room temperature. These materials, particularly metal oxide frameworks and clathrate hydrates, represent new storage ideas and should be studied to determine the potential for the near future

Other hydrogen storage system (Glass Microspheres, Organic fluid sorption)

The basic concept for how glass microspheres can be used to store hydrogen gas onboard a vehicle can be described by three steps: charging, filling and discharging. First, hollow glass spheres are filled with H_2 at high pressure (350-700 bar) and high temperature (~300 °C) by permeation in a high-pressure vessel. Next, the microspheres are cooled down to room temperature and transferred to the low-pressure vehicle tank. Finally, the microspheres are heated to ca. 200-300 °C for controlled release of H_2 to run the vehicle (Figure 28).

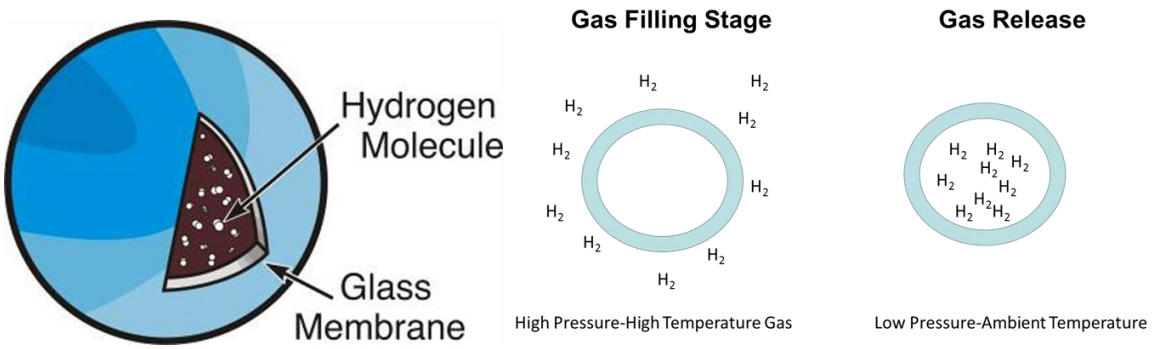

FIGURE 28 SCHEMATIC GLASS MEMBRANE HYDROGEN STORAGE AND WORKING CONCEPT

The main problem with glass microspheres is the inherently low volumetric density that can be achieved and the high pressure required for filling. The glass microspheres slowly leak hydrogen at ambient temperatures. Another practical challenge is that there is too much breakage during cycling.

The main operational challenge is the need to supply heat at temperatures higher than are available from the PEM fuel cell (ca. 70-80 °C). The high temperature required (ca. 300 °C) also makes rapid response-control difficult. However, there do exist some clear advantages. Glass microspheres have the potential to be inherently safe as they store H_2 at a relatively low pressure onboard and are suitable for conformable tanks. This allows for low container costs. The significant technical advantage is the demonstrated storage density of 5.4 wt.% H_2. R&D is needed to reduce the H_2 liberation temperatures to less than 100 °C for the microspheres[22]. A snapshot is showed in Figure 29.

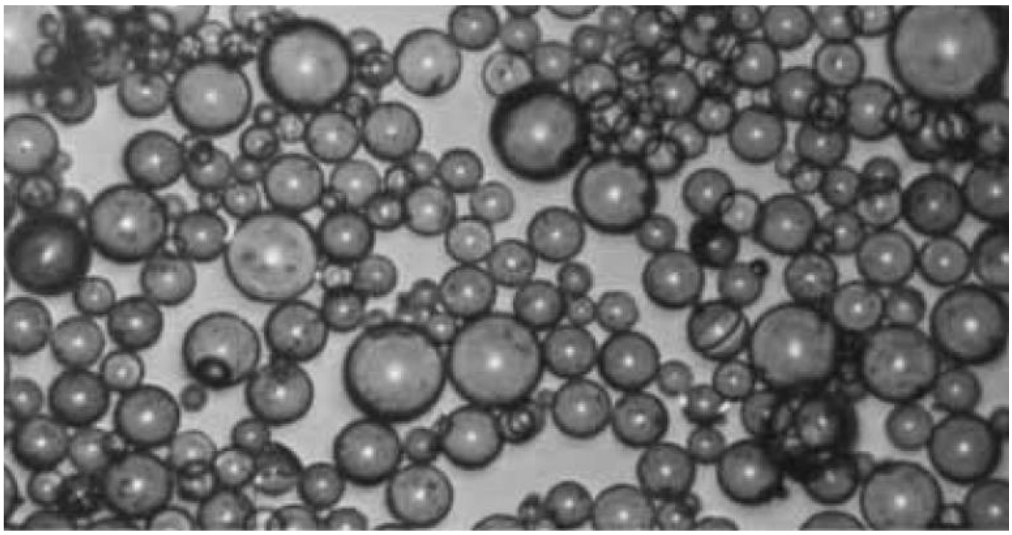

FIGURE 29 SNAPSHOT OF GLASS MICROSPHERES FOR HYDROGEN STORAGE

Some organic liquids can also be used to indirectly store hydrogen in liquid form. The following three steps summarize the basic concept. First, an organic liquid is dehydrogenated (in a catalytic process) to produce H_2 gas onboard. Second, the dehydrogenated product is transported from the vehicle tank to a central processing plant, while simultaneously refilling the tank with fresh H_2-rich liquid. Finally, the H_2-depleted liquid needs to be re-hydrogenated, brought back to the starting compound and returned to the filling station.
One example of a rechargeable organic liquid process is the dehydrogenation and hydrogenation of methylcyclohexane (C7H14) and toluene (C7H8).
Has to be noted that this solution may involve highly toxic chemical to work with, that must be handled with great care (methylcyclohexane is a clear colorless liquid that reacts violently with strong oxidants, causing fire and explosion hazards). This means that it is necessary to perform detailed safety and toxicity studies.

In Figure 30 (*A*) The volume of 4kg of hydrogen compacted in different ways, together with the weight of hydrogen storage material (note: weight and volume of a container are excluded). (*B*) At normal conditions, 4kg of hydrogen occupies a volume of 48M³, the volume of a medium size balloon are compared the volume mass of the different storage technologies and showed compared to a vehicle.

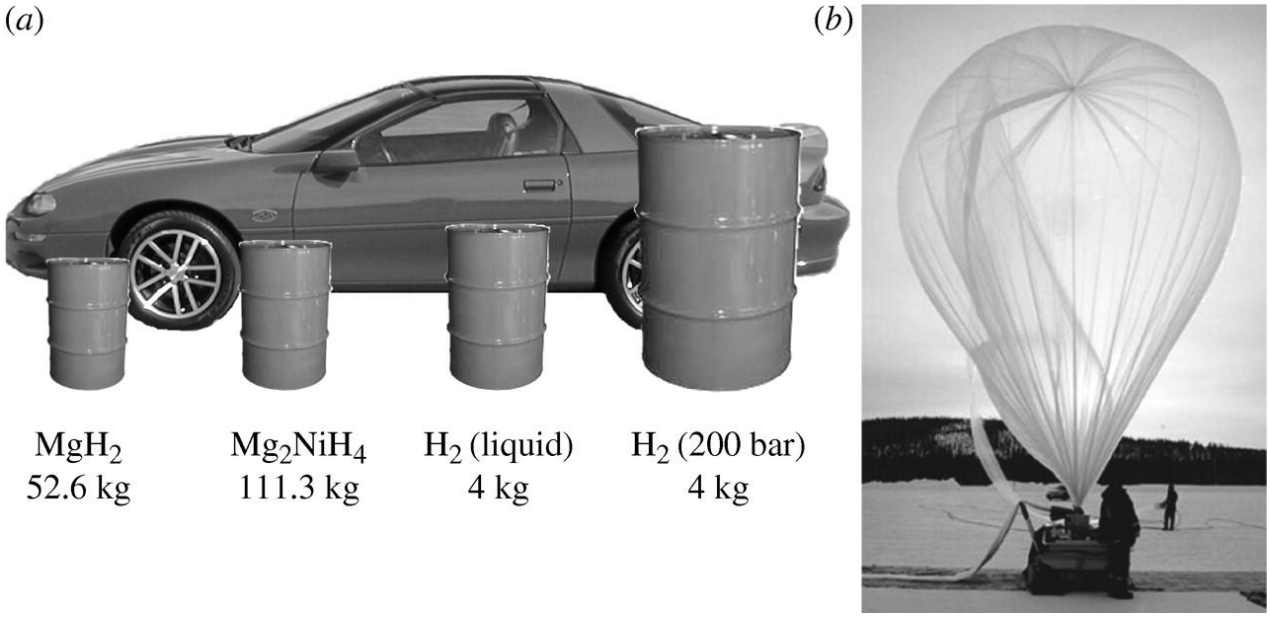

FIGURE 30 (*a*) THE VOLUME OF 4 KG OF HYDROGEN COMPACTED IN DIFFERENT WAYS, TOGETHER WITH THE WEIGHT OF HYDROGEN STORAGE MATERIAL (NOTE: WEIGHT AND

VOLUME OF A CONTAINER ARE EXCLUDED). (*b*) AT NORMAL CONDITIONS, 4 KG OF HYDROGEN OCCUPIES A VOLUME OF $48\,m^3$, THE VOLUME OF A MEDIUM SIZE BALLOON

4.HYDROGEN DELIVERY AND REFUELING STATION

Hydrogen fueling stations are the final component in the hydrogen delivery infrastructure. In contrast to conventional gas stations where gasoline is delivered by tanker trucks, hydrogen fuel can be either delivered by trucks, by hydrogen pipelines, or produced onsite at the fueling stations. In conventional (compressed or liquid) delivery scenarios, the fueling station is likely to account for 30-60% of the total hydrogen delivery cost, thus highlighting the need to properly evaluate and estimate the fueling station cost. The use of alternative carriers has the ability to significantly alter the design and required components at a hydrogen fueling station.

There are two basic types of hydrogen refueling station:

- Stations in which the hydrogen is made elsewhere and delivered to the station for local storage and dispensing to vehicles;
- Stations in which hydrogen is made on site, and then stored there ready for transfer to on-board hydrogen storage.

Some stations may be a combination of both types using delivered hydrogen to supplement on-site production as required.

4.1 Hydrogen distribution

The analysis of the above strategies needs to include all the stages necessary to produce and distribute the fuel for a widespread use, and should start from the following two options for hydrogen transport and distribution:

- A centralized management of the hydrogen production and distribution, corresponding to the existent energy production strategies;
- A distributed territorial production and utilization, for which H_2 is produced onsite at small–medium-scale filling station.

In Figure 31, the most significant fuel supply options are represented, evidencing individual steps concurring to the realization of each production–distribution chain.

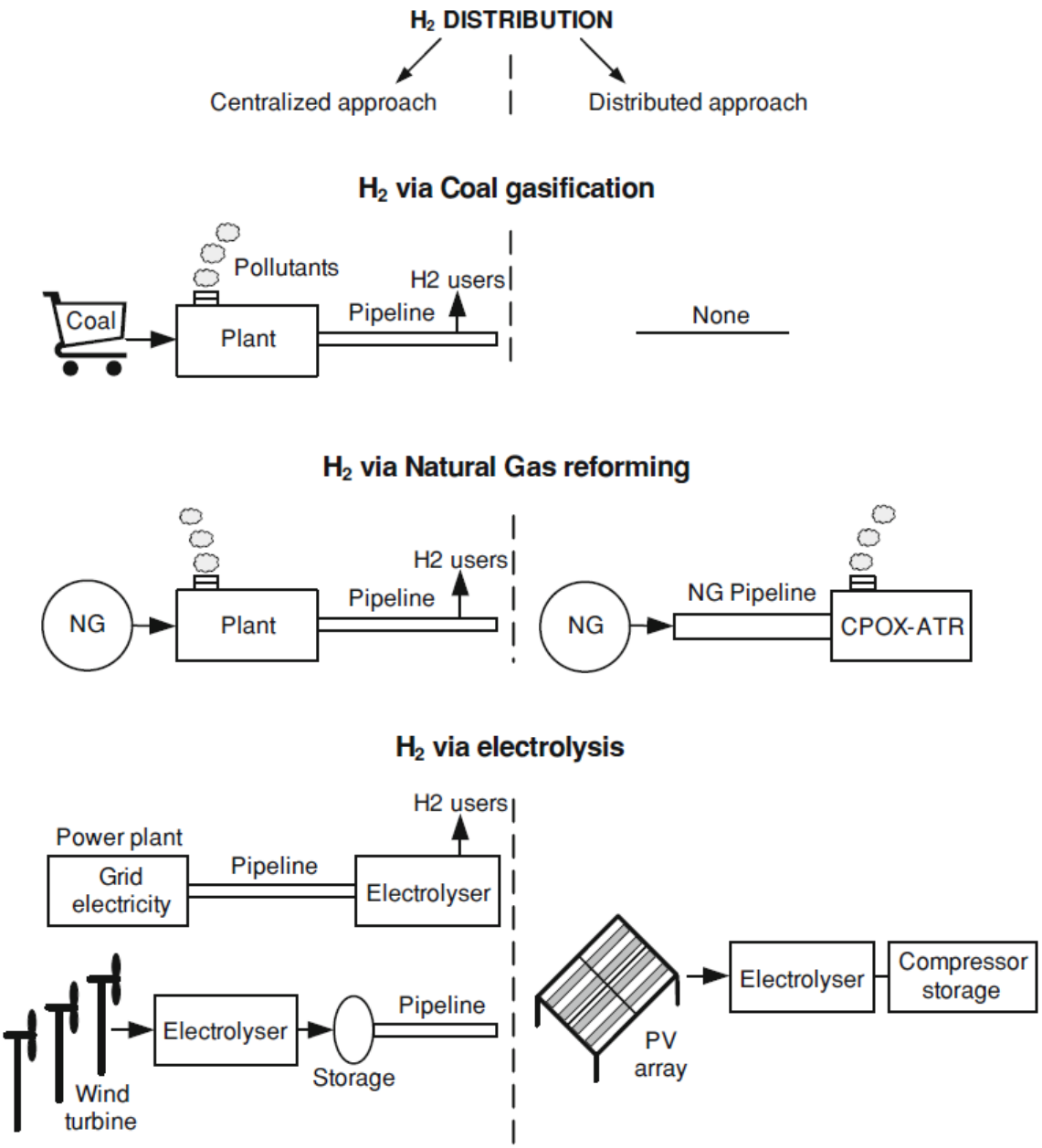

FIGURE 31 H2 SUPPLY OPTIONS IN CENTRALIZED AND DISTRIBUTED APPROACHES

Centralized hydrogen manufacture

Large-scale, industrial hydrogen production from all fossil energy sources can be considered a commercial technology for industrial purposes, though not yet for utilities. Hydrogen production at a large scale has the potential for relatively low unit costs, although the hydrogen production cost from natural gas in medium sized plants may be reduced towards the cost of large-scale production. An important challenge is to decarbonize the hydrogen production process. CO_2 capture and storage options are not fully technically and commercially proven.

A principle sketch of hydrogen distribution from a natural gas-based centralized hydrogen production plant is presented in Figure 32.

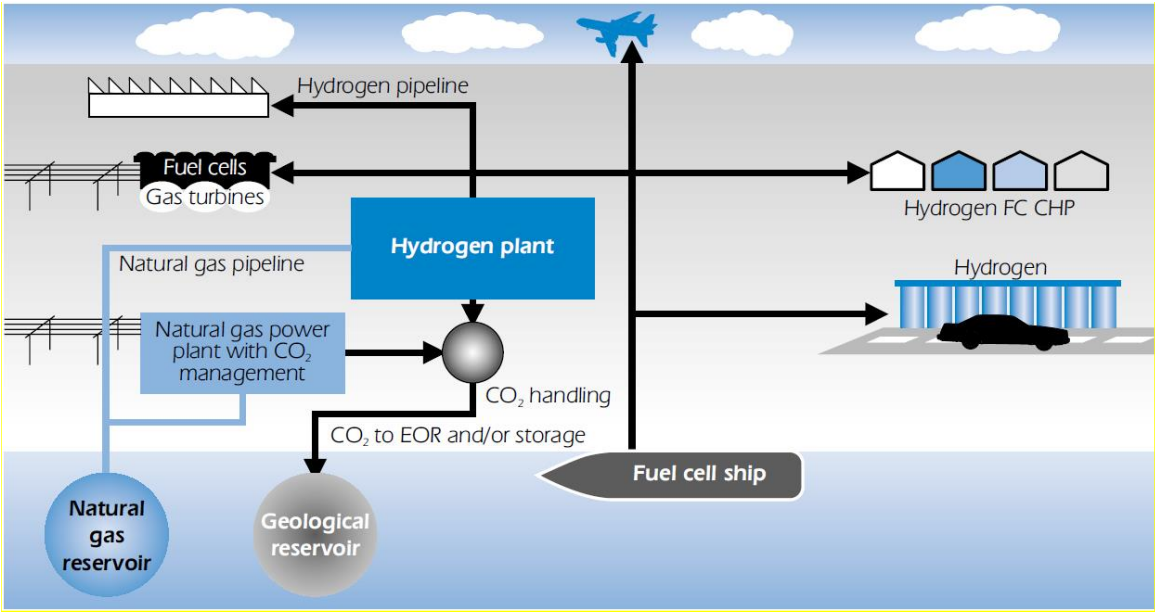

FIGURE 32 PRINCIPLE SKETCH FOR LARGE SCALE CENTRALISED HYDROGEN PRODUCTION

They require further researches on absorption or separation processes and process line-up, as well as acceptance for CO_2 storage. It is also important to increase plant efficiency, reduce capital costs and enhance reliability and operating flexibility.

Also, the processes of purification in order to have suitable hydrogen for fuell cells and on gas separation need to be further developed, especially in the sector of material science. Successful centralized hydrogen production requires large market

demand, as well as the construction of a new infrastructure to dinstribute the hydrogen and store the CO_2.

Distributed hydrogen manufacture

Distributed hydrogen production can be based on both water electrolysis (Figure 33) and the natural gas processes discussed above and then, when is generated, it will be transferred from the reformer or electrolyzer via a compressor to a compressed storage vessel. The benefit would be a reduced need for the transportation of hydrogen fuel, and hence less need for the construction of a new hydrogen infrastructure. Distributed production would also utilize existing infrastructure, such as natural gas or water and electric power. However, the production costs are higher for the smaller-capacity production facilities, and the efficiencies of production will probably be lower than those of centralized plants. In addition, carbon capture and sequestration would be more difficult and costly in small fossil-fueled plants. Also, it is unlikely that CO_2 from fossil fuels will be captured and stored when hydrogen is produced from distributed reformers.
Small-scale reformers will enable the use of existing natural gas pipelines for the production of hydrogen on-site. Such reformers therefore represent an important technology for the transition to a larger hydrogen supply. The availability of commercial reformers is limited and most reformers are currently in a researching stage.

FIGURE 33 HYDROGENICS HY-STAT A ALKALINE ELECTROLYSIS UNIT. THIS PACKAGED UNIT HAS AN INTEGRATED COMPRESSOR TO DELIVER HYDROGEN AT STORAGE PRESSURES.

4.2 Delivery systems

Hydrogen when produced through a centralized system, need to be delivered to the point of usage. There are different possibilities to deliver hydrogen, the three most common are:

- Liquid tanker truck, for liquid hydrogen (LH_2);
- Tube trailers truck, for compressed gas (CcH_2);
- Pipelines, for gas hydrogen.

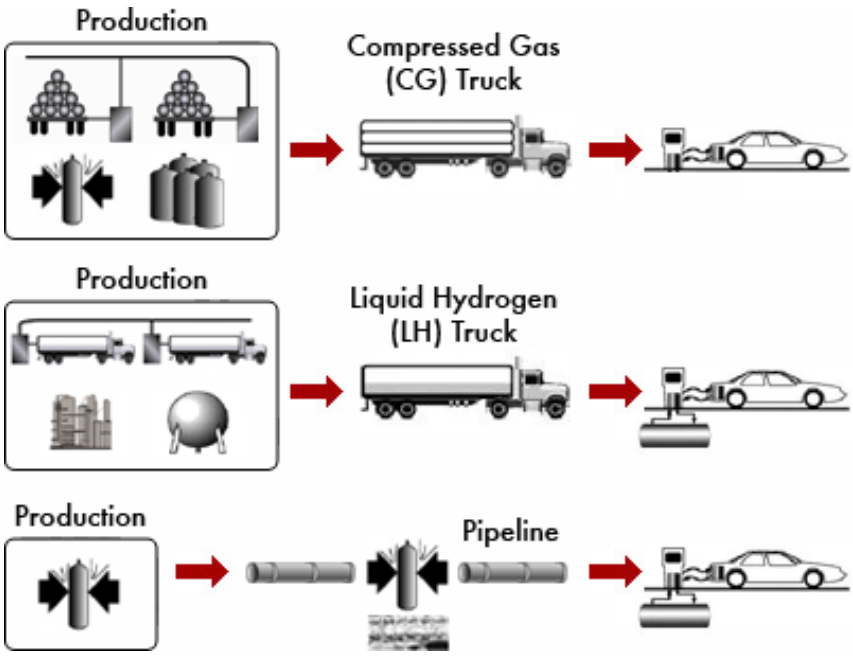

FIGURE 34 THREE PATHWAYS TO DELIVER HYDROGEN WHEN THE PRODUCTION IS OFF-SITE

Road liquid tanker transport

Cryogenic liquid hydrogen trailers (Figure 35) can carry up to 4,000 kg of hydrogen and operate at near atmospheric pressure. Some hydrogen boil-off can occur during transport despite the super-insulated design of these tankers, potentially on the order of 0.5% per day. Hydrogen boil-off of up to 5% also occurs when unloading the liquid hydrogen on delivery. If cost effective, a system could be installed to compress and recover the hydrogen boil-off during unloading if warranted. Based

on the economics of off-loading liquid hydrogen into a customer's tank (distance from source, driver hours, losses), most organizations plan deliveries to serve up to three customer sites.

FIGURE 35 CRYOGENIC LIQUID HYDROGEN TANKER TRUCK

It is estimated that merchant liquid hydrogen suppliers possess more than 140 liquid hydrogen trailers. Current markets include food processing; refineries; chemical processes; oil hydrogenation; and glass, electronics, and metals manufacturing.

Ship liquid hydrogen transportation

Hydrogen can be transported by sea over large distances as a liquid in tankers with cryogenic storages. Hydrogen ships are expected to be similar to the liquefied natural gas (LNG) ships that are widely used at present (Figure 36).

FIGURE 36 LIQUEFIED NATURAL GAS SHIP TRANSPORTATION

In particular, very high- grade insulation of tanks is required to maintain the very low temperatures needed to keep the hydrogen as a liquid (in the order of 20K). In addition, there is an opportunity to use some of the hydrogen carried as fuel for a fuel-cell powered ship. Kawasaki Heavy Industries Ltd (KHI) and Royal Dutch Shell will partner to develop technologies for transporting large volumes of liquefied hydrogen by sea. Liquefied hydrogen evaporates at a rate 10 times greater than LNG. To address this, the pioneering test vessel will employ a cargo containment system of a double shell structure for vacuum insulation, offering support that demonstrates excellent insulation performance and safety.

Kawasaki Heavy Industries aims to build the first distributed hydrogen energy ship to carry liquefied hydrogen as a demonstration by 2020. Currently the company has two conceptual designs for hydrogen tanker, spherical tank (Figure 37) and prismatic tank design (Figure 38). These are based on existing technologies for LNG tankers[23].

FIGURE 37 CONCEPTUAL DESIGN OF 160000 m^3 LH2 CARRIER SHIP

FIGURE 38 CONCEPTUAL DESIGN OF 2500 m^3 LH2 CARRIER SHIP

Compressed hydrogen tube trailer transport

Most existing hydrogen fueling stations dispense fuel from compressed gas canisters (Figure 39) that are delivered to the station.

The principle advantage of tube trailer delivery is that it avoids the high liquefaction energy cost and high pipeline investment costs that affect other delivery systems. Tube trailer fueling stations can be cheaper than other hydrogen fueling stations because the hydrogen is dispensed directly from the tube trailer that is dropped off at the station, so little on-site storage is required. Fueling stations tend to be small because a single tube trailer can store only 250–500 kg and it is impractical to replace the trailer several times each day.

FIGURE 39 TRUCK WITH TUBE TRAILER FOR COMPRESSED HYDROGEN DELIVERY

High costs are the principle disadvantages of tube trailer delivery, particularly for long-distance deliveries.

Tube trailers are currently limited by DOT (Department of Transportation) regulations to pressures at most as 250 bar. Further development and testing of Types II, III, or IV higher-pressure composite vessels for hydrogen (Figure 40), along with the development of appropriate codes and standards, will eventually allow the use of higher-pressure hydrogen tube trailers. Other approaches being researched for more cost-effective stationary gaseous hydrogen storage may also be applicable for transportation. This includes the use of cryo or cold gas and possibly the use of solid carriers in the tube vessels. With sufficient technology development

to minimize capital cost, high pressure composite tube trailers could dramatically decrease the cost of hydrogen transport via tube trailer by significantly increasing the carrying capacity.

FIGURE 40 NEW GENERATION OF TUBE TRAILER

Hydrogen leak detection, in the absence of odorizers, is a challenge. Currently, commercially available leak detection equipment is handheld. Ideally, an online leak detector (direct or indirect measurement) would be a desirable addition to a tube trailer. Improved monitoring and assessment of the structural integrity of tubes and appurtenances may be called for in the presence of higher containment pressures.

Gaseous hydrogen pipeline transport

Pipelines are the most efficient method of transporting large quantities of hydrogen, particularly over short distances. Almost 3000 km of hydrogen pipelines have been constructed since 1938 in Europe and North America. Transporting hydrogen through high-pressure steel pipelines (Figure 41) is more difficult than transporting methane because of hydrogen embrittlement, which makes strong steel pipes vulnerable to cracking, and because of hydrogen attack that allows reactions with the steel carbon atoms under certain operating conditions, again leading to cracks. Hydrogen has a lower energy density by volume than methane but a faster flow rate; this means that the total pipe capacity is around 20% lower for hydrogen than methane but the total hydrogen stored within the pipe is only a quarter of the total methane at the same pressure in energetic terms. Low-pressure hydrogen pipelines are not generally used for hydrogen except in a few niches, such as hospitals, town gas, a mixture of hydrogen and carbon monoxide, was delivered at low pressure to buildings across the UK for 150 years. There is much more flexibility over the choice of pipeline material at low pressures.

FIGURE 41 PIPELINE

Pipeline investment costs can be split into four main categories: materials, labor, right-of-way fees and miscellaneous. Only the material costs are likely to differ from pipelines used for methane. One method is to estimate the cost as the equivalent methane pipeline cost + 20%. Pipeline costs are affected by the diameter but also crucially by the topography, land use and labor costs as shown; for instance, urban area are the most expensive.

4.3 Hydrogen Fueling Station

Hydrogen is delivered to customers at fueling stations. Stations can be split into two broad categories, according to whether the hydrogen is stored in liquid or gaseous form.

LH_2 is substantially cheaper to store than GH_2 because it has a much greater volumetric energy density and can be stored in a single tank, but fuel losses are higher due to boil-off (at temperatures above −253 °C). Hydrogen liquefaction is expensive so LH_2 storage would only be economically-viable if the hydrogen were being delivered by LH_2 tanker. For GH_2 delivery or on-site generation, gaseous storage is cheaper because customers require high-pressure GH_2 for fuel cell vehicles. LH_2 and CGH_2 are three and six times less dense than petrol, respectively, so both types of station will require more physical space and more equipment than is deployed at current petrol stations to supply the equivalent amount of fuel. This difference will be partially reduced by the higher efficiency of fuel cell vehicles relative to ICEs.

Little storage is required for continuous GH_2 pipeline deliveries but bi-weekly LH_2 tanker deliveries would require a large LH_2 storage tank. Space limitations are likely to be most acute for stations with on-site hydrogen production. Current petrol fueling stations are not suitable for hydrogen delivery and would have to be completely rebuilt. Storing hydrogen at high pressure allows drivers of hydrogen vehicles, to fuel their tanks in about the same time as for gasoline vehicles, that is, in three to five minutes. The process of refueling vehicles with hydrogen is similar to filling a vehicle with compressed natural gas or propane and the sound is similar to that produced when blowing up a car tire with compressed air.

Both types of fueling station would require substantial capital investments. The small stations have a throughput of approximately 500 kg/day, while large stations deliver around 1500 kg/day. The cost variability in the literature mostly results from three factors: (i) the design of the station (primarily the amount of on-site storage and the deployment of spare compressors to ensure high station availability); (ii) the cost of each station component; and, (iii) the assumed utilization factor of the station.

FIGURE 42 SHELL HYDROGEN STATION IN WASHINGTON D.C.

Despite the many variations on station design, most stations contain the following pieces of hardware:

- Hydrogen production equipment (e.g. electrolyzer, steam-reformer) (if hydrogen is produced on-site) or a receiving port, used to receive compressed or liquid hydrogen from a tanker or pipeline when delivered;

- Purification system: purifies gas to acceptable purity for use in hydrogen vehicles;
- Storage vessels (liquid or gaseous);
- Heat exchangers to heat the liquid hydrogen and change it to a gas before it is compressed;
- Compressor: compresses hydrogen gas to achieve high pressure abov 350-700 bar for fueling and minimize storage volume;
- Dispensers taking high-pressure hydrogen from storage tanks and filling the on-board high-pressure hydrogen tanks of hydrogen vehicles usually through 350- or 700 bar nozzles;
- Safety equipment (e.g. vent stack, fencing, bollards);
- Mechanical equipment (e.g. underground piping, valves);
- Electrical equipment (e.g. control panels, high-voltage connections).

Stations typically have the following recurring operating expenses: equipment maintenance, labor (station operator), feedstock costs (e.g. natural gas, methanol, electricity, delivered hydrogen), insurance, and rent.
It is important for station economic analyses to include all of these capital and operating costs when evaluating hydrogen production costs. Many analyses in the existing body of literature omit some of these; particularly costs associated with permitting and site preparation.

Compressed gas hydrogen refueling station

As seen compressed gas can be delivered by trailer trucks or pipelines, typical schematics of the two categories of fueling station are shown in Figure 43 in and Figure 44 .

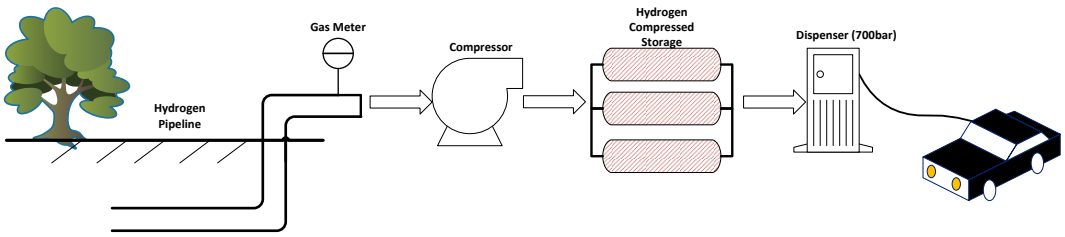

FIGURE 43 SCHEME OF A TYPICAL HYDROGEN REFUELING STATION WITH PIPELINE GH_2 DELIVERY

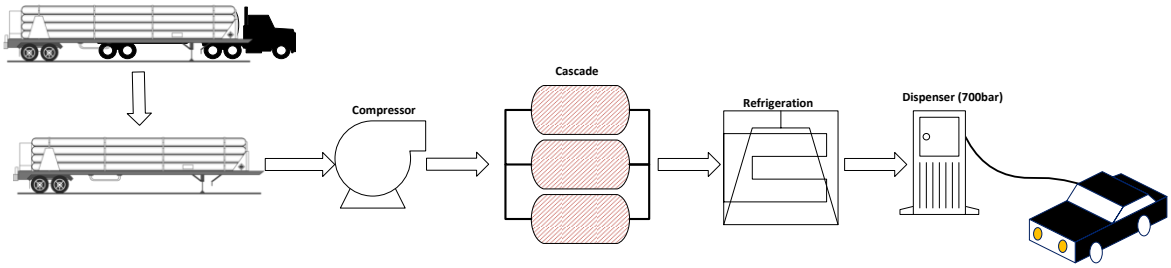

FIGURE 44 SCHEME OF A TYPICAL HYDROGEN REFUELING STATION WITH CCH2 DELIVERY AND STORAGE

For pipeline supply, the compressor operates in one of two modes[24]:

1. During periods of low station demand, it brings 20 bar hydrogen from the distribution pipeline to 170 bar for input to the fuel storage unit;
2. During periods of high station demand, it draws from both the distribution pipeline and the fuel storage unit to deliver higher pressure hydrogen to the cascade charging system.

For compressed gas tube-trailer truck supply, the compressor draws hydrogen from the tube-trailer, and delivers it to the cascade charging system. A high-pressure electrically powered compressor plus a hydrogen pressure booster is used to pressurize the hydrogen up to 875 bar for storage in high-pressure tanks. To transfer

and distribute hydrogen between components, suitably manufactured materials, pipes, valves and elements should be used to avoid any failure in the system that can be caused by direct contact with hydrogen. Compressed hydrogen is conveyed at high pressure (current standard 170–200bar) in containers that are resistant to hydrogen embrittlement.

Liquid hydrogen refueling station

The current LH_2 fueling stations (Figure 45) store liquid hydrogen in a large liquid Dewar, then the hydrogen is vaporized a pressure close to ambient, and then compressed. To downsize the compressor is normally present a cascade charging system typically comprising three vessels. Can be present also a booster compressor for the refueling process, this permits to use a cheaper cascade rated for lower pressure. It is necessary also a refrigerator to be able to refill a -40°C[25] limiting the heat due to the rapid refill process.

For stations dispensing less than 20% of a liquid tanker truck load (approximately 800 kg/day) cryogenic liquid tanks are sized to store a third of a tanker's load (approximately 1300 kg); for larger stations, on-site storage tanks are sized to satisfy 150% of average daily demand.

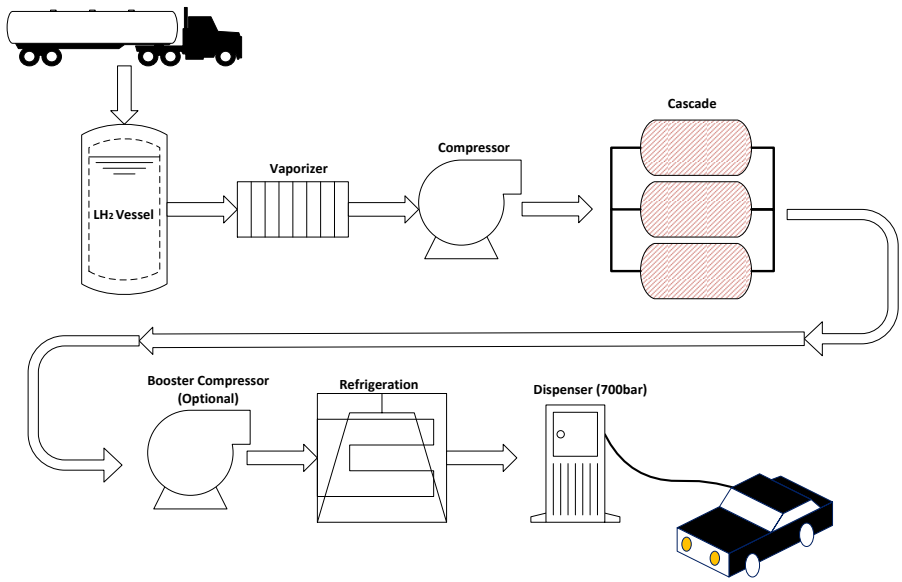

FIGURE 45 SCHEME OF A TYPICAL HYDROGEN REFUELING STATION WITH LH2 DELIVERY AND STORAGE

Mobile refueling station

Mobile refuelers deliver hydrogen storage tanks to a fueling site where they are stationed temporarily (Figure 46). This method is commonly used temporarily for fueling stations that are under construction or for short term events.

A number of companies have developed flexible refuelers which can be deployed on a customer's own facility and moved if required. These fuelers include built in compressors, ready to be connected up to a source of hydrogen (delivered cylinders or generated onsite).
These relatively low cost solutions are relevant for small fleet trials and demonstration projects[26].

FIGURE 46 MOBILE HYDROGEN REFUELING STATION

Station fuel demand

Much like gasoline stations, hydrogen stations will experience seasonal demand. Summer demand is assumed in HDSAM to be approximately 10% higher than the average demand whereas winter demand is 10% lower. During early infrastructure

development especially, a long-term storage system will be needed to store the 10% production excess in production during the winter for release to supplement production in the summer months[27]. Figure 6.3.1 shows the annual schedule of production and demand used in the H2A models.

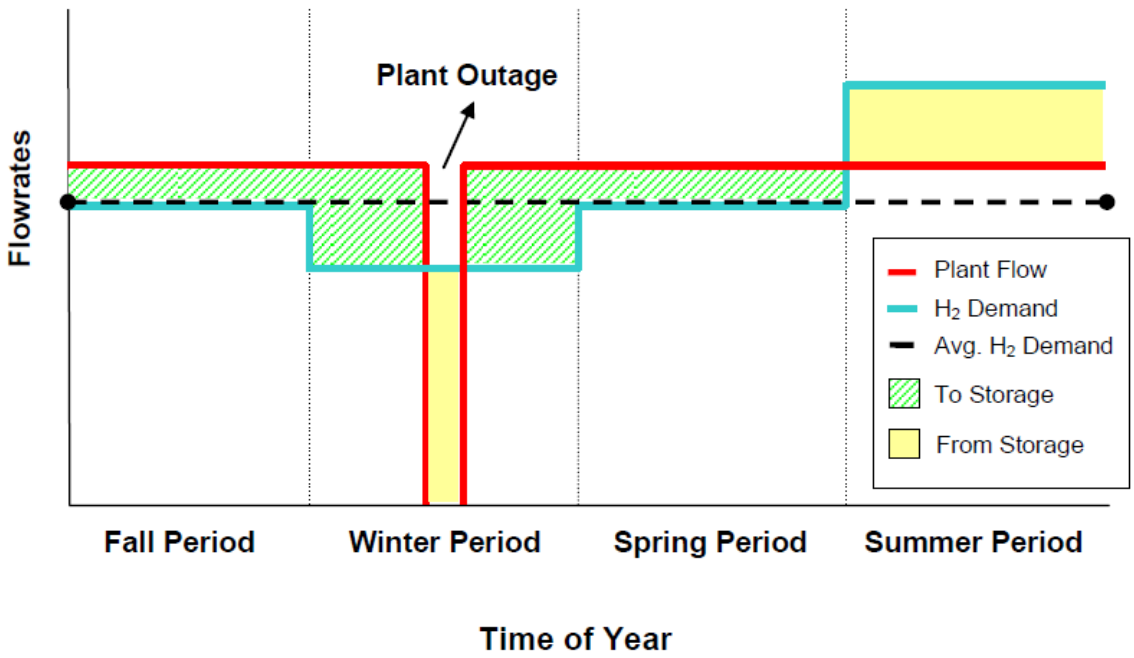

FIGURE 47 SEASONAL VARIATION IN PRODUCTION PLANTS AND STORAGE OPERATION

Addition to seasonal demand, demand variation occurs daily during the week (Figure 48) as well as hourly during the day. Friday demand is approximately 8% above average daily demand.

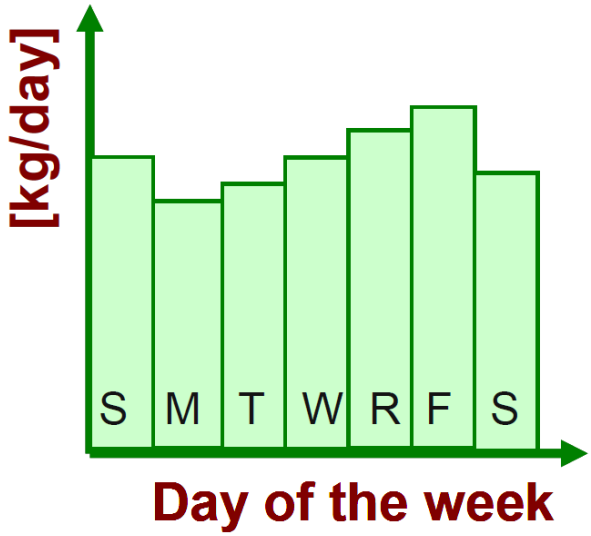

FIGURE 48WEEKLY DISTRIBUTION OF FUEL TRANSACTION OR "FILLS"

Peak demand occurs on Fridays between 4:00 and 6:00 p.m.[27] and is approximately 87% above Friday's average hourly demand. Figure 49 shows the hourly Friday demand profile at a refueling station over 24 hours. The area under the curve above the daily average hourly demand represents the minimum storage requirement to satisfy the station demand during peak hours (approximately 30% of daily demand).

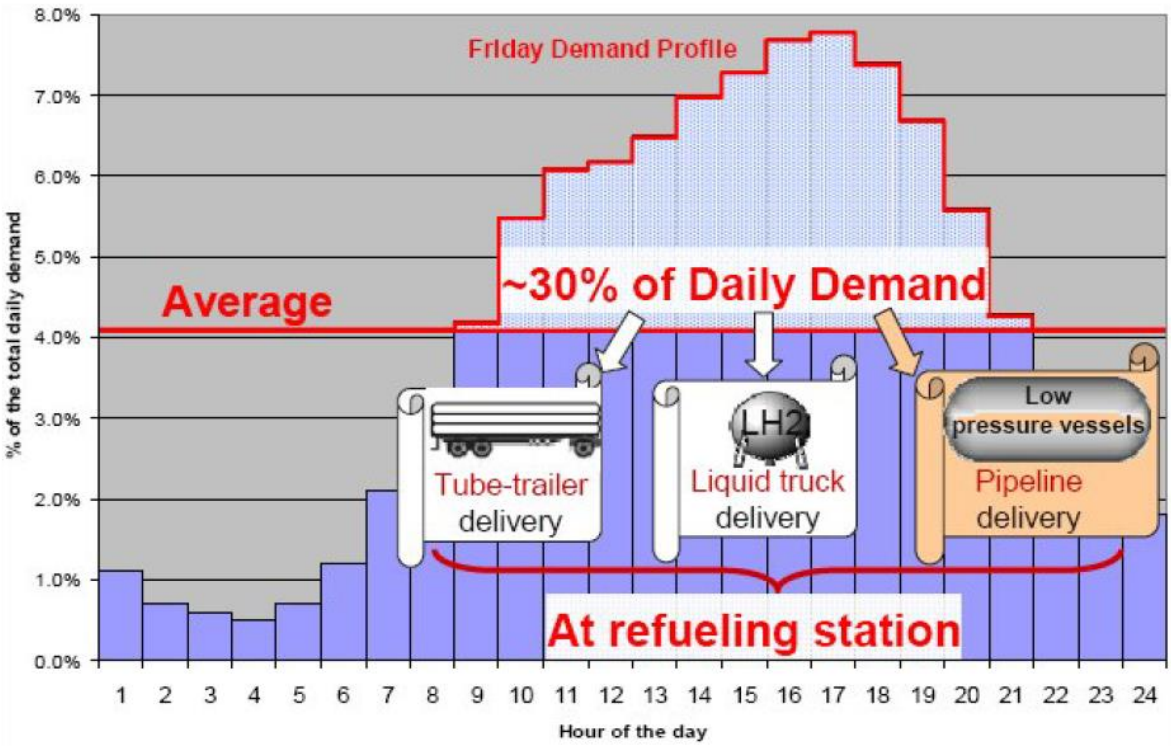

FIGURE 49 HYDROGEN DAILY AVERAGE DEMAND

The refueling site is the best location to handle daily and hourly fluctuations in demand and as stated above, pipeline distribution requires low pressure storage to absorb the difference between the steady supply rate from the production plant (via the pipeline) and hourly variations in refueling demand. To satisfy these two peaks, as well as the possibility that all hoses will be occupied for the first few minutes of the peak hour, low pressure storage equivalent to at least one-third of average daily demand is required at the refueling station.

For liquid trucks, the liquid storage tank would satisfy the increase in additional storage. Because truck deliveries do not exceed two deliveries per day, the truck would carry half the daily demand plus the 30% excess.

The number of dispensers is determined by the metric utilized in gasoline stations known as hose-occupied fraction (HOF). The HOF is the average fraction of time that each hose is occupied during the peak hour of the day. By determining the HOF of a gasoline station, the number of dispensers at a hydrogen station can be selected such that the HOF is approximately equal to that of a gasoline station

5. COMPRESSOR-LESS THERMAL COMPRESSION LH_2 REFUELING STATION: PHYSICAL MODEL AND TANK DESIGN

The LH_2 path is often considered too expensive due to the high energy necessary for the liquefaction, in fact to produce liquid hydrogen is required about 3 times[28] the energy necessary to produce hydrogen gas. On the other hand, the delivery of liquid hydrogen presents the advantage to be less energy consuming than delivering gas. Recent studies have shown that the total cost of the liquid path is comparable to the CcH_2 one[29], this because: the LH_2 trucks have larger capacities , reducing capital and drivers costs; LH_2 can be stored at the station into inexpensive Dewars and the transfer of liquid hydrogen into the delivery trucks it is easier (in Table 4 is shown the comparison).

TABLE 4 COMPARISON BETWEEN THE TWO PATH TO DELIVER HYDROGEN: LH_2 DELIVERY TRUCKS AND CH_2 TUBE TRAILER DELIVERY TRUCKS

	Liquid Hydrogen	**Tube Trailer Compressed Hydrogen (250 bar)**
Hydrogen delivered, kg[29]	4000	550
Equivalent number of filled H_2 vehicles*	~870	~120
Capital cost per kg H_2 capacity[29]	$160	$950
Loading time per truck (seconds/kg H_2)	2h(1.6s/kg)	6h(40s/kg)

* Assuming the average mass to refill a vehicle is 4.6 kg.

Figure 50 obtained through the HDSAM tool, shows the influence of each part of the process to the final price of the dispensed hydrogen in a refueling station with liquid and compressed hydrogen storage.

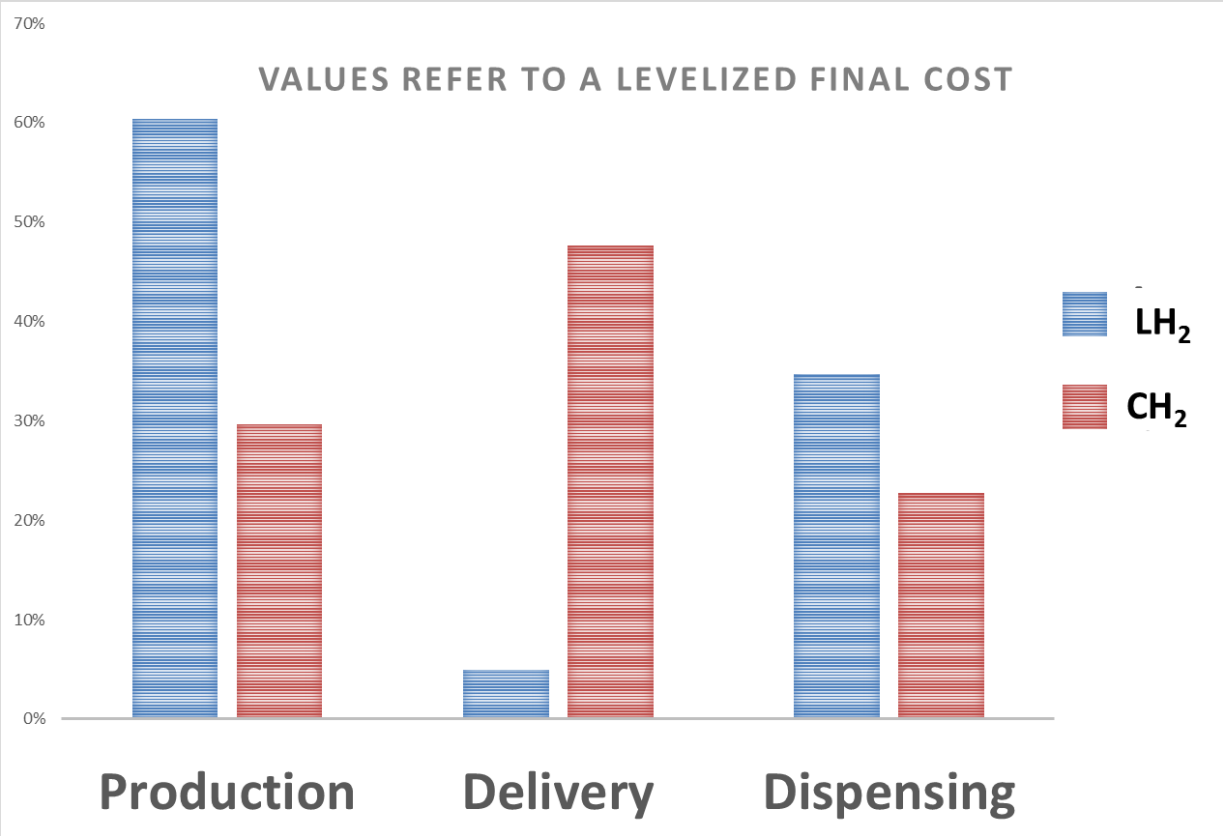

FIGURE 50 PERCENTAGE IN THE FINAL COST INFLUENCE OF PRODUCTION, DELIVERY AND DISPENSING CH_2 VS. LH_2 REFUELING STATION. THE COSTS CONSIDERED ARE FOR A STEAM METHANE REFORMING PRODUCTION PLANT

The refueling station investment impacts for a 35% on a refueling station with liquid hydrogen storage, this means that reducing the cost of the station is a key element for a reduction of the overall price. Figure 51, also obtained through the HDSAM tool, shows the breakdown of the station costs. It is clear that the compressor is the most expensive component, almost half of the cost of the station, being able to avoid to use a mechanical compression would be then reflected on significant save of money.

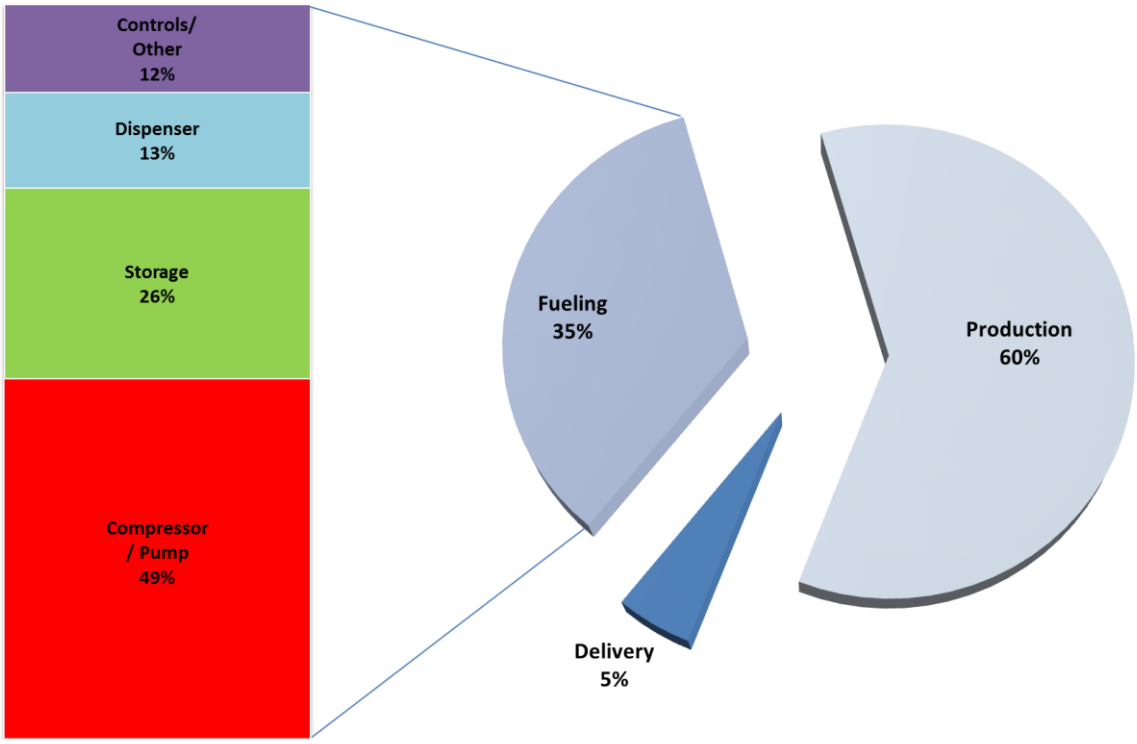

FIGURE 51 COST BREAK DOWN LH_2-CcH_2 REFUELING STATION

TABLE 5 CAPITAL COST CONTRIBUTION TO THE LIQUID REFUELING STATION OF THE DELIVERED REAL LEVELIZED HYDROGEN COST ($/KG OF HYDROGEN)		
	Cost	
Dispenser	$0.82	
Storage	$1.66	**Source H2A**
Compressor	$3.15	[30]
Electrical	$0.23	
Controls/other	$0.52	
	TOTAL	$6.38

The stations using liquid hydrogen storage with the standard design shown in Figure 45, waste LH_2's thermomechanical exergy trough the low pressure evaporation. The exergy, that represents the maximum useful work possible during a process that brings the system into equilibrium with the environmental conditions of pressure and temperature; while negligible for fuel as gasoline and diesel, for the LH_2 represents the 10.4% of the lower heating value (LHV) of hydrogen[31].

To take advantages of this exergy, can be used the concept of thermal compression LH_2 station. This was developed at Lawrence Livermore National Laboratory[32] and has a great potential for capital cost reduction by making a better use of the thermo-mechanical exergy of liquid H_2. This kind of station that is schematically shown in Figure 52, does not need to have either compressors that as we have previously seen is the most expensive element of the station and moreover need many hours of maintenance; averagely each month are require three maintenance events that count 12 hours total with 158kg hydrogen dispensed for the maintenance[33].

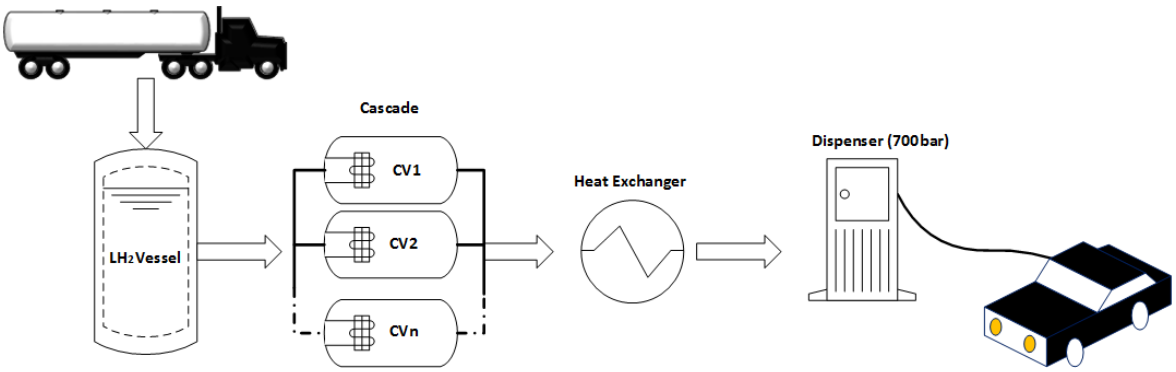

FIGURE 52 SCHEMATIC THERMAL-COMPRESSION COMPRESSOR LESS REFUELING STATION

In a LH_2 thermal compression station liquid hydrogen from the Dewar fills the cascade that is consequently pressurized by in-tank heat exchanger; when fully pressurized the dispensing process can start. Before to flow into the vehicle tank the cold hydrogen extracted from the cascade passes through another heat exchanger to further heat the hydrogen and reach the required -40°C[25].

The simplification of not having expensive and as seen maintenance-prone compressors has actually the drawback of potential H_2 evaporative losses during the cascade's refueling process.

Compressor-less thermal compression fueling stations, present other advantages compared to the standard design:

- A 350 bar mechanical compression station delivers only 350 bar H_2, while the thermal compression station dispenses both 350 and 700 bar H_2;
- Maintenance and electricity consumption at the station are minimum: no mechanical components are required, aside from vessels and valves;
- Thermal compression stations are intrinsically modular and offer capacity flexibility: the refueling station capacity can be increased as the demand expands by adding extra vessels in the cascade.

The aim of this study is to understand how the several design variables of the problem impact the hydrogen losses and the capital cost. The optimization work has been done writing a code with the language Fortran 90, the fluid real gas equation of states have been simulated using the subroutines from REFPROP 9.1[34], and the capital, operation and maintenance, and energy costs have been estimated using the HDSAM tool[30]. This has been addressed to find the right combination of the influence parameters, design and mode of use in order reduce of the overall refueling station cost, and more particularly explore the trade-offs between capital (size and ratings of the cascade) and energy costs (boil-off and heat input).

5.1 Description of the compressor-less thermal compression concept

The station consists of a stationary low pressure Dewar where liquid hydrogen is stored, a cascade of insulated high pressure vessels, heat exchangers and a dispenser.

The operation mode can be synthetized in 5 steps shown in Figure 53. Figure 54 shows the trend of temperature and density for a cryogenic vessel of the cascade during an entire cycle.

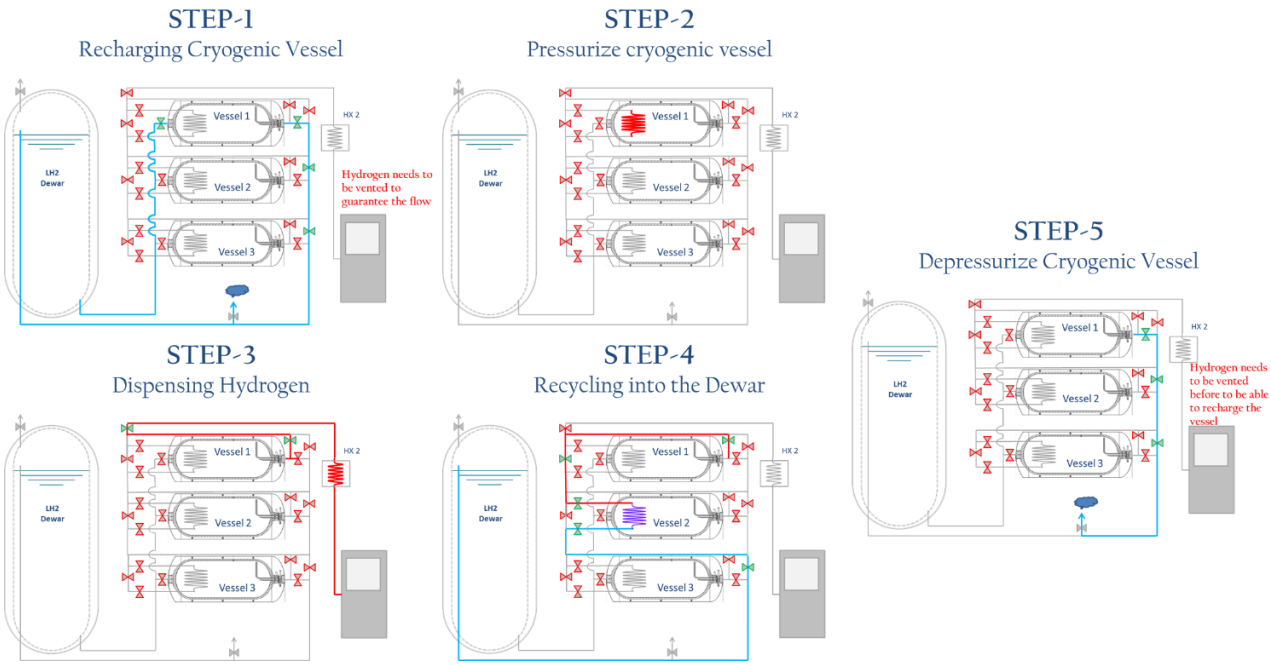

FIGURE 53 OPERATIONAL CONFIGURATION THERMAL-COMPRESSION COMPRESSOR LESS LH_2 REFUELING STATION

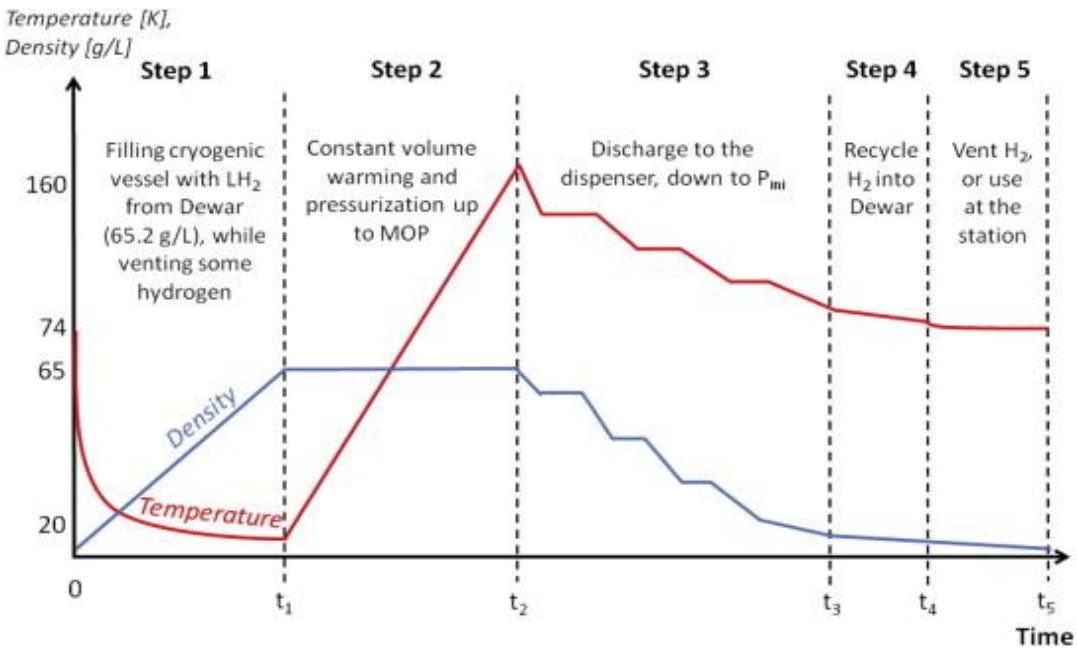

FIGURE 54 CYCLE OF CHARGING-DISCHARGING FOR A CRYOGENIC VESSEL OF THE CASCADE. REFERS TO A STATION THAT DISPENSES VEHICLES WITH 700 BAR TANK AND COME WITH 90 BAR INITIAL PRESSURE, SO THE MINIMUM PRESSURE OF DISCHARGE WILL BE 91.4 BAR CONSIDERING 1.4 BAR OF PRESSURE DROP ALONG THE HOSE AND DISPENSER

Step 1: Recharging of the cascade from the Dewar

Here the liquid hydrogen is taken from the Dewar and transferred for natural difference of pressure into the cascade. To guarantee the flow of hydrogen we have to make sure that the difference of pressure is maintained above a certain minimum level, and to do that we need to vent some of the hydrogen (boil-off). The recharging process continues until we have the cryogenic vessel completely full of liquid hydrogen, allowing to reach the maximum density.

This process is the most delicate to simulate because the fluid conditions, especially the quality, inside the cryogenic vessel are varying with the advancement of the process.

As shown in Figure 55, inside the vessel the cold liquid hydrogen that comes from the Dewar at the beginning finds a warmer environment, so it rapidly vaporizes reaching super-heated conditions and causing a fast increase of pressure inside the vessel. Venting some vapor hydrogen is therefore necessary in order to guarantee the continuity of the hydrogen flow, otherwise the process would stop and without one way valves, could even occur that the heated hydrogen would flow back into the Dewar warming this up, activating the safety vent valve wasting additional fluid. Continuing, the overall quality decreases because the fluid filled is liquid hydrogen, so the system moves toward saturated conditions. After a while indeed, under certain conditions the liquid hydrogen does not evaporate completely anymore. And yet, it starts to condense part of the hydrogen that had previously evaporated. We can observe a pressure drop. This phenomena is due to the vapor condensation, that occupies a smaller volume and being in a sealed ambient causes an expansion on the remaining part of super-heated vapor. Also the flow of vented hydrogen drastically decreases or can even stop if the pressure drops enough to guarantee the flow, not activating the vent valve. This effect continues until we reach overall saturated conditions (saturated vapor quality=1). At this point the liquid that goes inside the cryogenic vessel, keeps condensing the vapor, but now the system is in two-phase conditions, hence the vapor that condenses it is negligible as compared to the liquid that goes in and the pressure increases again, so some venting is necessary. The process goes on until the cryogenic vessel reaches its maximum capacity (i.e. maximum density based in the saturated pressure of the Dewar).

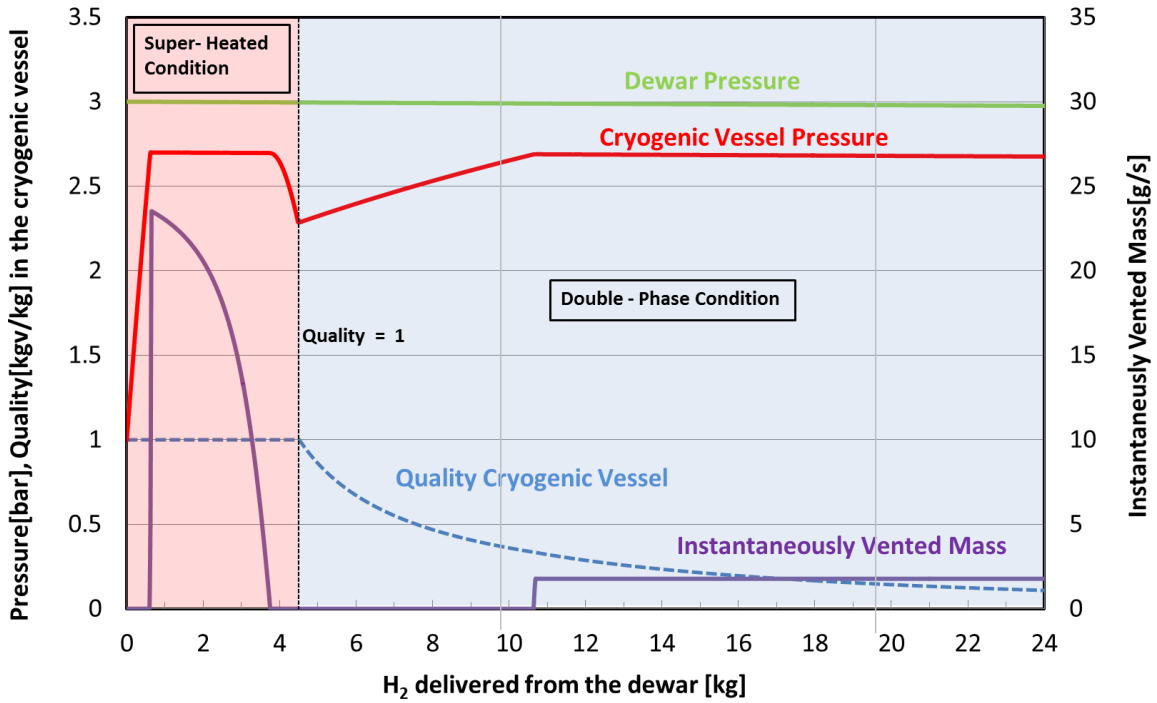

FIGURE 55 TREND PRESSURE AND VENTING DURING THE STEP 1 (RECHARGE CRYOGENIC VESSEL). THE RED LINE SHOW THE PRESSURE TREND INSIDE OF THE CRYOGENIC VESSEL, WHILE THE GREEN ONE INDICATE THE PRESSURE IN THE DEWAR, THE DOTTED BLUE LINE INDICATES THE OVERALL QUALITY OF THE HYDROGEN INSIDE THE CRYOGENIC VESSEL, AS SHOWN AT THE BEGINNING IS SUPER-HEATED THEN BE-PHASE WITH DECREASING QUALITY. THE PURPLE LINE SHOWS THE MASS OF HYDROGEN THAT NEEDS TO BE VENTED IN CORRESPONDENCE OF THAT TIME TO GUARANTEE THE FLOW CONTINUOUSLY WITHOUT INTERRUPTIONS

Step 2: Warm up of the full cryogenic vessels

With the in-tank heat exchanger, the cryogenic vessels of the cascade are warmed up until reaching the operative pressure condition, between 700 and 900 bar. We can obtain this result in different ways (e.g. with an electrical resistance), but this could be an expensive solution, therefore a good choice could be to exploit the hydrogen being dispensed to the vehicles as thermal energy carrier. This solution eliminates the need of recirculating pumps, since the pressure inside the cryogenic vessel drives the process. Use of hydrogen also eliminates the risk of tube blockage due to the freezing that might happen when utilizing fluids different from hydrogen or helium due to the low operative temperature (down to 25 K).

Step 3: Refueling vehicles

During that step, the hydrogen flows from the pressure vessels in the cascade to the vehicles.

We are always starting using the vessel with the lowest pressure that can still guarantee the flow: when the difference of pressure between the cryogenic vessel and the tank in the vehicle is too small we switch to the next available vessel. Between cryogenic vessel and the dispenser there is an heat exchanger to make sure that the hydrogen that goes into the vehicle's tank has a temperature not lower than 233K (-40°C)[25].One way to warm this hydrogen up before it goes inside the vehicle tank is using the heat from the ambient atmosphere, can considered at 288-300K.

Once the cryogenic vessel reaches the minimum pressure this is not used anymore to refill the vehicles and it starts its process of refueling going through step 4, 5 and 1, 2.

Figure 56 is shows the pressure trends inside of the cascade and the vehicles. This is for a station of 400 kg/day with two hoses (dispensing to two vehicles at the same time) filling to vehicles with a 700 bar tank and 140 liter of inner volume (5.6 kg of capacity). We assume that the cars come to the station with 1 kg of leftover hydrogen at 90 bar, and that the pressure drops due to the hoses valves and other component is 1.4 bar. The vessels of the cascade are, when completely full, at 860 bar with 69 kg/m^3 of hydrogen density in it and a volume of 1 m^3 (the influence of those parameters will be analyzed in the optimization section). No lingering time between the vehicles is considered.

Looking at the first cryogenic vessel (CV1), step 3 can be described as follows. CV1 fills the vehicles up to its minimum dispensing pressure (150 bar), and then goes offline to go through the other 4 steps in order to be recharged and pressurized and become ready to be used again after, in this case, 45 minutes offline.

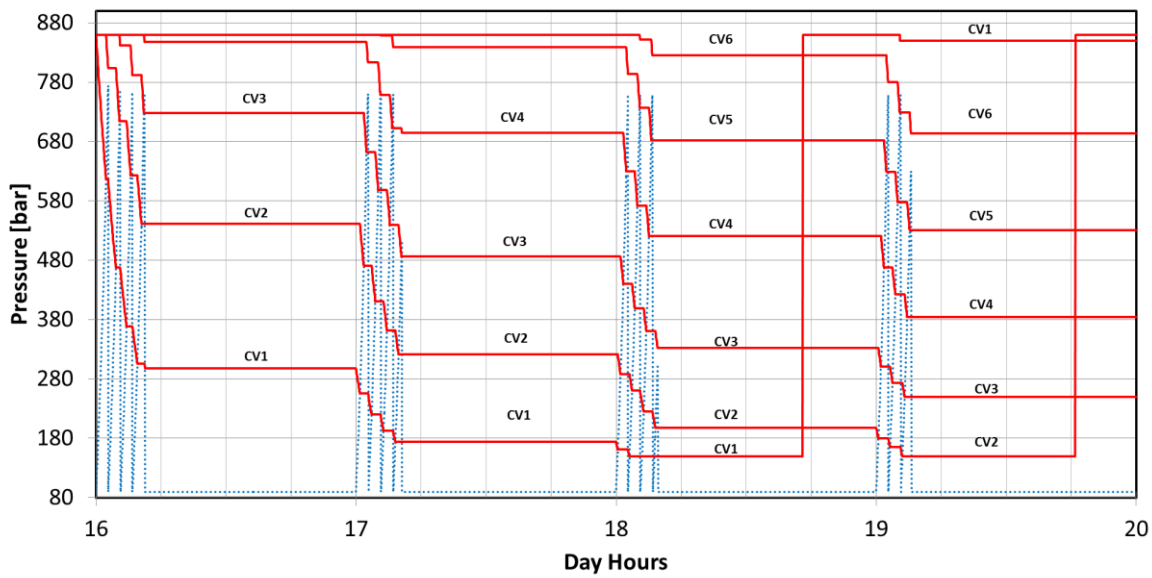

FIGURE 56 VESSEL PRESSURES (RED LINE) VS. VEHICLES PRESSURES (BLUE LINES). CRYOGENIC CASCADE VESSELS WITH RATING PRESSURE OF 860 BAR, INNER VOLUME OF 1 m^3 AND THE DISPENSING MINIMUM PRESSURE OF 150 BAR. VEHICLES WITH 140 LITER OF TANK VOLUME RATED FOR 700 BAR PRESSURE AND 5.6 KG OF CAPACITY.

Effort has been also spent trying to understand if using the cascade in a "traditional" way would actually be a good strategy or we could use some better control in order to minimize the number of vessel in the cascade. Several combination of rules have been tried, but did not show clear advantage, and it seems that the best solution is to use the cascade in the way we explained earlier. In Figure 57 are shown some of these.

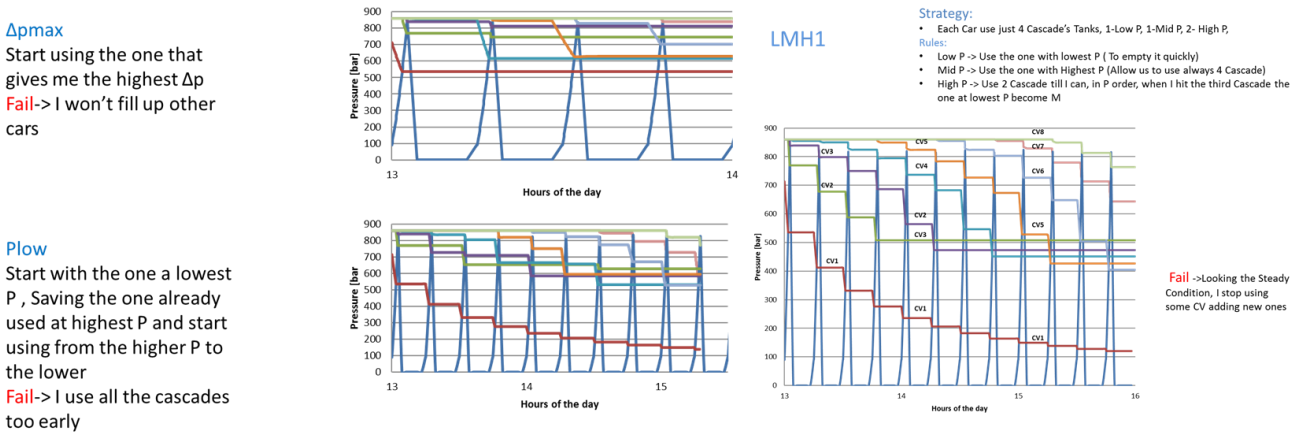

FIGURE 57 TRIES OF STRATEGIES TO A BETTER USE OF THE CASCADE TO MINIMIZE THE VESSELS NUMBER

Step 4: Recycle hydrogen left in the cascade into the Dewar

In the fourth step the remaining part of hydrogen that is still in the cryogenic vessel is recirculated into the Dewar to restore the initial operating pressure in it. Before flowing into the Dewar, the hydrogen is recirculated through a full, cold cryogenic vessel that comes out from the *Step 1*. The hydrogen is thus cooled down before entering into the Dewar, allowing a recirculation of a bigger amount of hydrogen. This also has the benefit of warming up the liquid hydrogen inside of the full cryogenic vessel, allowing to save some energy during the *Step 2*. The process goes on until the pressure is completely restored to the initial value of the Dewar. This process brings some mass inside the Dewar, increasing a bit its percentage of full, expressed as the liquid mass over the total mass (kg_l/kg_{tot}) and restores its working pressure allowing to refill a new cryogenic vessel of the cascade (Figure 58).

The heat exchange into the cold full vessel has been considered in this analysis as perfect, letting reach the two fluids the same temperature with no losses.

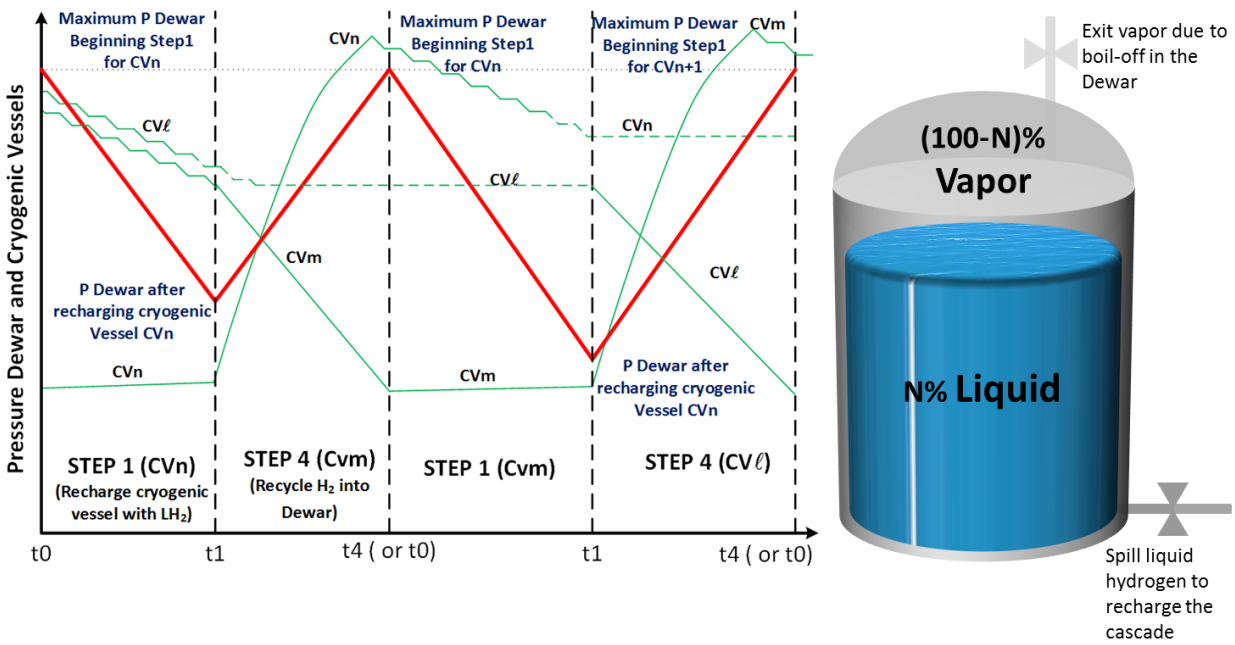

FIGURE 58 DEWAR PRESSURE CYCLES

Step 5: Venting unusable hydrogen leftover in the cascade

The fifth step is where the last part of hydrogen leftover into the cascade vessel can't be recirculate anymore into the Dewar because it reached its maximum pressure, and thus needs to be vented (boil-off) to bring the pressure inside of the vessel at a level that allows to start the recharging process in step 1 (Figure 59).

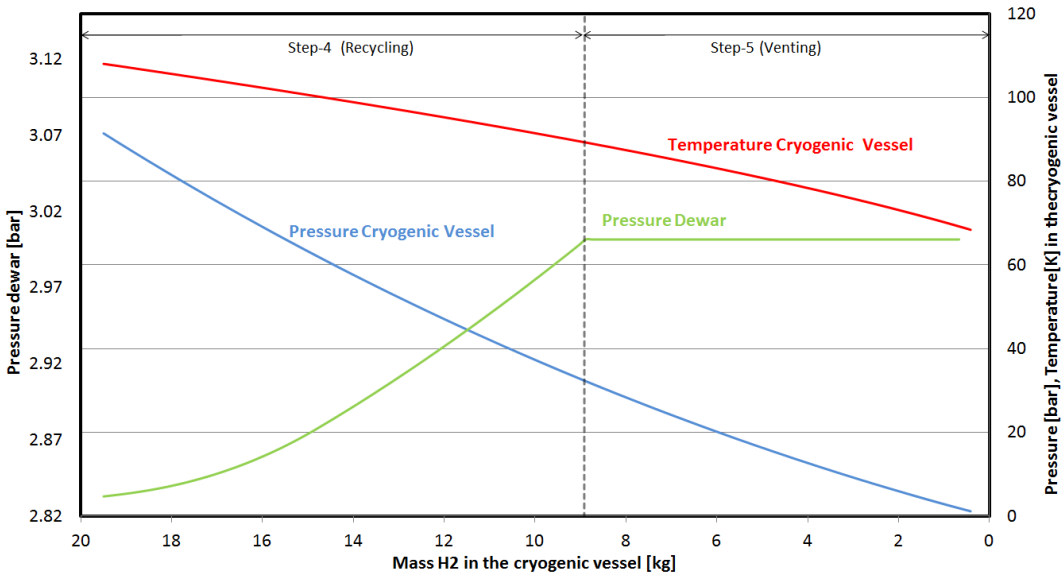

FIGURE 59 PRESSURE IN THE DEWAR, AND PRESSURE AND TEMPERATURE OF THE CRYOGENIC VESSEL, AS FUNCTION OF THE HYDROGEN MASS IN THE CRYOGENIC VESSEL DURING STEP 4 AND 5

5.2 Description of the tank design model

In this section, we describe the tank design model that was developed and implement in this simulation work. This model allows to estimate the mass of the pressure vessel given a rated pressure, an inner volume and a diameter, that is subsequently use in both the thermodynamic (thermal mass of the vessel) and the cost (based on the amount of material needed to fabricate the vessel) models. In this work, a type III vessel was considered, which consists of a composite carbon or glass fiber outer laminate to withstand the high pressure of the stored gas and a metal inner liner to store the gas at a very low permeation rate. The design of these vessels

can be really complicated and is normally approached with finite-element techniques[35][36], our purpose it is to made a baseline design to estimate the thermal masses and price.

Mechanical analysis for the design

The masses of the tanks we are designing either for the vehicles and the cryogenic cascade's vessels is estimated by the Swanson method[36], assuming type III tanks with an aluminum liner with cylinder with elliptical end closures and carbon fiber in an epoxy matrix as overwrap material. The composite is applied by filament windings continued over the domes.

The cylindrical section is wound by helical layers with an angle of ± α and 90º hoop windings (Figure 60). The helical windings are carried out over the domes and angle α is determinate by the design of the dome and the diameter of the dome end fittings related to the diameter of the cylinder. We have not taken into account the specifically design of the domes here, but the strains in the helical fiber are designed to be no more than 70% of those in the hoop windings, which makes the hoop windings critical for rupture.

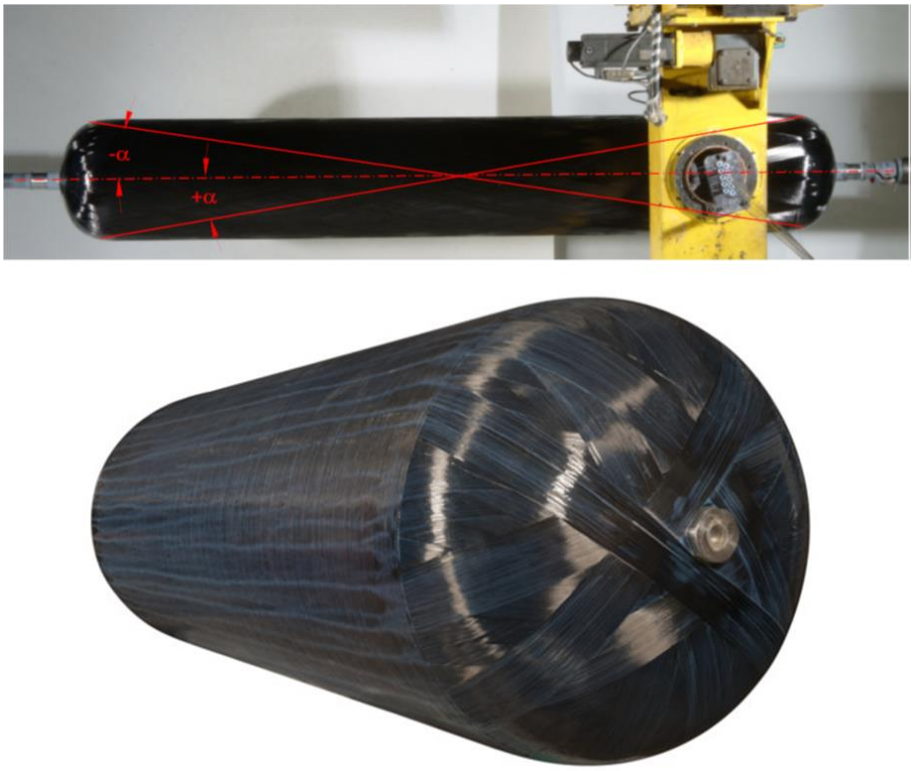

FIGURE 60 FILAMENT WINDING PROCESS

The load sharing between liner and overwrap material depends on the relative stiffness and is found with the assumption of thin-shell vessel, it means consider that the strains between the two is the same.

To do this, we construct a matrix for the liner and the overwrap material that relates the strains in the cylinder due to the pressure loads and then to calculate the stresses in the two from the strains. An expression of this matrix is given as:

$$A_{ij} = \sum_{k=1}^{N} \left(\overline{Q_{ij}}\right)_k (h_k - h_{k-1}) \quad (5.1)$$

Q is the stress-strain matrix in the overall system, and the term $(h_k - h_{k-1})$ is the thickness of each layer. The stress-strain matrix for the orthotropic liner is given by:

$$\begin{Bmatrix} \sigma_x \\ \sigma_h \\ \tau_{xh} \end{Bmatrix} = [Q_l] \begin{Bmatrix} \epsilon_x \\ \epsilon_h \\ \gamma_{xh} \end{Bmatrix} \quad (5.2)$$

$$\text{with } Q_l = \begin{bmatrix} \frac{E}{1-\nu^2} & \frac{\nu E}{1-\nu^2} & 0 \\ \frac{\nu E}{1-\nu^2} & \frac{E}{1-\nu^2} & 0 \\ 0 & 0 & G \end{bmatrix} \quad (5.3)$$

x and h stand for axial and hoop directions, respectively. E is the Young's modulus, ν is the Poisson's ratio, and G is the shear modulus.

The stress-strain matrix for the composite depends on the fiber angle. Thus, for the overwrap material the matrix will be:

$$[\bar{Q}] = [T^{-1}][Q][R][T][R^{-1}] \quad (5.4)$$

$$\begin{Bmatrix} \epsilon_1 \\ \epsilon_2 \\ \gamma_{12} \end{Bmatrix} = [R] \begin{Bmatrix} \epsilon_1 \\ \epsilon_2 \\ \frac{\gamma_{12}}{2} \end{Bmatrix} \quad (5.5)$$

where T is the transformation of coordinates matrix; R as shown, just give as result the engineering strain shear divided by 2 and Q is defined as follow:

$$Q = \begin{bmatrix} \frac{E_{11}}{1-\nu_{12}\nu_{21}} & \frac{\nu_{12}E_{11}}{1-\nu_{12}\nu_{21}} & 0 \\ \frac{\nu_{12}E_{22}}{1-\nu_{12}\nu_{21}} & \frac{E_{22}}{1-\nu_{12}\nu_{21}} & 0 \\ 0 & 0 & G_{12} \end{bmatrix} \quad (5.6)$$

$$\begin{Bmatrix} \sigma_1 \\ \sigma_2 \\ \tau_{12} \end{Bmatrix} = [Q] \begin{Bmatrix} \epsilon_1 \\ \epsilon_2 \\ \gamma_{12} \end{Bmatrix} \quad (5.7)$$

Where E_{11}, E_{22}, G_{12} are the elastic module in respectively the fiber and transverse directions and the shear modulus of a unidirectional layer, ν_{12} and ν_{21} are the Poisson's ratios satisfying the following symmetry condition: $E_{11}\nu_{21} = E_{22}\nu_{12}$.

As failure criteria we use the maximum fiber-direction strain, the rupture pressure is the value of the overpressure at which fails the overwrap. The overwrap is designed so that the highest strains are concentrated in the cylindrical part. It is reasonable to have strain in the helical fiber of the order of 60-70% the ones in the hoop. To calculate it, we are using the follow equation:

$$p_{ult} = p_y + \frac{1}{r}\left\{\left(A_{c21}R_{\Delta_\epsilon} + A_{c22}\right)\left(\epsilon_{ult} - \epsilon_{hy}\right)\right\} \quad (5.8)$$

$$\begin{Bmatrix} \epsilon_x \\ \epsilon_h \\ \gamma_{xh} \end{Bmatrix} = [A_c]^{-1} \begin{Bmatrix} p_y r/2 \\ p_y r \\ 0 \end{Bmatrix} \quad (5.9)$$

Where p_y is the initial yielding pressure calculated from the follow relation $p_{work} \leq \alpha\, p_y$, α is an experimental parameter that indicates the ratio of the working pressure to yield pressure and it is 0.75. R_{Δ_ϵ} represents the ratio of the additional axial-and-hoop-directions strains due to the initial overpressure cycle. This cycle

induces residual compressive stresses in the liner and residual tension in the composite. This is calculated as follow:

$$R_{\Delta_\epsilon} \equiv \frac{\Delta\epsilon_x}{\Delta\epsilon_h} = \frac{A_{c11}^{-1} + 2A_{c21}^{-1}}{A_{c21}^{-1} + 2A_{c22}^{-1}} \quad (5.10)$$

where A_c is the A matrix just for the composite.

Thermal mass estimation

To determine the thermal masses (Figure 61) and the cost of the cascade we have designed Type III tank based on the Swanson method [37].

The specific thermal masses showed in the Figure 61 are showed in kJ/kg because to calculate the value for the carbon fiber, the empiric equation used from BMW, gives results in J/kg.

For the liner the equation used is[38]:

$$C_{th,liner} = 10^{\log(Cth)} * T \left[\frac{kJ}{kg}\right] \quad (5.11)$$

$$\log(\mathrm{Cth}) = a + b * \log(T) + c * \log(T)^2 + d * \log(T)^3 + e * \log(T)^4 +$$

$$+f * \log(T)^5 + g * \log(T)^6 + h * \log(T)^7 + i * \log(T)^8 \left[\frac{kJ}{kg\ K}\right] \quad (5.12)$$

For the carbon fiber, the equation used is the following:

$$C_{th,carbonfiber} = \left(a * T + b * \frac{T^2}{2} + c * \frac{T^3}{3} + d * \frac{T^4}{4} + e * \frac{T^5}{5} + f * \frac{T^6}{6} + g * \frac{T^7}{7}\right) \left[\frac{J}{kg}\right] \quad (5.13)$$

TABLE 6 COEFFICIENTS FOR THE SPECIFIC THERMAL MASSES OF THE TWO METHODS			
Coefficient	**Aluminum 6061-T6**	**304 Stainless Steel**	**Carbon Fiber T700(epoxy)**
a	46.6467	22.0061	11.5488036
b	-314.292	-127.5528	3.11030698
c	866.662	303.6470	-0.0388055309
d	-1298.30	-381.0098	$7.71849531*10^{-4}$
e	1162.27	274.0328	$-5.15153348*10^{-6}$
f	-637.795	-112.9212	$1.42533974*10^{-8}$
g	210.351	24.7593	$-1.42078589*10^{-11}$
h	-38.3094	-2.239153	0
i	2.96344	0	0
		DATA RANGE	3-300K

a, *b*, *c*, *d*, *e*, *f*, *g*, *h*, and *i* are the fitted coefficients, and *T* is the temperature.

While the equations degree may seem like an excessive number of terms to use, it was determined that in order to fit the data over the large temperature range, we required a large number of terms. It should also be noted that all the digits provided for the coefficients should be used, any truncation can lead to significant errors.

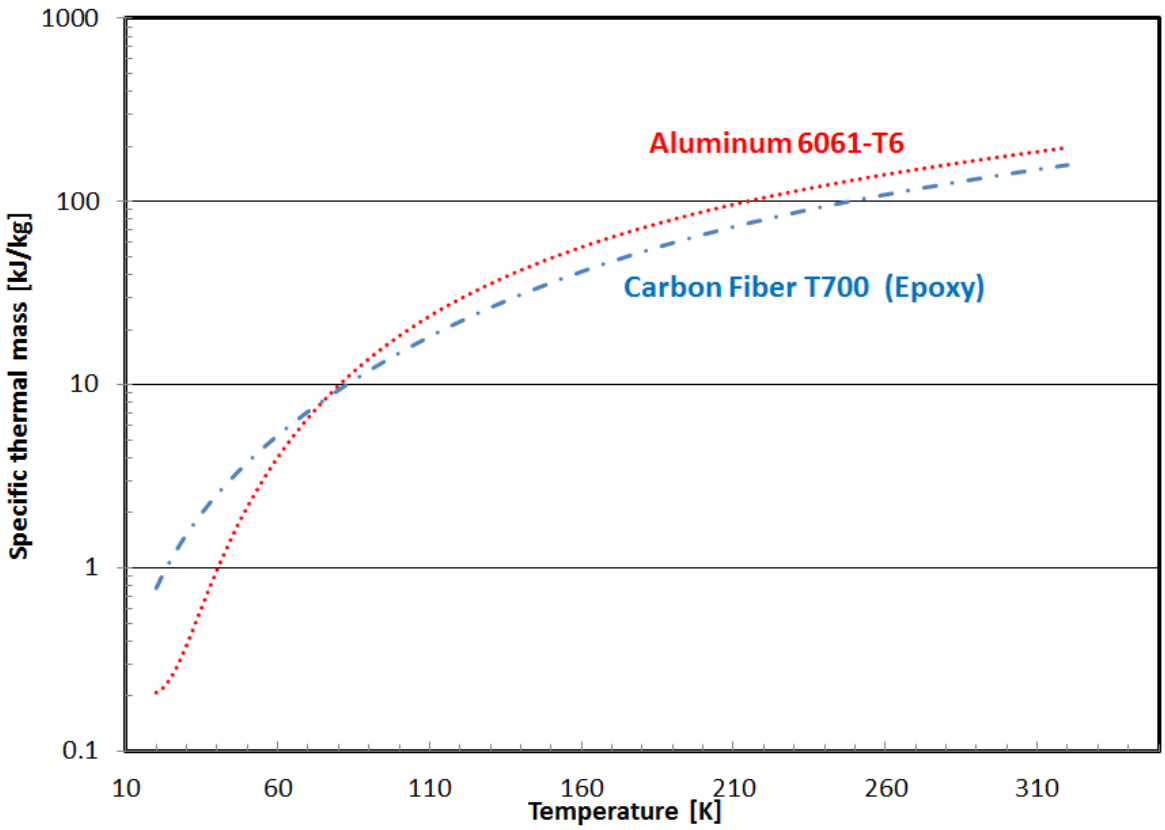

FIGURE 61 THERMAL MASS FOR ALUMINUM AND CARBON FIBER[38]

6.MODEL CODING AND IMPLEMENTATION

The overall cost of the fueling station includes capital and operating cost. In order to minimize that cost for the thermal compression fueling station concept, it is thus necessary to study how to optimize the design of the cryogenic vessels and cascade (capital cost) and the venting losses (operating cost); including also how those two parameters interact with each other.

The first step in the model implementation task was to implement all the tank design equations and the thermodynamic equations simulating the entire cycle of the station in a preliminary model on Excel (Visual Basic), in order to make sure that the physics was well captured. Using this method was however limited because of the size of the data we had to deal with a 17250 x1 80 cells spreadsheet was necessary simulate a station with 20 cryogenic vessels in the cascade and needed more than 24 hours of computing time, causing the computer to sometime “freeze”.

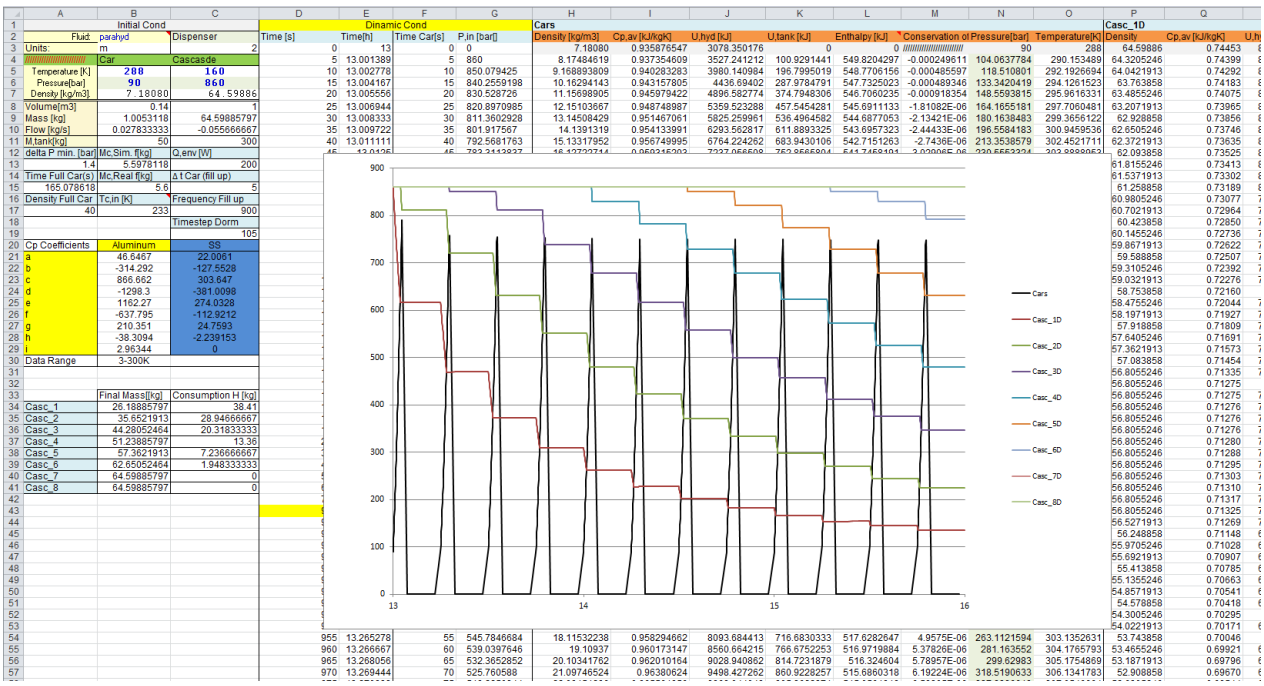

FIGURE 62 EXCEL SPREADSHEET TO SIMULATE STEP-3 WITH 20 CRYOGENIC VESSELS IN THE CASCADE

As a result, a new modeling framework was developed using with the Fortran 90 language. This choice, although the GUI was not as friendly as Excel, had a stiffer

learning curve and the debugging was not straight forward, but it drastically reduced the computational time. This feature was a necessity for the optimization due to the multitude of runs necessary. Using Fortran 90 was also based on the good integration with the subroutines of REFPROP 9.1[33] (program utilized to model the fluid properties with real equations of state), that are written with the same language.

```
ncv_3 = 120                          ! max number of Cryogenic Vessel availables

!!!!!!!!!!!!!!!!!!!!!!!!!!!!!!!!!!!!!!!!!!!!!!!!!!!!!!!!!!!!!!!!!!!!!!!!!!!!!!!!!!!!!!

pcv_3 = 800          ! Rated pressure of cryogenic vessel, in Bar
Vcv = 390            ! Internal volume of cryogenic vessel, in Liters
Ri = 350             ! Radius of cryogenic vessel, in mm
L_th = 6             ! Liner Thikness, in mm
SF = 2.25            ! Design Safety Factor


Pmin = 150           ! Minimum pressure to deliver to the car, in Bar
time_offline= 120    ! Amount of time to empty and refill cryogenic vessel, in minutes
number_h = 2         ! Number of hoses per dispenser
Dp_3 = 1.4           ! Maximum delta P to refill vehicles, in Bar
tw_3 = 360000        ! Physical ime window for calculation, in seconds

Ssd=400              ! station size, in kg/day
```

FIGURE 63 SCREENSHOT OF THE INPUT FILE FOR THE TRANSIENT CASCADING SUB-ROUTINE

Two Fortran subroutines were written, with more than 2000 lines each, to simulate:

1. The wasted hydrogen (venting losses – boil-off) during the cryogenic vessel filling and recycling processes (Step1 and Step5);
2. The transient cascading system to determine the number and dimension of the bank of cryogenic vessel.

The computational time on one processor was less than one minute for the venting losses simulation, and from one to eight minutes for the transient cascading subroutine.

6.1 Venting losses minimization simulations

The goal of this section is to simulate different operating conditions and cryogenic vessel designs for the thermal compression station in order to identify the parameters that minimize venting losses. Those losses are estimated as a ratio of the amount of hydrogen vented during Steps 1 and Step 5 over the mass of hydrogen stored in a given cryogenic vessel design.

Controlling variables and their typical ranges are first selected, including cryogenic vessels and Dewar design (pressure rating, geometry), minimum delivery pressure to the vehicle, level of liquid in the Dewar. Then, various combinations of those inputs are run using a quasi-random low discrepancy sampling method (here: Sobol sequence), that typically offers higher levels of efficiency and uniformity than purely deterministic methods (Figure 64). At last, the results are post-processed using a High Dimensional Model Representation (HDMR) to identify the most important controlling variables with regards to venting (both in Steps 1 and 5).

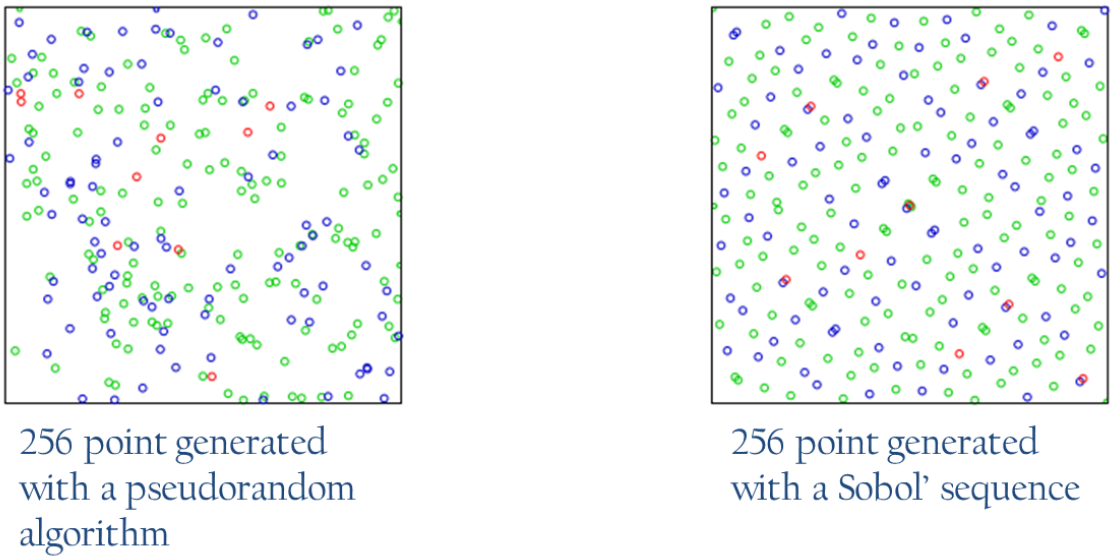

FIGURE 64 PSEUDORANDOM SAMPLING VS. SOBOL' SEQUENCE SAMPLING

The code has been verified to make sure that it gives reasonable results, the convergence was proved comparing the results with the ones obtained through the

Excel spreadsheets, timestep influence has been verified to make sure that it was not affecting the results.

Input parameters selection

After the input parameters to control were selected, also the range of value in which each of the parameters can vary have been chosen. With those, we get 2000 different combination of data input. We used the language Python to run the code through all the matrix of inputs, this also allowed to spot the last bags of the code; the boundaries are show in the Table 7:

TABLE 7 PARAMETERS RANGE FOR THE OPTIMIZATION PROCESS

Program Block	Variable	Range (MIN-MAX)
Tank Design	Pressure Work [bar]	350 - 900
	Inner Radius [m]	0.2 – 1.3
	Internal Volume[m^3]	0.5 - 10
Step1	Volume Dewar [m^3]	20 - 50
	Max Pressure Dewar [bar]	2 - 8
	Percentage of full Dewar	5% - 95%
	Min ΔP during the refill [bar]	0.3 - 0.5
Step3	Min Pressure Dispensing CV [bar]	92-250
Step4	Min Pressure admissible CV [bar]	1 -7.7
	Percentage of full Dewar	5% - 95%

These ranges where we look for the optimization are based on literature and typical values; regarding the Dewar: LH_2 tanks are usually filled only for 85-95% of their total capacity, an empty space has to be left because of the dormancy (defined as the

period of inactivity before a vessel releases H_2 to reduce pressure build-up), and to prevent spills due to the expansion of liquid hydrogen with the increase of temperature during the refill of it[39]; to understand the pressure boundaries we can look at the graph in Figure 65 ; since into the Dewar the two phases are in equilibrium, the rating pressure at which the Dewar is filled governs the density of the liquid, this can be explained thinking at our tank as a sealed ambient with a fixed amount of hydrogen inside it, this ambient at first has a pressure p, if now we imagine to increase this pressure to a value p' > p , as logic suggests the gas will increase its density, but having fixed volume and fixed mass, the overall density cannot change, it means that the density of the liquid has to decrease. The upper and lower bound therefore are 2 bar because it is the minimum value to guarantee a difference of pressure between Dewar and cascade during the recharging process (Step1) to flow hydrogen. The 8 bar are because with this pressure the density of the liquid is 54.5 g/l and we do not want to decrease anymore the density because filling the cascade with liquid a lower density increases unacceptably the boil-off necessary to complete the process.

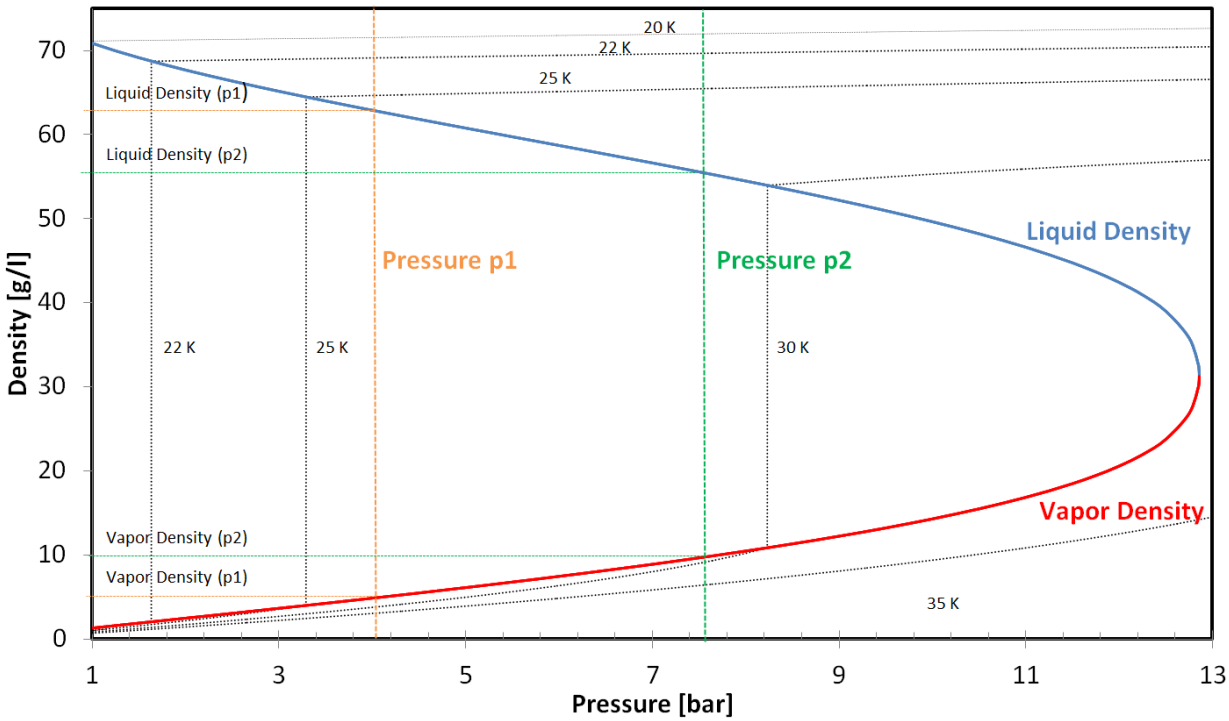

FIGURE 65 DENSITY VS. PRESSURE FOR SATURATED PARA-HYDROGEN (AT EQUILIBRIUM)

The minimum pressure admissible for the cryogenic vessel it is dictated from the maximum pressure of the Dewar (beginning step 1), this pressure cannot be greater than the Dewar pressure less the drop of pressure to refill (Min ΔP during the refill), otherwise there will be no flow. The pressure of work of the cascade are again typical values, a typical cascade in fact consists of three level of pressure; low 350-500 bar, medium, 500-700, and the highest can be above of 900 bar[40][41].

Logic and code routine

The logic of the program can be followed in Figure 66.

The green blocks are referring at the tank design, the orange ones are used when we initialize the program, and the blue blocks are referring at the fueling station cycle.

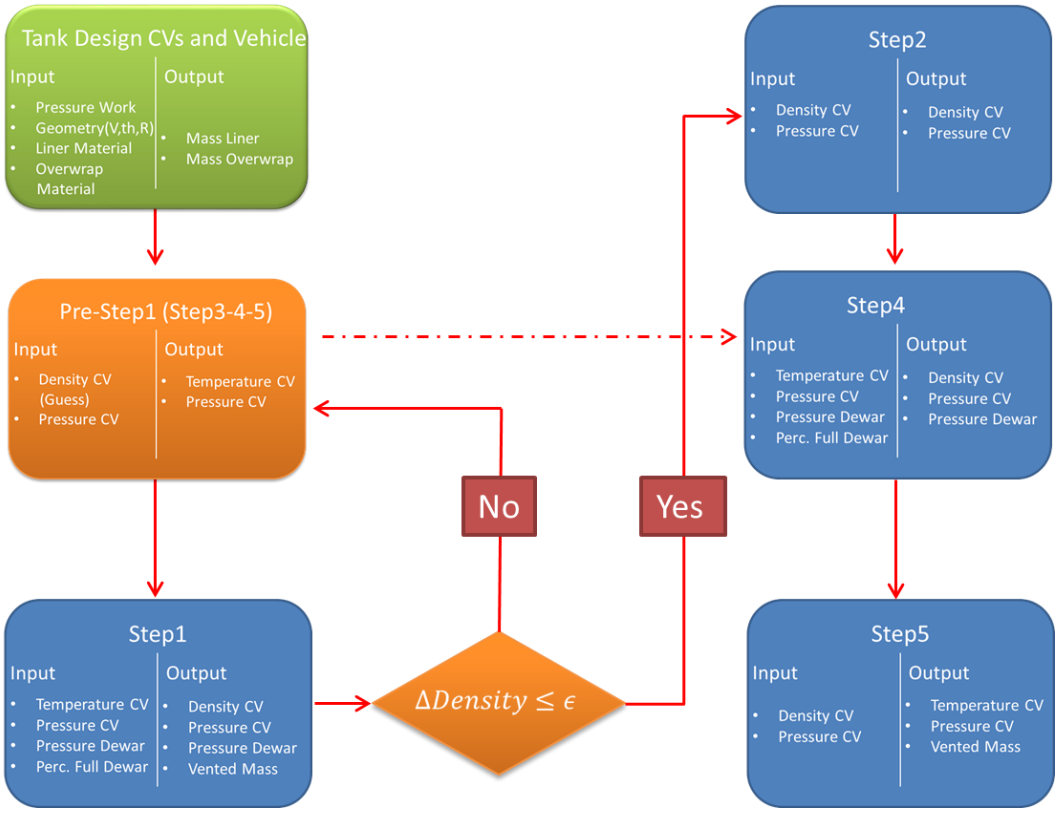

FIGURE 66 MAIN LOGIC OF THE PROGRAM TO SIMULATE THE ENTIRE PROCESS OF THE FUELING STATION. THE GREEN BLOCKS ARE REFERRING AT THE TANK DESIGN, THE BLUE ONES IS THE ACTUAL FUELING STATION

It can be divided in the following blocks:

- **Tank Design**

The input data are the geometry of the tanks: inner volume, inner radius and thickness, the operating pressure and the materials for liner and overwrap.

As previously said in this analysis only aluminum liner and carbon fiber as overwrap material has been taken into account, anyway the code allows to design tanks with other materials (e.g Stainless Steel for the liner, glass fiber for the overwrap material) or made with other technologies (Type I Type II Type IV). The equations shown before have been implemented with a safety factor of 2.25. With the baseline design also the final masses of the two components can be obtained. These can be used to estimate cost of the tanks and their thermal masses.

- **Pre-Step1**

The Pre-Step1 block, is used to determine the initial temperature and pressure of the cryogenic vessel at the beginning of the *Step1* when we first initialize the program. This is necessary, because at the beginning, the temperature of the cryogenic vessel at the end of the *Step5* in unknown. Also, the final density that the hydrogen inside the cryogenic vessel will reach is unknown, because this is determined at the end of Step1 and depends of the initial temperature. The code starts with a guessed value for the final density of the cryogenic vessel, then since the working pressure is known because is a controllable variable. From these initial values the hydrogen expands up to the minimum allowable pressure reachable inside the vessel (pressure cryogenic vessel end Step5). This first block is making a simulation of the: *Step 3*, *Step 4* and *Step5*, only from the cryogenic vessel point of view (in this case are not taken into account neither vehicles nor the Dewar). This block gives as result the cryogenic vessel's initial conditions to start the *Step1* block. In the *Step1* the final density of a full cryogenic vessel is determined. This value is then compared with the initial guess and adjusted to start over the *Pre-Step1*. This process is iterated until the error between the guessed density at the beginning of

the *Pre-Step1* and the result of density obtained at the end of the *Step1* block is less of a certain ε (0.1 kg/m^3).

- **Step1**

During the simulation of the *Step1*, liquid hydrogen is flown from the Dewar to the cryogenic vessel.

The equations implemented are balance of mass and balance of energy for both Dewar and cryogenic vessel as follow:

MASS BALANCE

$$Dewar:\ M_d(i) = M_d(i-1) - mass\ transfer \quad (6.1)$$

$$Cryogenic\ Vessel:$$

$$M_{cv}^n(i) = M_{cv}^n(i-1) + mass\ transfer - venting \quad (6.2)$$

ENERGY BALANCE

$$Dewar: U_d(i) = U_d(i-1) - H_l \quad (6.3)$$

$$Cryogenic\ Vessel:$$

$$U_{cv}^n(i) + U_{tank,cv}^n = U_{cv}^n(i-1) + U_{tank,cv}^n(i-1) + H_l - H_{vent} \quad (6.4)$$

Where U is the internal energy [J], M is the mass [kg] and H the enthalpy [J]; the i identifies the timestep and n is the number that identifies the cryogenic vessel in the cascade.

These equations are iterated until is reached one of the conditions of exit.

Normally the control done to decide whether or not the process is finished, is on the quality of the hydrogen into the cryogenic vessel, when this value reaches zero, the overall system is in subcooled liquid conditions so, the density cannot grow anymore and the flow stops. This is what happens in standard conditions, but since during the optimization process we can obtain also more extreme conditions that can lead to results not physically correct, temperature and density of the cryogenic vessel, and the quality of the Dewar are continuously checked. For the latter, the code stops compiling in case the hydrogen inside of the Dewar (that has to be in saturated liquid form) become super-heated. The temperature inside the cryogenic vessel as to be limited to a maximum of 300K[38], while for the density has to be checked the trend during the process, if it decreases the code stop compiling because the venting would be greater than the flow of the mass from the Dewar. Also, the end value that cannot be less than 20 g/l[34].

While when the trend of the density decreases the last value is taken as final density, there are two "safety rules" to exit the coding guarantee to have physically possible results, indeed when those condition happens, the specific set of values has not taken into account. The dynamic of this process it is really delicate to be simulated, due to the continuous change of phase and the venting, in fact those rules have been implemented after some bugs were found through the parameters sweep of the entire space, running the data set given to the Sobol' sequence with Phyton.

The two terms venting and the enthalpy correlated (the enthalpy is the energy that flow away with the vented mass), are zero when the pressure in the cryogenic vessel it is low enough to let the liquid flow from the Dewar and are becoming greater otherwise. As seen in Figure 55 the vented mass can have complicated trend, so the check of quality is necessary also to accurately simulate this behavior and make sure to vent the only vapor part. The hydrogen vented is in vapor phase, so the enthalpy refers at this condition.

- **Step2**

Starting from the values of density and pressure for the cryogenic vessel at the end of the *Step1*, a heat-exchanger into the vessel warms-up the hydrogen bringing it at working pressure. In this study, this process accounts of just the energy balance

equation for the cryogenic vessel, iterated up to the rating condition. Further studies would be needed to better understand the physic and mode to have this pressurization. But since it does not affect the boil-off, these were not done in this analysis.

- **Step4**

In the simulation of this step the heat exchange that happens between the hydrogen that flows from the cryogenic vessel that is emptying into the Dewar, and the cold hydrogen contained in the vessel that have just been recharged in the *Step1* has to be simulated. Has been considered an ideal condition of perfect exchange (equation 6.8) where the temperatures of the two fluids at the equilibrium are the same. The equations implemented are mass balance and energy balance for cryogenic vessel and Dewar, plus the one for the heat exchange. When in the Dewar is obtained its working pressure the code exits from this block.

MASS BALANCE

$$Cryogenic\ Vessel: M_{cv}^{n}(i) = M_{cv}^{n}(i-1) - mass\ transfer \quad (6.5)$$

$$Dewar: M_{d}(i) = M_{d}(i-1) + mass\ transfer \quad (6.6)$$

ENERGY BALANCE

$$Cryogenic\ Vessel:$$

$$U_{cv}^{n}(i) + U_{tank,cv}^{n} = U_{cv}^{n}(i-1) + U_{tank,cv}^{n}(i-1) - H_{out} \quad (6.7)$$

$$\Delta U_{cv}^{full} = \Delta U_{cv}^{emptying} \quad (6.8)$$

$$Dewar: U_{d}(i) = U_{d}(i-1) + H_{in} \quad (6.9)$$

- **Step5**

Last block of the cycle, here the only equations implemented are the ones for the cryogenic vessel (equation 6.6 and 6.7). The leftover part of hydrogen is vented until the minimum allowable pressure is reached.

6.2 Optimization of the cascade design

In this section, it is analyzed the cascade footprint (i.e. "capital cost") using the total masses of liner and overwrap materials as the metrics. Similarly to what was done in the previous section, various combinations of parameters are varied over pre-defined ranges and simulated to meet a given station size. The liner and overwrap masses of the vessel design are then multiplied by the number of cryogenic vessels in the cascade as outputs.

The main logic of the entire code is shown in Figure 67

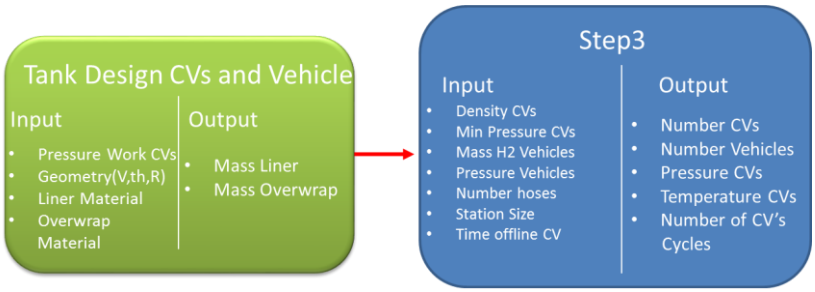

FIGURE 67 MAIN LOGIC OF THE TRANSIENT CASCADING SIMULATION CODE

Also this piece of code starts with the tank design block implementing exactly the same equations shown in the section 5.2 of this document. The only difference is that in this case the design is done twice, once for the cryogenic vessels of the cascade and then for the vehicles' tank.

Once we got the masses for the vessels, we can start the *Step3*.

Input parameter selection

It is assumed that all the cryogenic vessels in the cascade have the same design: pressure rating, diameter, volume. Additionally, the minimum delivery pressure to the vehicles is the same for all vessels. Also for the vehicles have been assumed that they were all the same and with the same initial and final conditions.

Also for this code have been checked the accuracy, comparing the results with the one obtained from Excel, then similarly as done before, 1,000 cases were run over the ranges described in Table 8. In this case this was done to make sure that the code was working properly, also control on the timestep influence were done.

TABLE 8 PARAMETERS RANGE FOR THE OPTIMIZATION PROCESS

Program Block	Variable	Range (MIN-MAX)
Tank Design	Pressure Work [bar]	350 - 900
	Inner Radius [m]	0.2 – 1.3
	Internal Volume[m^3]	0.5 - 10
Step3	Min Pressure Usage CV [bar]	92-250
	Time Offline [hrs]	1-3
	Station size[kg/day]	400-1000

Logic and code routine

Figure 68 shows the logic of implementation of the dispensing process with stressed attention on the bank of cryogenic vessels implementation.

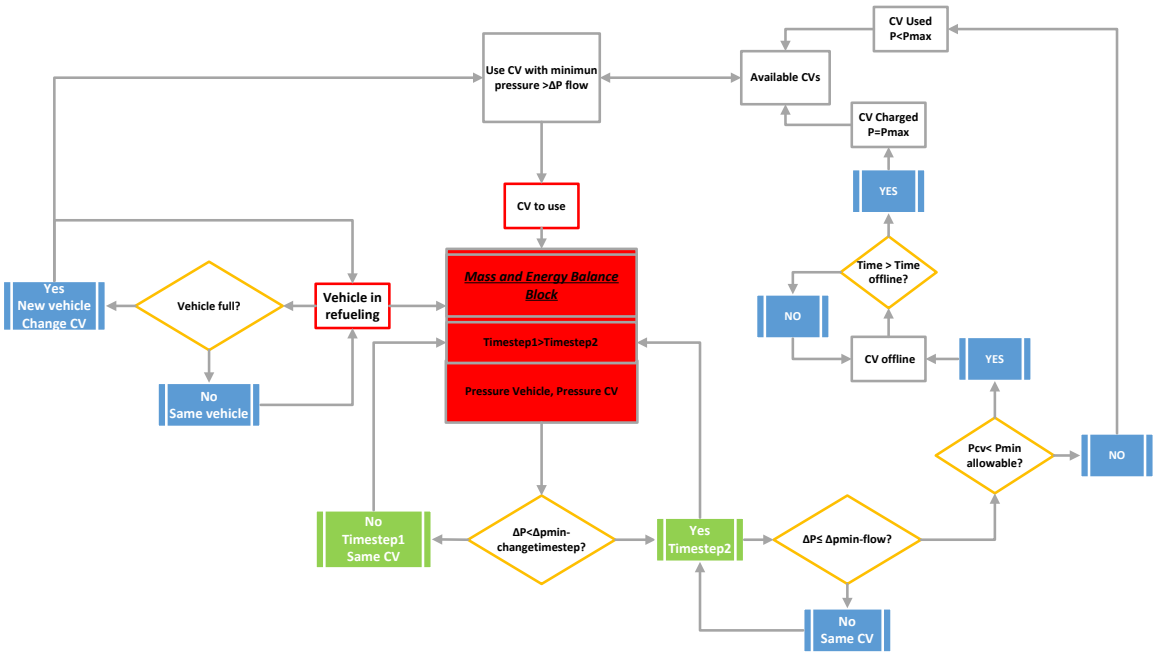

FIGURE 68 LOGIC OF THE STEP3 TRANSIENT MODEL CODE, THE RED BLOCK IS THE ACTUAL REFUELING PROCESS, THE BLUE ARE THE VEHICLES AND BANK OF CRYOGENIC VESSELS IMPLEMENTATION, THE GREEN ARE FOR THE TIMESTEP CHANGE

The explanation can be split in two parts:

- **Step 3**

As station demand we are referring at the Chevron profile in Figure 69[27]. In this step the calculation starts at 4:00 PM, on the peak demand of the so-called Chevron profile, to exploit at best the full cascade. This allows to reach a stationarity of the number of cryogenic vessels earlier. This is a conservative calculation since maximum daily demand (Friday in the summer) is assumed every day. Each vehicle is rated for 700 bar and at the beginning they have 1 kg of hydrogen in the tank at 90 bar, 288 K. The dispending process stops when the tank is full with 5.6 kg of hydrogen in it. We can choose the size of the station and the number of hoses. This number is checked once we have chosen the size of the station and if is not enough to flow the required mass during the peak of the demand, the code stops compiling and gives a warning, so the hoses number can be increased accordingly.

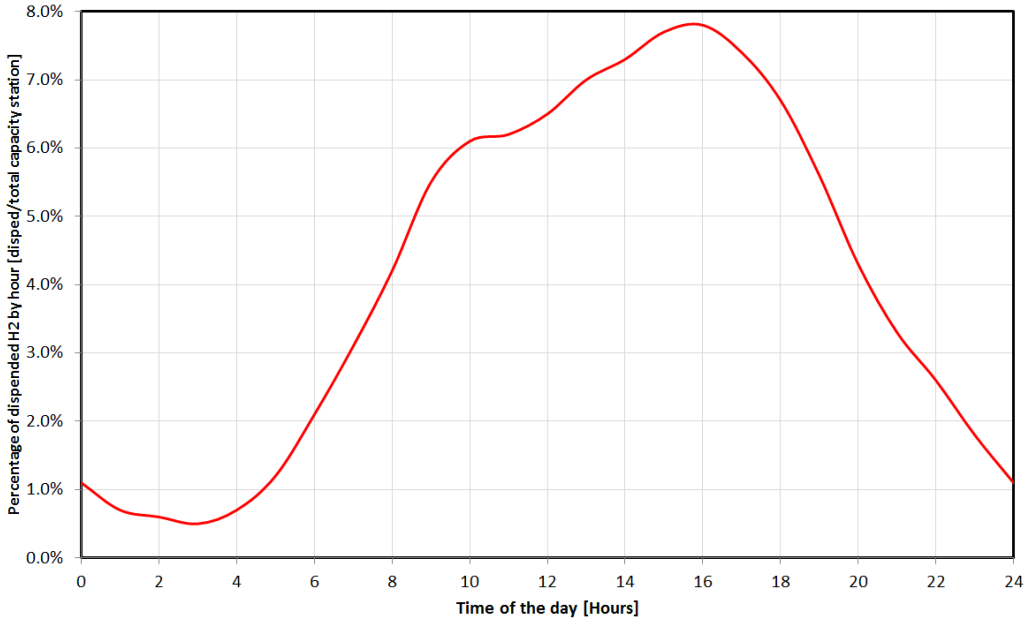

FIGURE 69 MAXIMUM STATION DEMAND PROFILE, FOR A FRIDAY OF SUMMER[30]

The equations iterated during this step, are again balance of mass and energy, for vehicles and cascade as follow:

$$M_{cv}^{n}(i) = M_{cv}^{n}(i-1) - mass\ transfer \quad (6.10)$$

$$M_{vh}(i) = M_{vh}(i-1) + mass\ transfer \quad (6.11)$$

$$U_{cv}^{n}(i) + U_{tank,cv}^{n} = U_{cv}^{n}(i-1) + U_{tank,cv}^{n}(i-1) - H_{out} + Q_{env} \quad (6.12)$$

$$U_{vh}(i) + U_{tank,vh}(i) = U_{vh}(i-1) + U_{tank,vh}(i-1) + H_{in} \quad (6.13)$$

should be noted that there is a term in the energy balance for the cryogenic vessel that there was not in the previous steps. It is the Q_{env}, this represents the loss of cold to the environment, in all the other steps it is considered negligible respect the flow of enthalpy in and/or out; while here it is important to take into account the dormancy. It is the only energy contribute we have while the specific vessel is not

used. Also has to be noted that the term H_{in} in the energy balance for the vehicle does not have the same value of H_{out} that comes from the cryogenic vessel; in order to respect the safety specification of 233K (-40°C)[25], an heat exchanger is needed to warm up the hydrogen which goes inside the vehicle. Also, the flow rate in this case have a fixed value, to accomplish the required time to refill the vehicle to be not more than 3 minutes[25]. To achieve this, the flow-rate of dispensed hydrogen is 1.67 kg/min. This part of code gives us important information about the mode of use and how to build the station, this can simulate as much days we want referring at the actual demand curve, allowing to bring the system a stationary condition to know how many vessels are needed in the cascade and how many times have been recharged, thus can be established how we want to manage our station choosing the minimum pressure of usage and the time offline of the vessels.

It is also important to note that the timestep change it is really important in this piece of code, have implemented this allow to have reasonable computational time and yet be accurate. In fact, the difference of pressure between the tanks of cascade and vehicle continuously checked. The timestep is changed when this values drops under a certain safety value, greater than the minimum allowable in order to let the hydrogen flow of 1.4 bar. Once we reach this value, the timestep becomes very smaller, increasing the number of iteration to make sure the pressures do not overlap and respecting the 1.4 bar limit. This happens just before to switch cryogenic vessel of the cascade. So, once this is changed and the difference of pressure between the two tanks it is large again, the bigger timestep can be used again to do not have too large computational time.

- **Bank of cryogenic vessels matrix**

The dispending step is also a delicate step to simulate, while all the other steps are processing one cryogenic vessel at a time, here it is needed to simulate the entire bank of cryogenic vessels in the cascade and also how one cryogenic vessel interacts with the others. There is also the possibility to choose different characteristic for each of the vessels in the cascade; each vessel is characterized with a flag number

(n) that is attached at that specific vessel to keep track of it from the first step of our program after it is designed.

As previously said the station starts with the vessel that has the lowest pressure, yet enough to guarantee the flow. This rule is taken into account and checked every iteration to make sure to use the correct vessel.

During the refueling process to the vehicles, when the pressure of the vessel is too low, this stops dispensing. We start dispensing hydrogen from the first one available according to the rule just explained. Once a vessel reaches the minimum pressure to be utilized, it stops dispensing hydrogen and goes through the steps 4-5, 1-2 so that it becomes available again in the Step 3 after a time offline; the time in which the cryogenic vessel will not be available because it goes through its refueling process it is also a variable that can be changed.

To correctly implement the bank of cryogenic vessels has been construct a matrix in which the vessels are divided in 4 categories.

1. Cryogenic vessel currently in use,
2. Cryogenic vessels that has been already used but has still dispensable hydrogen in it;
3. Cryogenic vessels that are going through the recharging process;
4. Charged cryogenic vessel that have not been used yet.

The last category, it is important, because at the beginning the final number of cryogenic vessel in the cascade is unknown. It takes some time to reach a stationarity in this number, so in case none of the already used cryogenic vessel can guarantee the sufficient difference of pressure, a new one is taken from the matrix. Dormancy considered to negligible under the typical timeframe for the design.

7. RESULTS AND CONCLUSIONS

In this chapter, the impact of venting losses and cascade design on a thermal compression Hydrogen fueling station are simulated and evaluated.

The boil-off problem has been analyzed with a Quasi-Monte Carlo method in order to make sure the parameter space is correctly sampled. The results from the first code (Section6.1), have been post-processed with the HDMR tool in order to carry out a global sensitivity analysis with the variance reduction method on the output data and understand the correlation between the input parameters and the vented mass. After that, the data outputs have been mapped in function of these parameters to understand how we should change it in order to minimize the boil-off.

In Figure 70 are shown the results from the HDMR for the first order Sobol index S_i that measures the main effect of the input variable xi on the output, or in other words the fractional contribution of xi to the variance of $F(x)$.

In Figure 71 the second order sensitivity index S_{ij} measures the interaction effect of x_i and x_j on the output.

TABLE 9 SYMBOL MEANING IN THE HDMR ANALYSIS RESULTS		
#	**Symbol**	**Meaning**
1	Pwork	Pressure Work
2	Pmin	Min Pressure Dispensing CV
3	pd_1	Pressione iniziale Dewar Step 1
4	Md_1perc	Percentage of full Dewar Step 1
5	Vd	Volume Dewar
6	Dp_1	Min ΔP during the refill
7	Pmin_empty	Min Pressure admissible CV
8	Md_4perc	Percentage of full Dewar Step 4
9	pd_4	Max Pressure Dewar Step 4
10	Vi	Internal Volume CV
11	Ri	Inner Radius CV

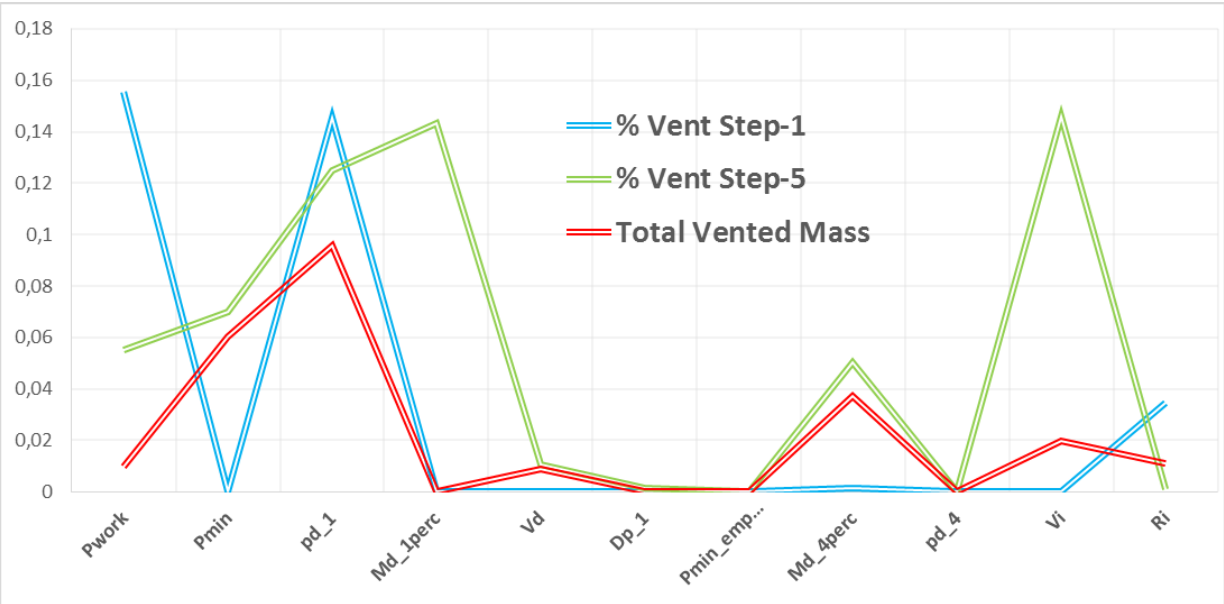

FIGURE 70 FIRST ORDER SOBOL INDICES FOR THE INPUT PARAMETERS

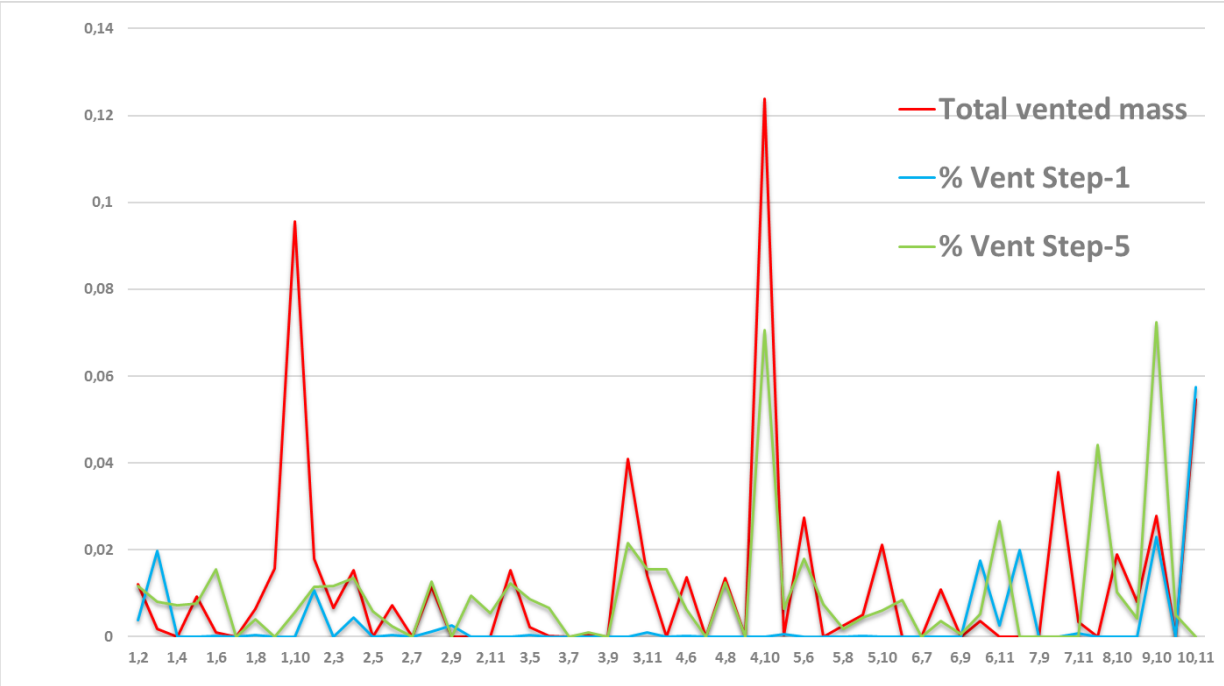

FIGURE 71 SECOND ORDER SOBOL INDICES FOR COUPLED PARAMETERS

Figure 72, shows the comparison of the accuracy of the results we would assuming a linear approximation, that is only looking at the first order Sobol indices with the one obtained looking also at the second order ones.

It is clear that in order to have a trustworthy result we cannot the linear approximation it is not enough and it is needed to look at the correlation between the parameters, that is the second order Sobol indices.

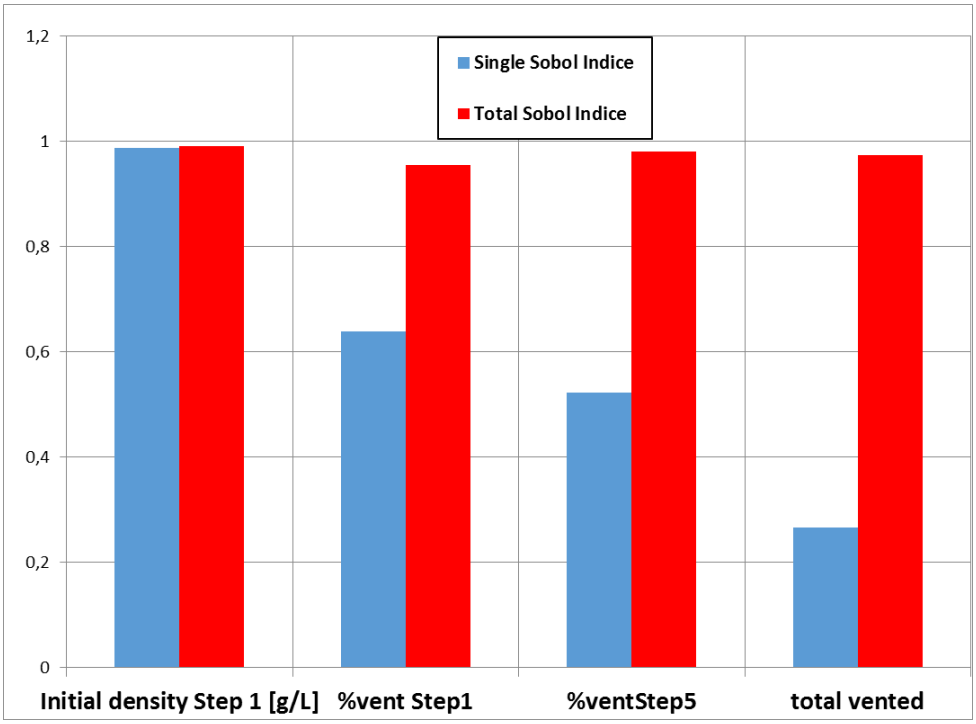

FIGURE 72 COMPARISON OF FIRST ORDER AND TOTAL SOBOL INDICES

In Figure 73 are shown maps of the inputs whose interaction has been identified to have an influence on the vented mass (cf Figure 71). In blue are all the results while red dots represent the combination where the boil-off is less than 10%.

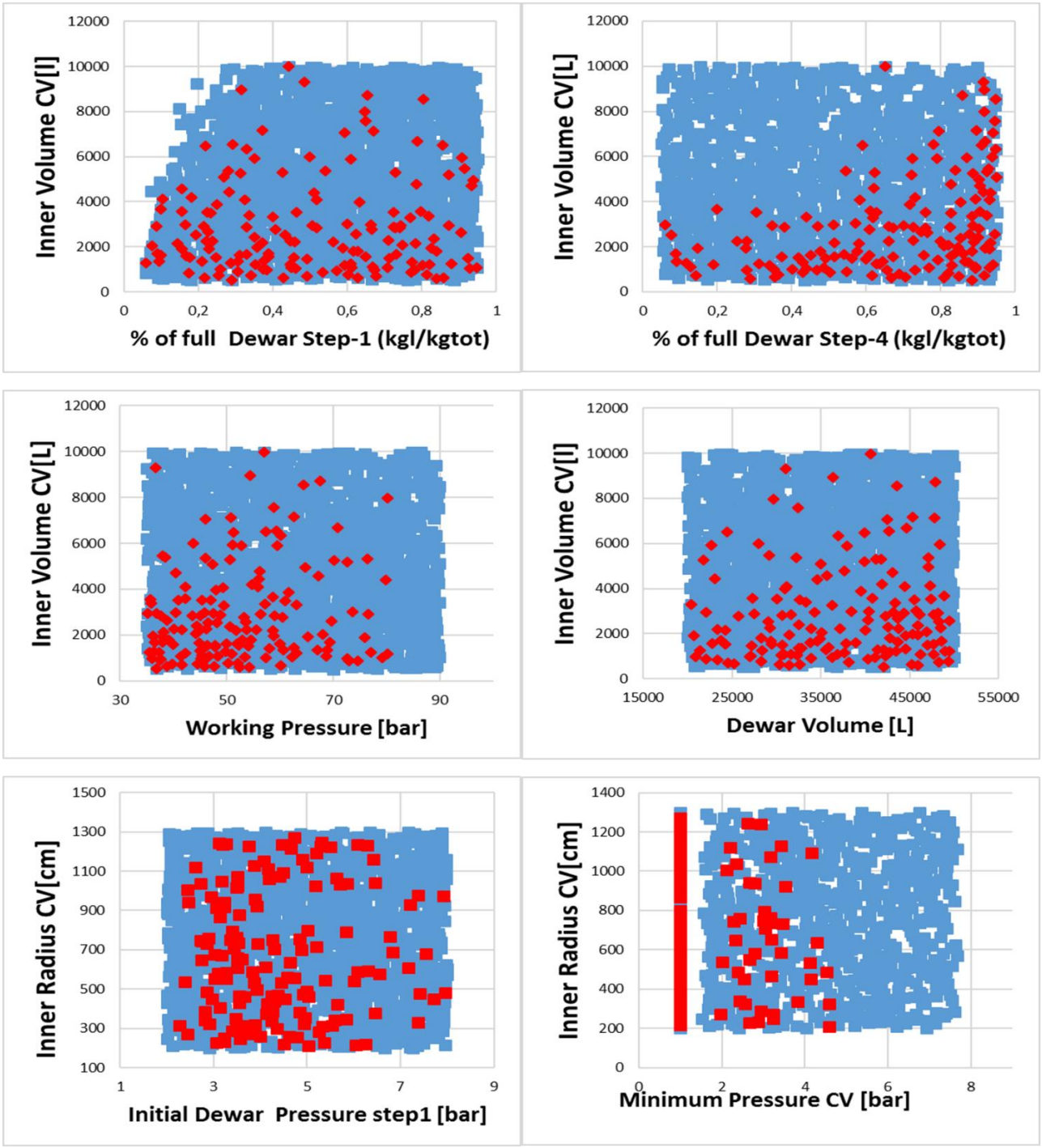

FIGURE 73 OUTPUT DATA MAP. TOTAL PERCENTAGE VENTING FUNCTION OF TWO INPUT PARAMETERS. RED DOTS BOIL-OFF ‹ 10%, BLUE DOTS ALL THE VALUES

These maps on Figure 73 help understanding what would in the best way to reduce the wasted H_2. For example, we can see that a small volume for the cryogenic vessel with a small value of inner radius and minimum allowable pressure would reduce the boil-off, as would lowering the Dewar pressure at the beginning of the *Step1* and

Step4. At last, a large volume of the Dewar and high percentage of full at again at the beginning of the *Step1* and *Step4* would be beneficial.

For the second subroutine (Section 6.2) we analyze a mid-size station of 400 kg/days dispensing from 2 hoses with a cascade with 860 bar as working pressure.For this station have been studied the effect of the volume, minimum dispensing pressure and time offline on the cost of the cascade.

Logic at first would suggest that the best way to dispense hydrogen is up to the maximum allowable (pressure of the car + drops through the hoses and valves, in our case ~92 bar), this to exploit as much as possible the hydrogen contained into the cryogenic vessel. Also we thought that this would have had a good impact on the venting since the quantity of hydrogen leftover to recycle would have been less.

Yet, in our process of optimization for the boil-off we have explored also higher values of minimum dispensing pressure, to better understand how this variable count on the total venting. We found out that having a high minimum pressure of dispensing has some advantages. And also it does not affect sensibly the vented mass.

The first analysis conducted was to run the code simulating enough time to bring the bank of cascade vessels at stationary, here meaning no additional vessels needed.

In Figure 74 can be noted how setting a higher value for the minimum pressure of dispensing has advantages.

Having a higher value of minimum pressure of dispensing allow, to reach stationarity earlier e.g. 60 hours are needed for 120 bar and less than 30 hours for 150 bar, with one hour of time offline, moreover the number of vessels needed are less, more than 30 for the first case and less than 30 for the latter.

Comparing the cryogenic vessels with the same characteristics but different time offline this impact greatly the number of cryogenic vessels in the cascade's bank, again in Figure 74 are compared two cryogenic vessels with same characteristics and time offline, of 1 hour and 3 hours. In the first case the cascade counts a bit more than 20 vessels in the bank while the latter need almost 30 cryogenic vessels. This give an indication, that further research has to be conducted on the recharging time for the cryogenic vessels. Especially the pressurization in the *Step2* that should be further studied to find a compromise between the power needed to warm up the vessels and time needed for the process. As previously said, we could use the environment temperature instead of giving an extra energy input from another source, this would warm up the vessels no adding costs but would take extra time so, a bigger bank of cryogenic vessels in the cascade.

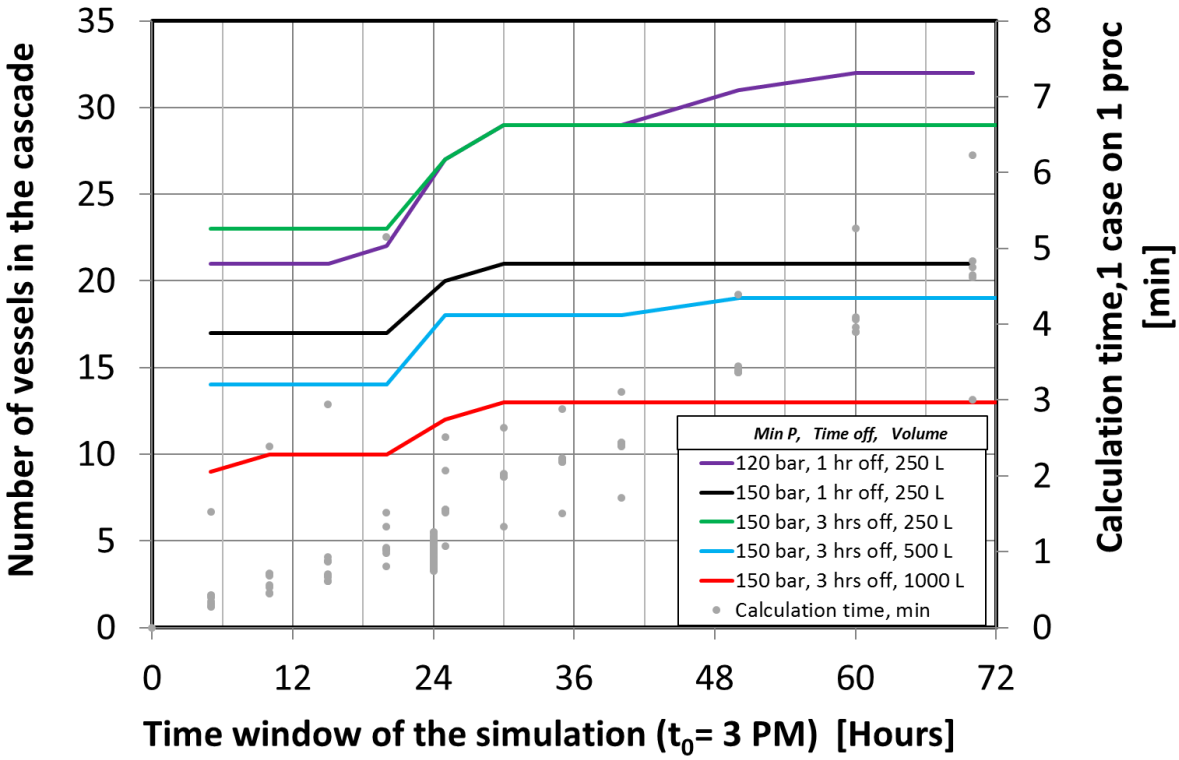

FIGURE 74 TIME WINDOW INFLUENCE AND NUMBER OF NEEDED VESSEL IN THE CASCADE

Once the cascade is at its stationary conditions (fixed number of cryogenic vessels) looking at Figure 75, can be seen also another vantage that there is in having a higher minimum pressure of dispensing. Here are shown the trends of the pressures inside the bank of cryogenic vessels in the cascade vs. the pressure in the vehicles. Have been taken the two most extreme cases to better show, that in the case (A) with 250 bar of minimum dispensing pressure, only 4 cryogenic vessels are used to refill completely a vehicle. In the case (B) with a lower pressure of 92 bar the entire cascade (8 tanks) is used, in which someone of those will dispense only a really small amount of hydrogen (CV6-CV7), this could exploit the valves that has to be open and close quickly to dispense only few grams of hydrogen.

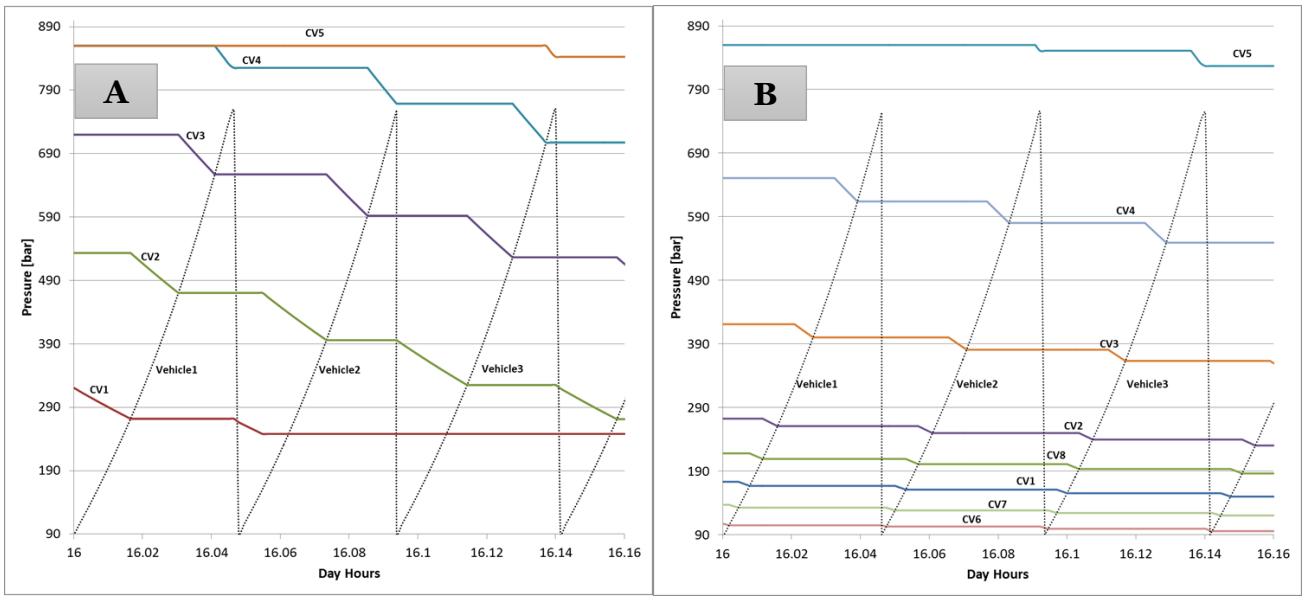

FIGURE 75 COMPARISON DURING THE PEAK OF THE DEMAND (16.00) OF TWO MINIMUM DISPENSING PRESSURE SCENARIO. CRYOGENIC VESSELS PRESSURES VS. VEHICLES PRESSURES. SCENARIO (A) 250 BAR, SCENARIO (B) 92 BAR

At last with the results from the analysis previously showed in Figure 74, we analyzed the costs and mode of use for the entire cascade.

In Figure 76 (A) it shown how the minimum pressure of dispensing and the offline time plays on the entire price of the bank of cryogenic vessels.

In (B) and (C) are shown how is correlated the volume of one vessel with the number of cycle per day and the total number of cryogenic vessels in the cascade.

What we can conclude from these, is that a good solution for the designs would be "Smaller and more vessels" in order to reduce the cost, by enabling more cycles per vessel. The optimal is around 200-300 Liters and a bank of 30 cryogenic vessels.

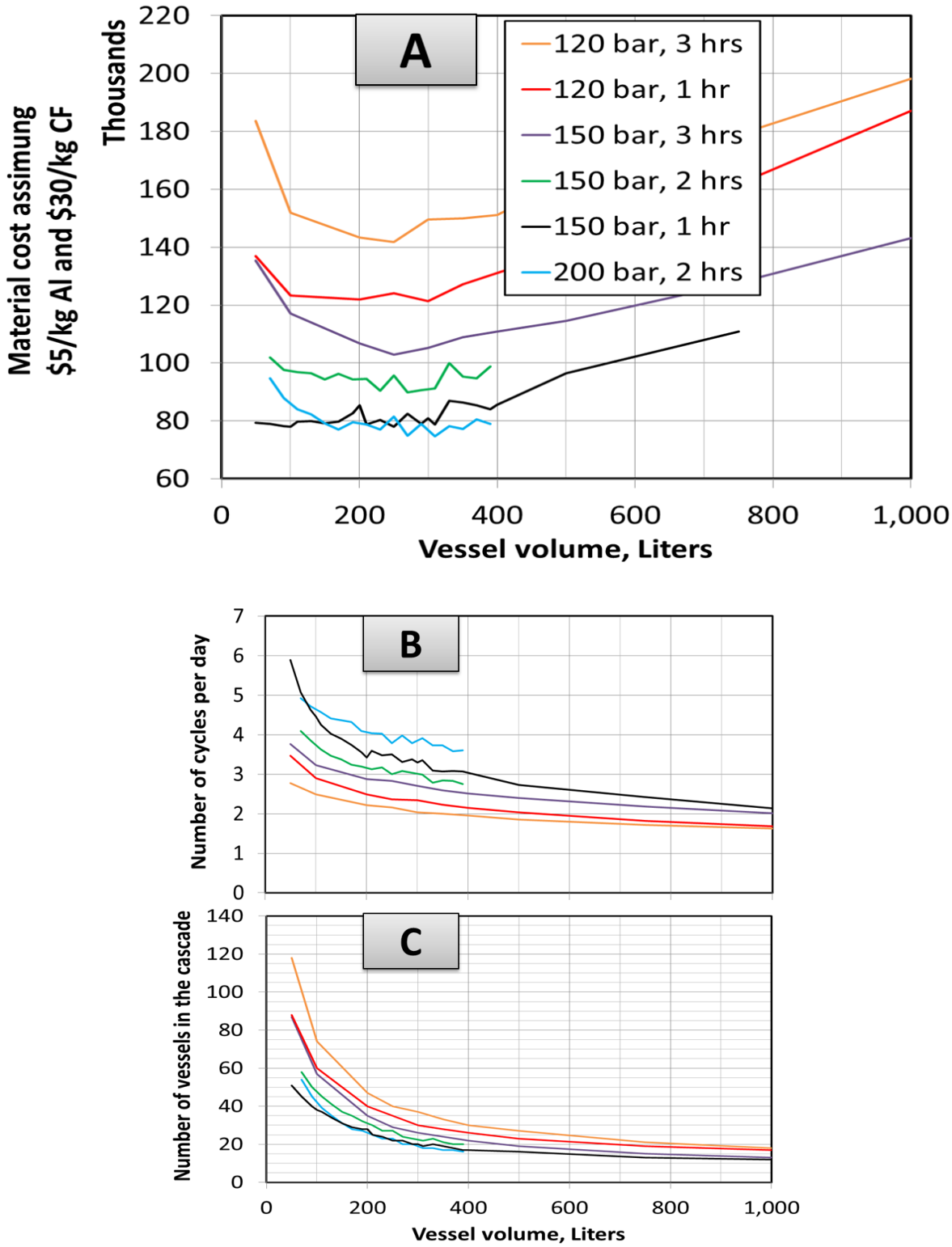

FIGURE 76 (A) ESTIMATION OF THE COST OF THE ENTIRE BANK OF CRYOGENIC VESSEL IN THE CASCADE CORRELATED WITH THEIR VOLUME. (B) AVERAGE NUMBER OF CYCLES PER DAY FOR ONE CRYOGENIC VESSEL. (C) CORRELATION NUMBER OF CRYOGENIC VESSELS IN THE CASCADE VS. INTERNAL VOLUME OF THE VESSEL

Using the results from the two codes, it is now possible to evaluate the impact of venting and cryogenic vessel design on the overall station cost.

HDSAM simulation tools were used to estimate the boundaries into which we need to stay to respect a target price. In our estimation, the cost in resulted to be $7.4 per kg of dispended hydrogen.

Figure 77 shows the trade-off between the operation cost (i.e. H2 losses) and the capital cost (i.e. amount of material in the cascade) in order to meet a given cost target for the dispensed H2; here $7.2/kg H2. Two cases are shown: the red line assumes no cost for dispensing (the cost to pressurize the cryogenic vessel and warm up the hydrogen during the refueling process (*Step3*) is negligible) while the blue line is considers the extra cost of energy of warming up the H_2..

We can see that in case we have a $300k bank of cryogenic vessels, the boil-off must not be more than 13% taken into account extra energy cost for dispensing. If we are able to avoid this extra cost, an extra 3% of vented hydrogen could be alowed. Having a cheaper bank of cryogenic vessel allows to have more venting and still be in the target price and the other way around.

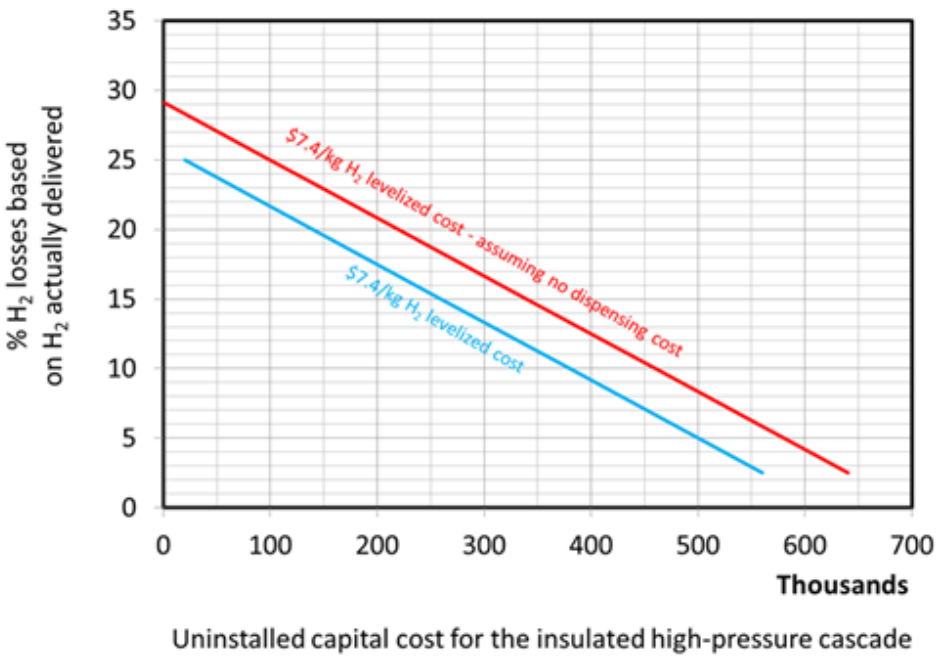

FIGURE 77 VENTING-CASCADE DESIGN COMPARISON AT A FIXED TARGET PRICE FOR THE DISPENSED HYDROGEN. BLUE LINE CONSIDERING THE ENERGY INPUT FOR THE PRESSURIZATION PROCESS, THE RED LINE THIS COST IS CONSIDERED NEGLIGIBLE

The results from the entire study and the two codes are resumed in the following table, were can be seen in which direction the controllable parameters have to be moved in order to get a minimum boil-off and overall cost of the cascade:

TABLE 10 PARAMETERS MANAGING TO OPTIMIZE CASCADE COST AND BOIL-OFF. ARROW POINTING UP: INCREASE VALUE. ARROW POINTING DOWN: DECREASE VALUE.

Parameters	Boil-Off	Cascade Cost
Cryogenic Vessel Internal Volume	↓↓↓	↓↓↓
Cryogenic Vessel Inner Radius	↓↓↓	
Minimum Dispensing Pressure		↑↑↑
Time offline Cryogenic Vessel		↓↓↓
Number of Cryogenic Vessels		↑↑↑
Number of Cycle for Cryogenic Vessel		↑↑↑
Minimum admissible Pressure CV	↓↓↓	
Dewar Volume	↑↑↑	
Percentage of Full Dewar Step1	↑↑↑	
Percentage of Full Dewar Step4	↑↑↑	

FUTURE WORKS

- In future should be done further studies to evaluate the possibility of using one/two low pressure liquid cryogenic pump/s during the recharging process. This could allow to eliminate in part or completely the need to vent in order to recharge the cascade. But has to be carefully evaluated the cost of such pumps.
- The pressurization of the cryogenic vessels need further research to better understand the optimal design and the actual impact on the overall price.
- Further studies on how to use the vented hydrogen on-site will be necessary in order to understand how we could use it to supply the energy demand of the station (e. g. electrical generator for the fridges of the bar etc.)

APPENDIX A: REFPROP 9.1

REFPROP is an acronym for REFerence fluid PROPerties. This program, developed by the National Institute of Standards and Technology (NIST), calculates the thermodynamic and transport properties of industrially important fluids and their mixtures. These properties can be displayed in tables and plots through the graphical user interface; they are also accessible through spreadsheets or user-written applications accessing the REFPROP DLL or the FORTRAN property subroutines.

REFPROP is based on the most accurate pure fluid and mixture models currently available. It implements three models for the thermodynamic properties of pure fluids: equations of state explicit in Helmholtz energy, the modified Benedict-Webb-Rubin equation of state, and an extended corresponding states (ECS) model. Mixture calculations employ a model that applies mixing rules to the Helmholtz energy of the mixture components; it uses a departure function to account for the departure from ideal mixing. Viscosity and thermal conductivity are modeled with either fluid-specific correlations, an ECS method, or in some cases the friction theory method.

These models are implemented in a suite of FORTRAN subroutines. They are written in a structured format, are internally documented with extensive comments, and have been tested on a variety of compilers. Routines are provided to calculate thermodynamic and transport properties at a given (T,,x) state. Iterative routines provide saturation properties for a specified (T,x) or (P,x) state. Flash calculations describe single- or two-phase states given a wide variety of input combinations [(P,h,x), (P,T,x), etc].

A separate graphical user interface, designed for the Windows operating system, provides a convenient means of accessing the models. It generates tables and plots for user-specified mixtures or a number of predefined mixtures (air, the commercially available refrigerant blends, and several reference natural gases). A help system provides information on how to use the program. Information screens that display fluid constants and documentation for the property models can be called up at any time. Numerous options to customize the output are available as well as capabilities to copy and paste to and from other applications.

The property models can also be accessed by other applications (such as spreadsheets) through use of a dynamic link library (DLL).

APPENDIX B: HDSAM

Although a number of analyses of hydrogen production and delivery infrastructures have been conducted and have produced important insights into technical and cost barriers, most studies have failed to provide the guidance needed for Research and Development (R&D) decisions. In particular, findings have appeared inconsistent or conflicting because of differences in the analytical base (e.g., whether the analysis is based on current or advanced technologies, on targets or empirical results, on "real world' or simulated duty cycles, etc.), or in the many economic, financial and technological assumptions used in the analysis. As a result, analytical results have not always contributed the rigor desired for oversight and guidance of the hydrogen program.

The H2A (or Hydrogen Analysis) project was initiated to remedy this problem. Begun in 2003, H2A sought to improve transparency and consistency so researchers and program managers could better understand similarities and differences among efforts, and industry could better validate results. To that end, DOE leveraged the talents and capabilities of analysts from several national laboratories, universities and the private sector, forming two teams to develop a set of tools for production and delivery analysis. More information on H2A can be found at www.hydrogen.energy.gov.

The H2A Delivery team was charged with developing tools to model the cost contribution of all activities/components between the central production of hydrogen and its use on-board a vehicle. Two tools have been developed – the Delivery Components Model and the Delivery Scenarios Model. Versions 2.0 of both models are available at the above web address. This report documents Version 2.0 of the **Delivery Scenarios Model**.

The H2A teams were supplemented by a group of Key Industrial Collaborators (KIC) who attended H2A meetings, reviewed draft documents, provided "rules of thumb" for default assumptions, and reviewed "beta" or test versions of H2A-developed tools. In addition to contributing their own technical expertise, KIC members provided access to their organization's publicly available knowledge base. The resulting tools benefited greatly from this input.

APPENDIX C: Sobol Sequence

Sobol sequences (also called LP_τ sequences or (t, s) sequences in base 2) are an example of quasi-random low-discrepancy sequences. They were first introduced by the Russian mathematician Ilya M. Sobol (Илья Меерович Соболь) in 1967.

The Sobol was the first digital sequence. It operates in base-2 and is still well-regarded for use in quasi Monte-Carlo. To generate one sequence (i.e., one dimension) of *N-bit* low-discrepancy Sobol numbers, we choose odd integers m_i $(0 \leq i \leq N)$, and define N direction vectors c_i:

$$c_i = \frac{m_i}{2^i} = 0._{c_i 1 c_i 2 c_i 3 \ldots\ldots} \quad (c.1)$$

where c_{ij} denote the binary expansion of c_i. Now, choose a primitive polynomial $P(x)$ of degree d with coefficients a_i from the two-element finite (or Galois) field GF (2) (i.e., binary):

$$P(x) = x^d + a_1 x^{d-1} + \cdots + a_{d-1} + 1 \quad (c.2)$$

These coefficients a_i are used to calculate each direction vector c_i as:

$$c_i = a_1 c_{i-1} \oplus a_2 c_{i-2} \oplus a_1 c_{i-1} \oplus \ldots . \oplus a_{d-1} c_{i-d+1} \oplus c_{i-d} \oplus [c_{i-d} \gg d] \quad \text{(c.3)}$$

where $\oplus$ is an exclusive-or (XOR), and the last term is c_{i-d} right-shifted by d bits. A one-dimensional N-bit wide low-discrepancy Sobol sequence x_1, x_2 ,... can be generated based on this set of direction vectors. Take the n-th term of this sequence, x_n, with $n = b_N b_{N-1} \ldots b_2 b_1$ in binary.
Then,

$$x_n = b_1 c_1 \oplus b_2 c_2 \oplus \ldots \oplus b_{N-1} c_{N-1} \oplus b_N c_N \ (c.4)$$

If the direction vectors ci are pre-computed, generating one number requires at most N lookups and

N - 1 XORs. This effort can be drastically reduced by considering a *gray-coded* representation of n. A gray-coded *n+1* differs from gray-coded n in only one bit. The gray-code representation for n can be obtained by

$$g_N \dots g_2 g_1 = b_N \dots b_2 b_1 \oplus \dots \oplus b_N \dots c_3 c_2 \quad (c.5)$$

and the bit gr that flips going from $n \rightarrow n + 1$ is simply the position r of the least-significant zero-bit (LSZ) in $n = b_N \dots b1$.
Now, since $n + 1$ differs from n by only one bit, x_{n+1} 'differs' from x_n by only one direction vector c_r. x_{n+1} can therefore be computed based on x_n as

$$x_{n+1} = x_n \oplus c_r \quad (c.6)$$

with only one lookup and one *XOR*; the complexity of finding the least-significant zero-bit r of n can also be decreased from the standard $O(\log n)$ in hardware by using a priority encoder.

APPENDIX D: HDMR

The high dimensional model representation (HDMR) method is a set of tools explored by Rabitz et al. (1999) in order to express the input-output relationship of complex models with a large number of input variables. The mapping between the input variables $x_1, \ldots, x_n$ and the output variables $f(x) = f(x_1, \ldots, x_n)$ in the domain Rn can be written in the following form:

$$f(x) = f_0 + \sum_{i=1}^{n} f_i(x_i) + \sum_{1 \le i < j \le n} f_{ij}(x_i, x_j) + \cdots + f_{12\ldots n}(x_i, x_j, \ldots x_n) \quad (d.1)$$

Here f_o denotes the mean effect (zeroth order), which is a constant. The function $f_i(x_i)$ is a first order term giving the effect of variable x_i acting independently (although generally non-linearly) upon the output $f(x)$. The function $f_{ij}(x_i, x_j)$ is a second order term describing the cooperative effects of the variables x_i and x_j upon the output $f(x)$. The higher order terms reflect the cooperative effects of increasing numbers of input variables acting together to influence the output $f(x)$. If there is no interaction between the input variables, then only the zeroth order term fo and the first order terms $f_i(x_i)$ will appear in the HDMR expansion.

The HDMR expansion is computationally very efficient if higher order input variable correlations are weak and can therefore be neglected. For many systems a HDMR expression up to second order already provides satisfactory results and a good approximation of $f(x)$ (Li et al., 2001).

The developed GUI-HDMR software is based on the RS-HDMR approach (Li et al., 2002) where a set of random sample points N over the entire domain Rn is used. The zeroth order term fo can be approximated by the average value of $f(x)$. The determination of the higher order component functions is based on the approximation of the component functions by orthonormal basis functions:

$$f_i(x_i) \approx \sum_{r=1}^{k} \alpha_r^i \varphi_r(x_i) \quad (d.2)$$

$$f_{ij}(x_i, x_j) \approx \sum_{p=1}^{l} \sum_{q=1}^{l'} \beta_{pq}^{ij} \varphi_p(x_i) \varphi_q(x_j) \quad (d.3)$$

where *k, l, l'* represent the order of the polynomial expansion, α_r^i and β_{pq}^{ij} are constant coefficients to be determined, and $\varphi_r(x_i), \varphi_p(x_i)$ and $\varphi_q(x_j)$ are the orthonormal basis functions.
Note that only one set of random samples *N* is necessary in order to determine all RS-HDMR component functions (Li et al., 2002).

A commonly used method in global SA is the method of Sobol' (Sobol, 2001), which is conceptually the same as the RS-HDMR approach. In statistics the decomposition of *f(x)* into summands of increasing dimensionality (see equation (1)) is called ANOVA decomposition which is also a member of the high dimensional model representations known as ANOVA-HDMR (Rabitz et al., 1999), (Rabitz and Ali¸s, 1999). However, the calculation of the partial variances on the basis of the RS-HDMR function expansion provides a much more efficient approach (Ali¸s and Rabitz, 2001).
The total variance *D* can be obtained by

$$D = \int_{K^n} f^2(x)dx - f_0^2 \quad (d.4)$$

and the partial variances $D_{i1,\ldots,is}$ can be calculated from each of the terms in equation (1):

$$D_i = \int_0^1 f_i^2\,(x_i)dx_i \quad (d.5)$$

$$D_{ij} = \int_0^1 \int_0^1 f_{ij}^2\,(x_i, x_j)dx_i dx_j \quad (d.6)$$

Once the partial variances are determined the sensitivity indices can be calculated as follows:

$$S_{i_1,\ldots i_s} = \frac{D_{i_1,\ldots i_s}}{D} \quad 1 \le i_1 < \cdots < i_s \le n \; (d.7)$$

so that all its terms add up to 1:

$$\sum_{i=1}^{n} S_i + \sum_{1 \le i < j \le n} S_{ij} + \cdots + S_{12\ldots n} = 1$$

The first order sensitivity index S_i measures the main effect of the input variable xi on the output, or in other words the fractional contribution of xi to the variance of *f(x)*.

The second order sensitivity index S_{ij} measures the interaction effect of x_i and x_j on the output and so on. More detailed information about the calculation of the sensitivity indices on basis of the RS-HDMR component functions can be found in Li at el. (2002a).

BIBLIOGRAPHY

[1] J. Marcinkoski, "U.S. Department of Energy Efforts in Electrified Vehicle Power."

[2] Kamel Bennaceur,Brian Clark, Franklin M. Orr Jr., T.S. Ramakrishnan, Claude Roulet, Ellen Stount, "Hydrgone: A Future Energy Carrier?"

[3] W. Dougherty, S. Kartha, C. Rajan, M. Lazarus, A. Bailie, B. Runkle, and A. Fencl, "Greenhouse gas reduction benefits and costs of a large-scale transition to hydrogen in the USA," *Energy Policy*, vol. 37, no. 1, pp. 56–67, Jan. 2009.

[4] Michael R. Swain and University of Miai, "Fuel Leak Simulation." [Online].

[5] CEC-600-2005-0012004 and 2005-0012004,California Energy Commission : California., "CEC.Failure modes and effects analysis for hydrogen fueling options."

[6] "Daimler, Ford, Nissan form hydrogen fuel cell alliance - Photos (1 of 2) | CarAdvice,"

[7] IEA- Hydrogen Coordination Group, "Hydrogen Production and Storage."

[8] O. Veneri, "Hydrogen as Future Energy Carrier," in *Hydrogen Fuel Cells for Road Vehicles*, Springer London, 2011, pp. 33–70.

[9] Wonihl Cho, Seung-Ho Lee, Woo-Sung Ju and Youngsoon Baek, "Conversion of Natural Gas to Hydrogen and Carbon Black by Plasma and Application of Plasma Black."

[10] N. Muradov, F. Smith, G. Bockerman, and K. Scammon, "Thermocatalytic decomposition of natural gas over plasma-generated carbon aerosols for sustainable production of hydrogen and carbon," *Appl. Catal. Gen.*, vol. 365, no. 2, pp. 292–300, Aug. 2009.

[11] *Carbon and Coal Gasification - Science and Technology | J.L. Figueiredo | Springer*.

[12] Paul Pickard, Sandia National Labs, "2005 DOE Hydrogen Program Review Sulfur-Iodine Thermochemical Cycle."

[13] "PEM electrolysis for production of hydrogen from renewable energy sources."

[14] J. Stephen Herring , James O'Brien, Carl Stoots, Paul Lessing and Ray Anderson, , Qiang Sunc, and , Siew Hwa Chan, "High-Temperature Solid Oxide Electrolyser System."

[15] Jan Pawel Stempiena,b, "Solid Oxide Electrolyzer Cell Modeling: A Review."

[16] Sunita Sharman, Sib Krishna Ghoshal, "Hydrogen the future transportation fuel: From production to applications."

[17] Jinyang Zheng, Jinxing Guo, Jian Yang, Yongzhi Zhao, Lei Zhao, and Xiangmin Pan, Jianxin Ma, Lifang Zhang, "Experimental and numerical study on temperature rise within a 70 MPa type III cylinder during fast refueling."

[18] D. Mori, K. Hirose, "Recent challenges of hydrogen storage technologies for fuel cell vehicles."

[19] Salvador M. Aceves, Francisco Espinosa-Loza, Elias Ledesma-Orozco,Timothy O. Ross, Andrew H. Weisberg, Tobias C. Brunner, Oliver Kircher, "High-density automotive hydrogen storage with cryogenic capable pressure vessels."

[20] P. E. D. and W. McDowall and UCL Energy Institute, University College London, "A review of hydrogen delivery technologies for energy system models.

[21] Andrew Burke and Monterey Gardiner, "Hydrogen Storage Options: Technologies and Comparisons for Light-Duty Vehicle Applications.

[22] Delbert E. Day, James E. Shelby, "Hollow Glass Microspheres (HGMS) Designed for Storing Hydrogen.

[23] "Green Car Congress: Kawasaki Heavy and Shell to partner on technologies for transporting liquefied hydrogen by sea.

[24] Amgad Elgowainy, Marianne Mintz, Bruce Kelly, Matthew Hooks, and Mark Paster, "Optimization of Compression and Storage Requirements at Hydrogen Refueling Station.

[25] Jesse Schneider, and SAE Fuel Cell Interface Group Chair, "SAE J2601 - Worldwide Hydrogen Fueling Protocol: Status, Standardization & Implementation

[26] Ian A. Richardson, Jacob T. Fisher, Patrick E. Frome, Ben O. Smith, Shaotong Guo, Sayonsom Chanda, Mikko S. McFeely, and Austin M. Miller, Jacob W. Leachman, "Low-cost, transportable hydrogen fueling station for early market adoption of fuel cell electric vehicles.

[27] Nexant, Inc., Air Liquide, Argonne National Laboratory, Chevron Technology Venture, Gas Technology Institute, National Renewable Energy Laboratory, Pacific Northwest National Laboratory, and TIAX LLC, "H2A Hydrogen Delivery Infrastructure Analysis Models and Conventional Pathway Options Analysis Results.

[28] Monterey Gardiner, "Energy requirements for hydrogen gas compression and liquefaction as related to vehicle storage needs.

[29] M. D. Paster, R. K. Ahluwalia, G. Berry, A. Elgowainy, S. Lasher, K. McKenney, and M. Gardiner, "Hydrogen storage technology options for fuel cell vehicles: Well-to-wheel costs, energy efficiencies, and greenhouse gas emissions," *Int. J. Hydrog. Energy*, vol. 36, no. 22, pp. 14534–14551, Nov. 2011.

[30] "H2A Delivery Scenario Analysis Mode: Version 2.0 (HDSAM 2.0) User's Manual -

[31] Y. Li, H. Chen, and Y. Ding, "Fundamentals and applications of cryogen as a thermal energy carrier: A critical assessment," *Int. J. Therm. Sci.*, vol. 49, no. 6, pp. 941–949, Jun. 2010.

[32] G. Petitpas, S. M. Aceves, and N. Gupta, "Vehicle refueling with liquid hydrogen thermal compression," *Int. J. Hydrog. Energy*, vol. 37, no. 15, pp. 11448–11457, Aug. 2012.

[33] Sam Sprik (PI), Jennifer Kurtz, Chris Ainscough,Genevieve Saur, Mike Peters, National Renewable Energy Laboratory, "Hydrogen Station Data Collection and Analysis.

[34] E. W. Lemmon, Marcia L. Huber, and Mark O. McLinden, "NIST Reference Fluid Thermodynamic and Transport Properties — REFPROP Version 9. 1.

[35] L. Parnas and N. Katırcı, "Design of fiber-reinforced composite pressure vessels under various loading conditions," *Compos. Struct.*, vol. 58, no. 1, pp. 83–95, Oct. 2002.

[36] D.-S. Son and S.-H. Chang, "Evaluation of modeling techniques for a type III hydrogen pressure vessel (70 MPa) made of an aluminum liner and a thick carbon/epoxy composite for fuel cell vehicles," *Int. J. Hydrog. Energy*, vol. 37, no. 3, pp. 2353–2369, Feb. 2012.

[37] S. R. Swanson, Ed., *Introduction to design and analysis with advanced composite materials*. Upper Saddle River, N.J.: Prentice Hall, 1997.

[38] E.D. Marquardt, J.P. Le, and Ray Radebaugh and National Institute of Standards and Technology, “Cryogenic Material Properties Database.

[39] R. K. Ahluwalia and J. K. Peng, “Dynamics of cryogenic hydrogen storage in insulated pressure vessels for automotive applications,” *Int. J. Hydrog. Energy*, vol. 33, no. 17, pp. 4622–4633, Sep. 2008.

[40] E. Rothuizen and M. Rokni, “Optimization of the overall energy consumption in cascade fueling stations for hydrogen vehicles,” *Int. J. Hydrog. Energy*, vol. 39, no. 1, pp. 582–592, Jan. 2014.

[41] Joseph Pratt (Sandia National Laboratories), Danny Terlip, Chris Ainscough, Jennifer Kurtz (National Renewable Energy, and Laboratory) Amgad Elgowainy (Argonne National Laboratory), “H2FIRST Reference Station Design Task: Project Deliverable 2-2.